ADHESION IN BITUMEN-AGGREGATE SYSTEMS AND QUANTIFICATION OF THE EFFECTS OF WATER ON THE ADHESIVE BOND

A Dissertation

by

ARNO WILHELM HEFER

Submitted to the Office of Graduate Studies of
Texas A&M University
in partial fulfillment of the requirements for the degree of

DOCTOR OF PHILOSOPHY

December 2004

Major Subject: Civil Engineering

ADHESION IN BITUMEN-AGGREGATE SYSTEMS AND QUANTIFICATION OF THE EFFECTS OF WATER ON THE ADHESIVE BOND

A Dissertation

by

ARNO WILHELM HEFER

Submitted to Texas A&M University
in partial fulfillment of the requirements
for the degree of

DOCTOR OF PHILOSOPHY

Approved as to style and content by:

Dallas N. Little (Chair of Committee)	Robert L. Lytton (Member)
Bruce E. Herbert (Member)	D. Wayne Goodman (Member)
	Paul N. Roschke (Head of Department)

December 2004

Major Subject: Civil Engineering

ABSTRACT

Adhesion in Bitumen-Aggregate Systems and
Quantification of the Effects of Water
on the Adhesive Bond. (December 2004)
Arno Wilhelm Hefer, B.S., University of Pretoria, South Africa;
M.S., University of Pretoria, South Africa
Chair of Advisory Committee: Dr. Dallas N. Little

This research is intended to contribute toward the understanding, development, and implementation of a more fundamental design process for bituminous pavement materials, utilizing thermodynamic properties of the materials involved. The theory developed by van Oss, Chaudhury and Good forms the basis of this research. Optimization of techniques to characterize surface energy, as well as consideration and evaluation of additional factors that influence adhesion in the presence of water, are pursued. A synthesis of theories and mechanisms of bitumen-aggregate adhesion is presented, and existing and potential techniques for surface energy characterization are reviewed to establish firm background knowledge on this subject.

The Wilhelmy plate technique was scrutinized and improved methodologies and analysis procedures are proposed. Inverse gas chromatography (IGC) is introduced as an alternative technique. A reasonable comparison of total surface energy values form these techniques with mechanical surface tension values were found. Results suggest that bitumen surface energies do not vary substantially. Inability of these techniques to detect the effect of a liquid additive is rationalized by the 'potential' surface energy concept. Suggestions for a more realistic characterization of bitumen polar surface energy components are presented.

A static gravimetric sorption technique was employed to characterize aggregate surface energies. Dynamic vapor sorption was identified as a candidate alternative technique for aggregate surface energy characterization.

A study on the effect of pH on surface energy components of water revealed that this effect is practically negligible. Calculation of the free energy of electrostatic interaction (ΔG^{EL}) indicated that this term contributes less than 1% to the total free energy of adhesion. Despite this finding, it is shown that ΔG^{EL} alone is able to distinguish moisture sensitive mixtures. The significance of electrical phenomena at the interface is elucidated through another mechanism following the work of M.E. Labib. The relationship between pH and electron donor-acceptor properties of aggregate surfaces is presented. The Labib approach potentially offers the solution to quantify the effect of pH on adhesion. In addition, it should be possible to resolve issues with the acid-base scale proposed by the founders of the current theory, by replacing it with a more absolute donor-acceptor scale.

MASHA

ACKNOWLEDGMENTS

I would like to express my appreciation and gratitude to my advisor, Dr. Dallas Little, for his trust and support, and for giving me the opportunity to be a part of this interesting and important research. I wish to thank Dr. Lytton for sharing his knowledge so passionately, it was inspirational and a privilege to have him on this committee.

Appreciation and thanks go to Dr. Bruce Herbert from the Department of Geology and Geophysics (GEPL) for his encouragement and time spent in valuable discussions. It was a privilege to have Dr. Wayne Goodman from the Department of Chemistry on this committee. I appreciate and thank Dr. Ray Guillemette from GEPL for acting as a temporary substitute committee member and for memorable discussions on mineralogy.

I wish to express my appreciation and gratitude to Dr. Carel J. van Oss, Professor at the State University of New York at Buffalo for many interesting discussions and literature made available. I am also grateful to Dr. van Oss for his initiative in conducting the study on the effects of pH on the electron accepticity-donicity of water.

I am indebted to Dr. Mohamed E. Labib, CEO and President of Novaflux Technologies for his guidance and contribution to this research by making indispensable research material available.

I would like to thank my friend and collogue, Amit Bhasin, for his support and so many interesting and valuable discussions that helped stimulate and solidify my thinking on many aspects of this research.

I gratefully acknowledge the role AFRICON Engineering International played, especially Dr. Ian van Wijk and Dr. Gustav Rohde, in granting me the opportunity to acquire this knowledge and gain this life enriching personal experience.

The love, encouragement, and prayers of my family carried me through this time. This research would not have been possible without having my wonderful wife, Masha, by my side. Many thanks to my friends for their encouragement and support.

Most importantly, all the Honor and the Glory to my Lord and Savior, Jesus Christ.

TABLE OF CONTENTS

Page

CHAPTER Page

LIST OF FIGURES

FIGURE Page

FIGURE Page

FIGURE Page

LIST OF TABLES

TABLE Page

CHAPTER I

INTRODUCTON

BACKGROUND

The word ‘adhesion’ comes from the Latin word *adhaerere*, which means ‘to stick to’. A definition of ‘adhesion’ in its scientific context is given by ASTM D907 as “the state in which two surfaces are held together by valence forces or interlocking forces, or both”. ‘Fundamental’ adhesion refers to forces between atoms at the interface, also called ‘true’ adhesion. ‘Practical’ adhesion, on the other hand, is a term that can be used to describe the results of destructive adhesion tests, such as a tensile test. The parameter recorded reflects the fundamental adhesion at the interface as well as the mechanical response of the adhesive glue, substrate, and interfacial region. The mode of failure in tests of this nature can be adhesive (rupture of bonds between molecules of different phases), cohesive (rupture of bonds between molecules within the same phase), or mixed (Packham, 1992). The research of interest in this dissertation is concerned with fundamental adhesion, with the emphasis on surface energy or surface tension.

The intrinsic surface forces that take part in fundamental adhesion can be attributed to the fact that atoms and molecules in that region usually possess reactivity significantly different from units in the bulk. In the bulk phase, a unit experiences a uniform force field due to interaction with neighboring units. However, if a surface is created by dividing the bulk phase, the forces acting on the unit at the new surface are no longer uniform. Due to the missing interactions, the units are in an energetically unfavorable condition, i.e. the total free energy of the system increased. This increase in energy is termed the “surface free energy” or more accurately the “excess surface free energy”. In order to restore equilibrium, molecules and atoms at the surface of liquids will experience a net positive inward attraction, normal to the surface and resultant lateral

---

This dissertation follows Geoarchaeology for style and format.

tension along the surface, referred to as “surface tension”. Hence, liquid water tends to contract into a sphere when free from other phases and gravitational forces. The phenomenon of insects walking on water is often used as an example of surface tension at work. When one contacting phase is vacuum or gas, it is common to refer to “surface energy” or “surface tension”. Equilibrium can also be restored by interaction with atoms or molecules from another condensed phase. When two condensed phases are involved the terms “interfacial energy” or “interfacial tension” are used. The two terms are interchangeable for liquids, are dimensionally equivalent, and numerically equal. In solids, however, the application of the surface tension concept becomes less clear and surface “energy” and surface “tension” are not necessarily equal. Solid surface characteristics such as reduced mobility of atoms and molecules, and varying surface morphology give rise to a heterogeneous “solid surface tension” condition. It is therefore more accurate to use the term surface energy, rather than surface tension for solid surfaces (Myers, 2002).

The fact that good adhesion between bitumen and aggregate is a key ingredient for good performance is as old as the first bitumen bound macadam pavements constructed in the late 1800s. Road builders at the time would not only test the consistency, but also the stickiness of a piece of bitumen by chewing on it – bitumen sticking to their teeth passed the test! Literature suggests that concern about adhesion of bitumen to aggregate stimulated research into this matter since the 1920s. The main concern that would lead to extensive research over decades to come was adhesive failure induced by water entering the bituminous mix, called moisture damage, or simply stripping. Efforts to resolve adhesion problems in bituminous mixtures led to establishment of ‘The Committee on Interfacial Surface Tension’ in the early 1930s (Nicholson, 1932). Saville and Axon (1937) stated that this subject had been studied so extensively and discussed so frequently, that the fundamental principles of bitumen-aggregate adhesion were generally known to the industry. The most significant outcome of research during this time was identification of chemical compounds that could be used as adhesion promoters

between bitumen and aggregate. Although the stripping phenomenon was known to be an exhibition of interfacial tension relation between aggregate and bitumen in the presence of water, attempts to place this on a quantitative basis had not been too successful. Pavement engineers chose to use tests such as the boiling water test (Riedel-and-Wieber test), the wash test, swell test, and eventually wet-dry mechanical tests to assess water susceptibility of bituminous mixtures (Krchma and Loomis, 1943).

With the advent of technological advancement in the second half of the 20th century, significant contributions to the fundamental understanding of bitumen-aggregate interfacial relations were made. The extraction of bitumen from cores obtained from in-service pavements is everyday practice, and was probably one of the first techniques utilized to distinguish between strongly and weakly adsorbed chemical compounds in bitumen (or functional groups), often called *desorption by solvent extraction* (Petersen et al. 1974; Scott, 1978). By using solvents of increased polarity, concentrations of desorbed functionalities with each step can be determined using infrared spectroscopy or ultraviolet spectrophotometry. Plancher et al. (1977) also used this technique together with freeze-thaw experiments to isolate and identify sensitivities of these components to displacement by water from aggregate surfaces. They identified organic chemical compounds that represented the natural functional groups in bitumen, often called model compounds, in order to validate their findings through a more controlled experiment (Petersen and Plancher, 1998). Scott (1978) in his work on adhesion and disbonding mechanisms used this technique to analyze bitumen adsorbed from toluene solutions onto mineral powders and glass. Different acidic adsorption sites on quartz were characterized by Ernstsson and Larsson (1999) using desorption by solvent extraction.

Thermal desorption techniques were used by Petersen et al. (1982) and Park et al. (2000). In these studies model bitumen chemical compounds were adsorbed onto pulverized aggregates or pulverized model aggregates, dried, and heated at a predetermined rate. The higher the temperature at which these functionalities desorb, the higher the bond strength between the chemical compound and the aggregate surface. Petersen et al. (1982) also investigated pretreatment of these coated aggregate particles

with water and obtained fundamental information on some of the chemistries of moisture-induced damage (Petersen and Plancher, 1998).

Barbour et al. (1974) applied *inverse gas-liquid chromatography (IGLC)* to study bitumen-aggregate interactions. The time for a test compound in a gas state of certain polarity to elute through a column packed with an unknown substance, such as bitumen coated onto some support, served as an indication of how strong these interactions are. Retention times could then be used to calculate normalized interaction coefficients. Coefficients of different bitumen fractions coated onto inert supports as well as aggregate particles were used to obtain the net polarity of the complex system, hence providing a qualitative assessment of bitumen fractions with the aggregate particles.

During the Strategic Highway Research Program (SHRP), *adsorption by solvent depletion*, essentially a modified form of liquid chromatography, was the primary technique adopted for research on bitumen-aggregate interactions. In these experiments, aggregate particles are exposed to a solution containing a known concentration of bitumen or bitumen model compounds. The solution is then analyzed to determine the chemical functionality and amount adsorbed. Adsorption isotherms, which is the amount adsorbed at different initial concentrations at a given constant temperature, are usually developed from the data to obtain important thermodynamic parameters (Jeon and Curtis, 1990; Curtis et al., 1991). Introduction of water into the system and monitoring desorption of previously adsorbed species have also been conducted. During the SHRP research, Curtis and her co-workers developed the net-adsorption test from adsorption/ desorption studies (Curtis et al., 1989; Curtis, 1992; Curtis et al., 1992). Research at the Institute for Surface Chemistry in Sweden applied similar techniques at the time to characterize interaction of aggregates and minerals with bitumen model compounds (Ardebrant and Pugh, 1991a). Park et al. (2000) investigated the relative affinity of several bitumen model functionalities for a siliceous model aggregate substrate using solution depletion adsorption isotherms.

Microcalorimetry is used to measure sorption heats directly. Essentially, aggregates are brought into contact with bitumen and the energy released during interaction, and

over time, is measured with the sensitive microcalorimeter. This technique has been applied extensively for characterizing bitumen-aggregate interaction (Ensley and Sholz, 1972; Ensley, 1973; Ensley et al., 1984; Podoll and Irwin, 1990). Ernstsson and Larson (1991) incorporated this technique in their studies for identifying acidic adsorption sites on quartz.

The bitumen-water interface and influence of pH on interfacial activity have been studied by Scott (1978) using *electrophoresis*. Labib (1992) used electrophoreses to develop zeta potential – pH curves for selected aggregate and bitumen types. Zeta potential or electrokinetic potential is the electric potential that exists across the interface between a hydrated particle (fixed liquid) and the bulk solution (moving liquid), i.e. a measure of stability at the interface. In addition, this quantity is sensitive to changes in the pH of the system, which is significant, since the pH of water in contact with an aggregate surface changes (Scott, 1978; Labib, 1992).

Ross et al. (1991) and Podoll and Becker (1991) used several modern surface analysis techniques to investigate interactions at the bitumen-aggregate interface and the region around the boundary. In this research, bitumen-coated aggregate was cooled and then cut to expose the perimeter of interaction. An *autoradiographic (AR)* procedure was used to identify concentrations of specific compounds in bitumen that concentrates within boundary regions. *Scanning electron microscopy (SEM)* and *energy dispersive spectroscopy (EDS)* were then employed to closely investigate these regions and map chemical elements (Ross et al.,1991). In addition, elemental analysis from mass spectra obtained with *surface analysis by laser ionization (SALI)* on water stripped bitumen and aggregate surfaces were conducted by this group. The importance of cohesive failure within the aggregate during water-induced failure was one of the major findings (Podoll et al., 1991).

Fourier Transform Infrared spectroscopy (FTIR) as described by Petersen (1986) has been a valuable tool in identifying different functional groups in bitumen, e.g. during solvent extraction, or solvent depletion experiments. In-situ infrared spectroscopy studies on bitumen adsorbed onto aggregate powders, compressed into partly transparent

pellets, have also been conducted. However, Scott (1978) reports that the spectra were difficult to interpret. The Western Research Institute (WRI) in Wyoming used Attenuated Total Reflectance FTIR to investigate the hypothesis that polar groups form an interphase region at the bitumen-aggregate interface. This research confirmed that carboxylic acids migrate to the crystal-bitumen interface with time (WRI, 2001).

As part of a major Federal Highway Administration (FHWA) contract, WRI conducted fundamental work on bitumen-aggregate adhesion. *Atomic force microscopy (AFM)* measures the fundamental forces of adhesion on a substrate with a cantilever of a few hundred microns in length equipped with a minute tip. Surface energies and friction forces were measured on bitumen utilizing the AFM. The researchers also investigated the use of *differential scanning calorimetry (DSC)* to obtain the heat flow characteristics of bitumen and mastics. In DSC experiments, a small sample is heated and cooled at a predetermined rate while exothermic or endothermic heat flows, from and to the sample, are measured. The researchers used glass transition parameters as measures of interaction. Glass transition temperature is that temperature where molecular mobility is reduced dramatically from a liquid to a glassy state upon cooling. Accordingly, if strong interaction occurs when mastic aggregate is added to the bitumen, the bulk or non-interacting portion of the bitumen would have different glass transition properties than the original. In another part of this study, a high-speed *nuclear magnetic resonance (NMR)* sample spinner, was proposed as a rapid alternative to isolate bitumen components that truly adhere to aggregate surfaces facilitated by centrifugation. NMR imaging is also possible and combines the basic principles of magnetic resonance with spatial encoding to obtain the distribution of fluids in samples. This approach was used to obtain bitumen-water interfacial parameters, such as contact angles and surface tensions (WRI, 2003a)

The background on early fundamental research presented above, reveals that surface tension has long been considered an important parameter to elucidate adhesion in bituminous mixtures. Many methods are available to measure surface tension of liquids, while methods to determine the “surface tension” of solids are not common. These

methods are well documented in classic texts such as Adamson and Gast (1997). A renewed interest in the application of surface energy in adhesion science was gained when Fowkes (1964) proposed that surface energy could be divided into independent components, which represent different intermolecular forces on the surface, namely, polar and dispersive components. Ardebrant and Pugh (1991b) measured contact angles of water drops on polished aggregate surfaces by a goniometer telescope, facilitated by incorporating two immiscible hydrocarbon fluids. They used a two-component theory to calculate the work of adhesion of polar species between water and aggregates. Van Oss et al. (1988) developed a three-component theory, based on a modified form of the acid-base theory. In this theory, the total surface energy constitutes an acid, base, and an apolar or dispersive (also Lifshitz-van der Waals) component. Elphingstone (1997) determined contact angles of liquids on different bitumen types by employing the *Wilhelmy plate method*. Li (1997) adopted a gas sorption technique to determine the equilibrium spreading pressures of three organic solutes of different polarities when adsorbed onto road building aggregates and used these parameters to calculated surface energy. Cheng et al (2002) used both the Wilhelmy plate method and a vacuum sorption method or so-called *universal sorption device (USD)*, to determine the surface energy components of bitumen and aggregates respectively. The significance of determining surface energy components is its ability to be used in predicting the work of adhesion for any combination of bitumen and aggregate for which these values are known. The work of adhesion in the presence of a third medium, such as water, can also be predicted (Elphingstone, 1997; Cheng et al., 2002). In addition, surface energy and its components are fundamentally related to the fracture damage and healing phenomena induced by repeated wheel loads in bituminous paving mixtures (Little et al., 1997).

The fundamental nature of the surface energy theory and its potential versatility in quantitative application, have distinguished this approach as one considered for implementation by many in the pavement engineering community. This is evident from an National Cooperative Highway Research Program (NCHRP) project which was recently launched to further develop this technology for implementation.

PROBLEM STATEMENT AND HYPOTHESES

Adhesion between bitumen and aggregate is one of the important prerequisites in obtaining a successful bituminous paving mixture. The previous section indicates that problems with adhesion in these mixtures have historically been related to moisture damage. Although the impact of moisture sensitivity problems on pavement performance and maintenance costs is not clearly defined, studies in the USA showed that between 80% and 90% of the state road authorities require anti-strip additives and tests for moisture sensitivity of bituminous mixtures (Hicks et al., 2003). During the last few years, joint efforts to transfer experience and research available on moisture damage have resulted in significant contributions in this regard, such as the "National Seminar on Moisture Sensitivity" held in San Diego, in 2003.

Although it is well known that moisture damage can not be attributed to a single mechanism (Little and Jones, 2003), experience with the use of additives, such as hydrated lime and amine anti-stripping agents, illustrates the important role of chemical mechanisms in effectively mitigating moisture damage and improving pavement performance (Petersen and Plancher, 1998). The need for a fundamental approach to elucidate and quantify adhesion in these systems among researchers is evident from the literature. These highlights are only a glimpse into a body of research on the general subject of moisture damage. The major part of this research, however, is phenomenological, i.e. empirical, and accordingly also the state of practice. The importance of fundamental knowledge of materials and material behavior have become indispensable to pavement engineers with the trend towards privatization of infrastructure and long term concession contracts which demand a higher level of risk management. The introduction evidently shows the amount of valuable research that exists on bitumen-aggregate adhesion. Synthesis of this information is needed to complement recent advancements on the understanding and application of adhesion science in order to place the prediction of bitumen-aggregate bonding on a quantitative basis. In addition, research indicates that thermodynamic parameters, essentially surface energy, appear to be an appropriate way to describe adhesion. To utilize this approach

effectively, time efficient and reliable techniques need to be identified for quantification surface energy characteristics of the materials involved.

GOAL AND OBJECTIVES

The goal of this research is to contribute towards the understanding, development, and implementation of a materials design process for bituminous pavement composite materials, based on a fundamental macroscopic approach. This will be achieved by the following objectives.

- Synthesis of fundamental research on bitumen-aggregate adhesion.
- Review potential techniques for measuring surface energies of bitumen and aggregate.
- Optimize existing techniques to determine surface energies
- Introduce inverse gas chromatography as an alternative technique to determine surface energy.
- Investigate potential refinement of the current application of the thermodynamic theory to predict adhesive bond strength in the presence of water, with specific reference to the effect of pH of the interface water.

SCOPE

This research builds forth on the work conducted by Li (1997), Elphingstone (1997) and Cheng (2002), where surface energies of bitumen and aggregate were measured and utilized to calculate the work of adhesion as well as the work of cohesion, based on a physical chemistry theory developed by van Oss et al. (1988). The current research, is not intended to investigate and compare similar theories but to embrace the application of the current widely applied theory, by taking cognizance of subsequent developments and general critique.

In order to compliment the current research effort and in an attempt to gain a comprehensive perspective on the vast amount of research on bitumen-aggregate adhesion, a synthesis of theories and associated mechanisms was carried out. This work

is presented in a general framework of theories and mechanisms established in adhesion science. This approach is followed to help clarify ideas about these phenomena, stimulating development of new concepts and defining the current research. Due to the complexity of bitumen-aggregate adhesion, these theories or mechanisms can rarely be separated completely from each other. In addition, these discussions are focused on well-established theories and mechanisms, with reference to other factors or possible mechanisms. For example, the effect of binder aging is not discussed in detail, but certainly plays a role in adhesion.

Simple, efficient and reliable measurement of surface energy is an important consideration for implementation of this technology. Different techniques were identified based on their potential to characterize surface energy and its components according to the adopted theory. While the Wilhelmy plate technique and the universal sorption device (USD) have been used previously in this fashion, the sessile drop technique and inverse gas chromatography were selected as alternative techniques for the experimental part of this research. Of the aforementioned techniques, only the USD, a vacuum static vapor sorption technique, was employed for aggregate characterization. While it is possible to characterize aggregate surfaces using other techniques such as inverse gas chromatography, macroscopic heterogeneity of these materials undermines their suitability for this application. Surface energy characterization of five aggregate types and four bitumen types, representing different origins and a range of chemical composition, were performed during this research. The selected materials had been used previously during the Strategic Highway Research Program (SHRP) Research and were obtained from the materials reference library (MRL) in Navada. The motivation for using these materials is that their research history would benefit interpretation of results during this research, simultaneously making surface energy properties available on these well-known materials with which many researchers in this field identify. Aggregates with their respective MRL codes include Georgia granite (RA), sandstone (RG) from Pennsylvania, basalt (RK) from Oregon, Gulf coast gravel (RL) from Texas, and limestone (RD) from Maryland. The different bitumen types according to code and

crude source include AAD-1 from the Californian Coast, AAM-1 from West Texas, ABD from the California Valley, and AAB-1 from Wyoming. As the emphasis of this part of the research was on the techniques, three replicates on each sample were performed to evaluate reproducibility of the methodology employed.

An important objective of this research was to refine the application of the current theory to describe adhesion of bitumen and aggregate in the presence of water. Up to this point, the effect of pH of the water at the bitumen-aggregate interface has not been incorporated with other interfacial factors to assess its affect quantitatively. The first question to address within the context of the current theory is whether the surface energy components of water change at different pH levels. This work was performed in the laboratory of Professor Carel J. van Oss, a co-founder of the theory used in this research, at the State University of New York at Buffalo. Contact angles of water at three different pH levels were measured on electrostatically neutral dextran. Reference measurements were also performed on glass. The generalized theory proposed by van Oss (1994) includes a third term, namely, the free energy of electrostatic interaction (ΔG^{EL}). This term is introduced to account for the effect of overlapping electric double layers of two surfaces in the presence of water. Extension of the expression for the free energy of electrostatic interaction between two identical surfaces, to the interaction between two different surfaces is presented according to Ohshima (1998). Data from electrokinetic experiments obtained by Labib (1992) during the SHRP Program was utilized to calculate the free energy of electrostatic interaction between selected bitumen and aggregate types. These values are compared to the Lifshitz van der Waals (ΔG^{LW}) and the acid-base (ΔG^{AB}) free energy terms calculated from the surface energy measurements conducted during this research. In addition, the electrostatic term allows quantitative assessment of the effect of pH of the water at the interface on adhesion. The latter is illustrated by using data obtained by Labib (1992) as well as data reported on MRL aggregates during the SHRP Program. The selection of materials used in this research facilitated the compatibility between data generated during this research and

aforementioned data. Although no electrokinetic experiments were conducted during this research, detail account of the methodologies followed by Labib (1992) is presented.

ORGANIZATION OF DISSERTATION

This dissertation is organized into six chapters. Chapter I provides a background to research on bitumen-aggregate adhesion and describes the research goal, objectives and scope.

Chapter II synthesizes theories and associated mechanisms of bitumen-aggregate adhesion, which forms the basis for development of the material presented in subsequent chapters.

Chapter III identifies potential techniques for surface energy characterization of bitumen and aggregate and presents the concept and underlying theory of each technique. The applicability of each technique within the context of the adopted surface energy theory is also discussed.

Chapter IV introduces the materials selected for surface energy characterization and explains the experimental methodologies of the selected techniques. Details of the analyses and results are presented.

Chapter V proposes a refined application of the current theory to predict adhesion between bitumen and aggregate in the presence of water. First, the effect of pH on the surface tension components of water is addressed. In addition, the free energy of electrostatic interaction is introduced, which takes the effect of overlapping electric double layers into account and enables the assessment of pH of the interface water on the adhesive bond.

Conclusions of this research and recommendations for future research are outlined in Chapter VI.

CHAPTER II

THEORIES AND MECHANISMS OF BITUMEN-AGGREGATE ADHESION

INTRODUCTION

Based on the background sketched in the first chapter of this dissertation, it is evident that a wealth of research exists on bitumen-aggregate adhesion and the effect of water on the adhesive bond. Apart from a number of fundamental studies published in well-known transportation related journals, a significant amount of work in this regard has also been published sporadically in adhesion science, surface chemistry, and petroleum science journals. The general subject of adhesion science is multidisciplinary, encompassing aspects of engineering, as well as physical and organic chemistry. A very large and diverse technical literature on adhesion exists (Pocius, 1997).

The objectives of this chapter are: to review fundamental theories and associated mechanisms of bitumen-aggregate adhesion by synthesizing this research within the framework of theories generally established in the literature pertaining to adhesion science; to provide experimental evidence supporting these mechanisms; to consider the ability of these theories to place bitumen-aggregate adhesion and moisture damage on a quantitative basis; and to discuss the practical implications for materials and structural design.

Many practical applications of adhesion are based on simply controlling forces between surfaces (Pocius, 1997). The first part of this chapter is therefore devoted to a conceptual description of fundamental forces of adhesion. The theory of (weak) boundary layers, mechanical theory, electrostatic theory, chemical bonding theory, and thermodynamic theory are discussed with reference to bitumen-aggregate adhesion.

FUNDAMENTAL FORCES OF ADHESION

With this section, it is intended to establish a fundamental but conceptual understanding of interaction forces ultimately responsible for adhesion. The material presented is obtained from classical text on surface science (Adamson and Gast, 1997), treatises on adhesion (Good, 1966), and general texts on adhesion science (Pocius, 1997). This will set the stage for further discussions of theories that can be used to explain and in some cases quantify adhesive bonding.

Electrostatic Interactions between Ions

The basis for understanding intermolecular forces is the Coulomb force, which is the electrostatic force between two separated charges. Electrostatic forces play a primary role in the formation of ionic bonds. An ideal ionic bond is formed when a positive ion (cation) and negative ion (anion), as charged particles, attract each other according to Coulomb's law, each acting as a nucleus surrounded by a rigid spherical distribution of electrons. In this process, each ion pair gains classical electrostatic stabilization energy (Companion, 1979). Electrostatic forces in an ionic bond are the strongest forces of interaction and the energy required to break a mole of these bonds are typically in the order of 140 to 250 kcal (Good, 1966).

Electrodynamic Interactions through van der Waals Forces

The forces responsible for the deviation of behavior of a gas from an ideal gas are collectively known as van der Waals forces. J.D van der Waals first developed an equation of state to describe this deviation. Keesom, Debye, and London contributed much to the understanding of these forces, and for this reason, the three interactions are named for them. They include dipole-dipole interactions (Keesom orientation forces), dipole-induced dipole interactions (Debye induction forces), and induced dipole-induced dipole interactions (London dispersion forces). The van der Waals force is the sum of the three interactions. Usually, the London forces dominate (Butt et al., 2003). The

bonds formed by electrodynamic forces are small when compared to ionic or covalent bonds and typically exhibit strengths less than 10 kcal/mol. The potential energy of interaction is inversely proportional to the sixth power of the distance between interacting entities. Even though individual interactions are short-range, these forces are additive through the instantaneous propagation of an electric field and its contribution may be of considerable importance in interactions where large organic molecules are involved (Harter, 1977). Each of the contributing interactions are described in the following paragraphs.

Dipole-Dipole Interactions (Keesom Orientation Force)

Electronegativity is a measure of the ability of an atom to attract electrons and form a bond. A molecular dipole exists when an atom of high electronegativity on one end of the molecule draws electrons to reside more on that end than on the other, resulting in a partial separation of charge. The magnitude of these virtual charges and the distance separating them, characterize a dipole moment. When two dipoles interact, oppositely charged ends of the dipoles attract, while the other ends naturally repel. This changes their relative spatial orientation. The potential of two dipoles to interact, or Keesom potential, is more applicable to systems where free rotation is possible.

Dipole-Induced Dipole Interactions (Debye Induction Force)

In neutral atoms or symmetric molecules, with no dipole moment, the nuclei and electron clouds are attracted in opposite directions when exposed to an electrical field or dipole, i.e. polarization takes place. Molecules have different polarizability, a measure of how tightly the electrons are held, and depend on molecular or atomic volume. A dipole moment is therefore created in the otherwise spherical, symmetric molecule, and this is called an induced dipole.

Induce Dipole-Induced Dipole Interactions (London Dispersion Force)

For two atoms or molecules with spherical, symmetrical charge distribution, London proposed a type of force to explain the attraction between non-polar molecules. Based on the finite probability that, at any instant in time, electrons are all on one side of an atom or molecule with a partially unshielded nucleus on the other side, an instantaneous dipole is created. This process induces an instantaneous dipole in another species and results in forces of attraction. A dispersion force is created by this instantaneous force of attraction averaged over all instantaneous configurations of the electrons in the initial molecule. Apparently, the term "dispersion" comes from the need to quantify the natural frequency of a substance in one of London's earlier theories, and is determined by the dispersion of the refractive index as a function of frequency. Today, dispersion of refraction index is only of historical significance and use of the term "dispersive" is misleading. This type of interaction is fundamental to the study of adhesion, especially in polymeric materials.

In the preceding paragraphs, the interaction between two molecules due to van der Waals forces was described. In the quantitative consideration of such an approach, i.e. a microscopic approach, the influence of neighboring molecules on the interaction between any pair of molecules is ignored. In reality, the polarizability can change due to the influence of a third molecule and the description of additivity using such an approach becomes problematic. The theory of Lifshitz is based on a macroscopic approach and the discrete atomic structure is treated as a continuous material with bulk properties such as dielectric permittivity and refractive index. The problem of additivity is therefore eliminated (Butt et al., 2003). The Lifshitz approach plays an important role in the definition of surface energy components described in the section on Thermodynamic Theory.

Interactions through Electron Pair Sharing

While interactions facilitated by weak electrical forces resulting from oscillating charges is regarded as physical bonding, a union of two species through sharing of an

electron pair is often referred to as chemical bonding. Chemical interactions take place by rearrangement of bonding electrons within the interacting entities in order to establish balanced electron distributions between them. The latter are guided by the electronegativities of the atoms in the structure. Two broad categories of chemical bonding by electron pair sharing are discussed below.

Interaction through Contributions of Electrons from Both Entities

In this type of interaction, each atom contributes one of the shared electrons to form a new molecule. The bond formed in this way is called a covalent bond. A physical accumulation of electrons that occupy overlapping orbitals in space between nuclei takes place. Covalent bonds have directional character and interaction depends strongly on the exact position and orientation of the adsorbate with respect to the surface. Elements, which do not gain or lose electrons to form ions, will form covalent bonds. Covalent bonds and ionic bonds are the strongest type of bonds, with binding energies in the order of 170 kcal/mole. Values as low as 15 kcal/mol have, however, also been reported (Good, 1966).

Interaction through Donation of a Lone Pair of Electrons by a Single Entity

These interactions are also known as donor-acceptor interactions. One of the molecules, the donor, must have at least one unshared or lone pair of electrons. The other molecule, or acceptor, must be electron deficient and will interact with the lone pair from the donor. Bonds formed in this way are called coordination bonds. Unlike ionic and covalent bonds that can be formed between two atoms, a coordinate bond is formed between two molecules or between two ions. They are similar to a covalent bond with partial ionic character and the difference between them is indistinguishable. Compounds formed by these interactions, coordination compounds, consequently represent a whole range of characteristics that lie between covalent and ionic compounds.

Good (1966) describes this type of interaction as acid-base bonding and states that it can be considered weak-electron-sharing bonding. The Brönsted-Lowery and Lewis theories are the most widely accepted bases for describing acid-base concepts. The Brönsted-Lowery theory defines an acid as a substance capable of giving up a proton, and a base as a substance with the tendency to accept a proton. Acids in this theory are limited to hydrogen-containing compounds. According to the Lewis theory, an acid is an electron pair acceptor, and a base is an electron pair donor. The Lewis definition encompasses the Brönsted definition, but does not limit acids to hydrogen-containing compounds (Finston and Rychtman, 1982).

A Lewis acid-base system that forms a strong bond, in the order of 12 to 15 kcal/mole, can be regarded as an ordinary chemical bond. When a weak bond is formed, the system may dissociate readily even though the mechanism of electron sharing is the same as for a strong bond. These weak interactions may contribute significantly to adhesion forces across an interface or cohesion in a single phase.

It is appropriate at this point to introduce hydrogen bonding. This unique type of bonding involves a molecule with a lone pair of electrons to bond with a hydrogen atom, already covalently bonded to another molecule. The hydrogen therefore acts as a bridging atom between two electronegative atoms, holding one by a covalent bond and the other by electrostatic forces (Pimentel and McClellan, 1960). Hydrogen bonding can be described well by the Brönsted-Lowery theory. Naturally, it is also possible to describe this bonding in terms of the more general Lewis acid-base theory (Good and van Oss, 1991).

THEORY OF (WEAK) BOUNDARY LAYERS

This theory is commonly known as the theory of weak boundary layers and states that adhesive bonds fail in either the adhesive or substrate, due to the presence of an interphase region of low cohesive strength. Pocius (1997) reports that adhesion scientists have used this theory as a fallback position for any adhesive bonding situation that cannot be explained by other rationalizations. Early promoters of this theory

suggested that the cohesive strength of a weak boundary layer could always be considered the main factor influencing the level of adhesion. Since then, considerable experimental work has demonstrated that purely interfacial failure does occur (Schultz and Nardin, 1994). Although there is some controversy on how widespread these layers are, their existence is real and cannot be ignored (Brewis, 1992). However, some researchers consider certain types of boundary layers as important contributors to good adhesion (Ensley at al., 1984).

Low molecular weight (and therefore low cohesive strength) contaminants on the surface, such as some organics and water, are a common cause of weak boundary layers. Dusty substrates can prevent effective wetting and therefore intimate contact with the adhesive. Tarrar and Wagh (1992) report that dust on aggregates have a tendency to trap air when mixed with bitumen and consequently weaken the bitumen-aggregate bond.

Podoll and Becker (1991) used Surface Analysis by Laser Ionization (SALI) to examine water debonded surfaces of bitumen and aggregate pairs. This technique essentially produces an elemental depth profile through mass spectrometry. Calculation of the relative abundance of various elements on stripped and unstripped areas indicated that the locations of failure of some bitumen-aggregate pairs occurred on the aggregate side. Weak boundary layers of this nature may be intrinsic to the aggregate used, or can be developed by dissolution of surface complexes (Labib, 1992) or the mineral itself in the presence of water. The latter is dependent on the pH of the contacting water. Cohesive failure due to dissolution of surface layers in carbonates occur at pH levels lower than 6, while dissolution of silica minerals occurs at pH levels greater than about 8 (Jamieson et al. 1995).

Although chemical and physical properties of certain bitumen-aggregate combinations produce compatible, high quality interfacial bonds, other properties should be considered which might lead to the formation of weak boundary layers. Jeon and Curtis (1990) state that surfaces of aggregates exhibiting high porosity can act as molecular sieves, separating high and low molecular bitumen fractions. Phenomonological observation indicates that when absorption occurs, the bitumen

remaining on the outside becomes hard and brittle (Curtis et al., 1993). From the theory of weak boundary layers, it is postulated that a brittle interphase will form due to highly associated polar molecules left behind. This is similar to short term aging where volatiles evaporate during the manufacturing and construction process of hot mix asphalt. Curtis et al. (1993) report that no evidence of selective absorption could be found in separate research studies on this phenomenon.

It can be theorized that brittle, weak, boundary layers may form when the aggregate acts as a catalyst for oxidative aging. Harnsberger (2003) used inverse gas liquid chromatography (IGLC) to obtain interaction coefficients for bitumen model compounds eluted through a column packed with bitumen coated onto aggregate. The retention times of these compounds served as a measure of the degree of interaction. The catalytic effect of aggregate on the oxidation of bitumen was confirmed using this approach.

Ensley et al. (1984) postulated the formation of a structured interphase of bitumen molecules on an aggregate surface. The energy released during the interaction of aggregate submerged in bitumen, was measured using a sensitive microcalorimeter. Results indicated an extended energy release after initial bitumen-aggregate contact. They proposed that the initial peak might reflect the initial layer of molecules that adsorb onto the aggregate surface. The molecules become further polarized when attached to aggregate sites and opposite ends serve as bonding sites for other bitumen molecules. The extended energy release was attributed to the formation of an interphase region around the aggregate by propagation of this polarization mechanism. It was postulated that these layers should reduce water susceptibility and increase the strength of the bond. Ensley and his colleagues showed that the area under the energy-release-curve after two hours and the height of these curves could be related to tender and non-tender mixes. It was therefore argued that the proposed structured interphases increase stability near the bitumen-aggregate interface.

In addition to the formation of an interphase region by propagated polarization, Ross et al. (1991a) postulated that high mix temperatures initiate extensive acid-base complexation, altering and most likely agglomerating bitumen groups into larger,

probably cross-inked assemblies in the boundary region. While brittleness of this region may form a weak layer if too much cross-linking takes place, the aggregated region can form a seal that may inhibit adhesive failure due to water diffusion to the interface. In this research, bitumen-coated aggregate was cooled and then cut to expose the perimeter of interaction. An autoradiographic (AR) procedure was used to identify concentrations of labeled or "tagged" compounds in bitumen that concentrate within boundary regions. Ideally, it was expected that a gradient would be visible from radiographs if migration of the labeled compounds had taken place. The results from these images were, however, negative, suggesting no evidence of an interphase region (Ross, 1991b,1991c). Curtis (1992) supports this conclusion by stating that sampling of the boundary region every 24μm up to a 100μm, showed no differentiation in the chemical composition detectable with infrared analysis. It is also stated that the extended energy release found in earlier work by Ensley could not be reproduced during the SHRP Research. Nuclear magnetic resonance (NMR) spectroscopy, however, did show changes of rigidity within the boundary region for specific bitumen-aggregate systems (Curtis et al., 1993).

MECHANICAL THEORY

Mechanical theory describes the most intuitive adhesion phenomenon and traditionally involves mechanical gripping of the adhesive into the cavities, pores and asperities of the solid surface on a macroscopic scale (Allan, 1992; Schultz and Nardin, 1994). Improved adhesion through mechanical effects is rationalized by Pocius (1997) as follows:

- Physical "lock and key": The lock and key effect when the adhesive phase penetrates a pore in the solid substrate with consequent physical anchoring, is not difficult to visualize. Any movement of the two phases is restricted unless the adhesive plastically deforms and acts as an energy absorbing mechanism yielding an apparent increase in adhesive bond strength.
- Redistribution of stresses: Surface roughness prevents an abrupt plane of stress transfer. Rather, stresses are transferred across or into the adhesive, which in most cases

exhibits viscoelastic and plastic flow properties. The roughness therefore promotes energy dissipation around the crack tip and in the bulk by utilizing the properties of the adhesive.

- Increased surface area: Surface roughness also improves adhesion purely due to an increase in physical area of contact. The sum of interactions, as discussed in the previous section, increases by an amount proportional to the surface area.

McBain and Hopkins (1925) are generally considered the founders of the mechanical theory in the field of adhesion science (Allan, 1992; Schultz and Nardin, 1994; Packham, 1998). Interestingly, the two researchers (McBain and Hopkins, 1929) also contributed to relate adhesion between bitumen and aggregate to the surface characteristics of the aggregate, as reported by Hicks (1991) in his review of the literature. It is generally accepted that aggregates with a porous, slightly rough surface will promote adhesion by providing for a mechanical interlocking effect. However, the surface texture of an aggregate also affects its coatability, or wettability, in that a smoother surface coats easier than a rough surface (Tarrar and Wagh, 1992). In addition, wettability, including filling of pores, also depends on the viscosity of the binder and surface chemistry of both aggregate and bitumen. While many researchers postulate that surface texture of the aggregate is the main factor affecting adhesion (Kiggundu and Roberts, 1988) others report that chemical and electrochemical effects dominate (Yoon and Tarrer, 1988).

Many engineering surfaces are fractal, and possess similar structures over a range of scales. An analogy often used is a coastline, which might appear similar under successive magnifications. The assumption that this similarity is exact, is the basis of fractal analysis (Adamson and Gast, 1997). Particle form, angularity, and surface texture of aggregates were analyzed in recent years using imaging techniques. An aggregate imaging system (AIMS) has been used at Texas Transportation Institute for the characterization of these properties irrespective of size. A unique feature of this system is the ability to capture texture through wavelet analysis of black and white images. In wavelet analysis, signals or images are decomposed at different resolutions

to obtain different scales of texture. Surface texture essentially captures the surface irregularity at a scale that is too small to affect the overall shape (Chadan et al., 2004). Masad et al. (2004) obtained the texture of limestone, gravel and granite utilizing this imaging technique. The texture for fine fractions and coarse fractions were found to be different with all aggregates. The researchers presented an anisotropic viscoplastic continuum mechanics model, which was used to fit experimental data from compressive triaxial tests conducted at different confining pressures. One of the model parameters, a work-hardening parameter, $\bar{\kappa}$, represents the effect of adhesion between the binder and aggregate or cohesion within the binder. In Figures 1 and 2, the relationship between this parameter and aggregate texture suggests that it primarily represents adhesion in the mixture. In addition, it is shown that $\bar{\kappa}$ increases with an increase in applied pressure; the texture index of the fine fraction correlates with the initial $\bar{\kappa}$ at 1 percent viscoplastic strain, while the texture for the coarse aggregate correlates with the final $\bar{\kappa}$ at 8 percent viscoplastic strain. The coarse fraction of granite exhibits the highest texture index and, accordingly, the highest final $\bar{\kappa}$ value.

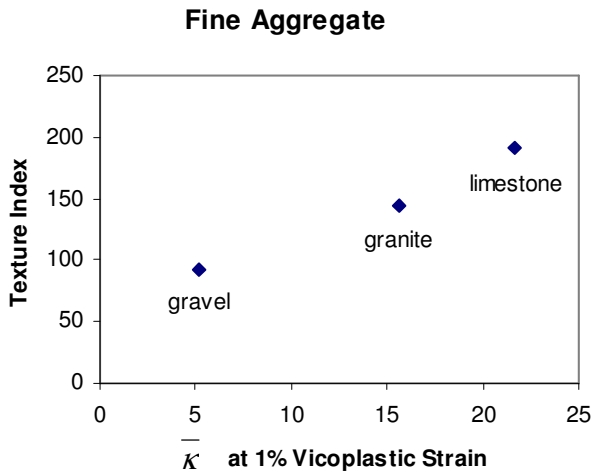

Figure 1. Relationship between the hardening model parameter and fine aggregate surface texture. Data from (Masad et al., 2004).

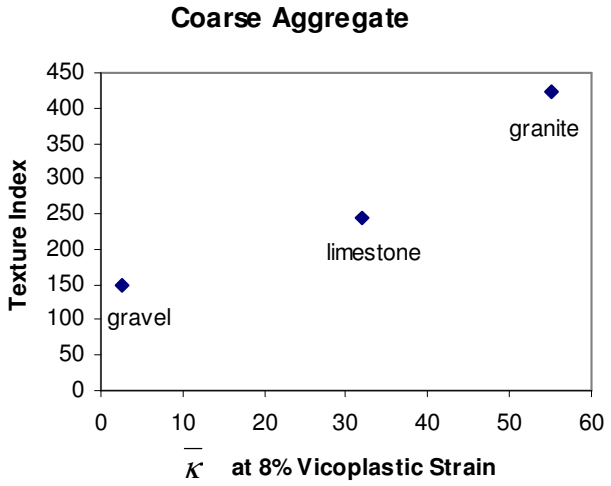

Figure 2. Relationship between the hardening model parameter and coarse aggregate surface texture. Data from (Masad et al., 2004).

Although the effect of surface chemistry of the materials cannot be excluded, these correlations suggest that the fine fraction, with higher surface area, dominates initial resistance to lower induced shear strains, while coarse aggregate supposedly forms a more stable phase at higher induced shear strains and controls adhesion under these conditions.

The mechanical theory not only applies on a macroscopic scale but also on a microscopic scale. These studies are normally performed using scanning probe microscopy techniques. The surface forces apparatus (SFA) and atomic force microscope (AFM) measure normal and frictional surface forces by detecting vertical or torsional deflection, respectively, of a flexible cantilever scanned over the substrate under consideration. Discussions on determining the relationship between friction at a molecular level, and adhesion appear in the literature. Extensive experimental work has been done with the SFA (Israelachvili et al, 1994) and AFM (Tsukruk and Bliznyuk, 1998). Houston and his colleagues developed and used the prototype interfacial force

microscope (IFM) extensively to quantify friction on a molecular level due to mechanical effects (Houston and Kim, 2002). Pauli (WRI, 2003a) characterized bitumen films solvent-cast onto glass slide substrates by AFM. TappingMode™ AFM height and phase-contrast imaging was employed. In this application, the probe-tip is oscillated at a resonance frequency characteristic of the cantilever, above the sample, only contacting the sample briefly in each oscillation cycle. Images are produced by capturing vibration changes of the cantilever due to interactions between the cantilever tip and the surface. Figure 3 is a typical image depicting a topographic (height) image on the left and the coinciding phase image on the right hand side of the figure.

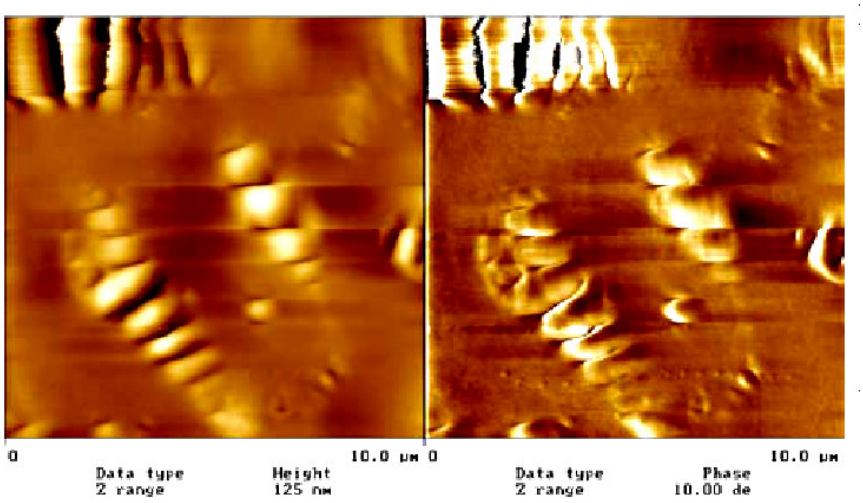

Figure 3. AFM height and phase-contrast imaging showing "bee structures" on bitumen surfaces (with permission from A.T. Pauli, WRI)

So-called "bee" structures appear in most of the discontinuous patches and are responsible for surface undulations covering several square microns of surface area. Friction force measurements indicated two distinct phases of material at the surface interface based on feature hardness. It is hypothesized that these morphological features

at the air-bitumen interfaces are due to associations of asphaltenes, along with other polar species, which nucleate by transport of material from the bulk of the film through a thermal gradient. Ongoing research at the Western Research Institute in Wyoming (USA) attempts to relate this to the adhesive nature of bitumen in asphalt mixtures.

ELECTROSTATIC THEORY

Solid surfaces can be characterized as electropositive or electronegative. This can be attributed to assemblies of atoms having an electronegative character and the consequent formation of molecular dipoles as previously discussed. Derjaguin, in 1955, proposed that essentially all adhesion phenomena could be explained by electrostatics. He considered, in particular, the peeling of a pressure-sensitive tape from a rigid substrate and the subsidiary phenomena of noise and emission of light, which accompany the separation. Essentially the electropositive material donates charge to the electronegative material thereby creating an electric double layer at the interface. Derjaguin analyzed the system as a capacitor. During interfacial failure of the system, separation of the two plates of the capacitor leads to an increasing potential difference up to a point where discharge occurs. The adhesive strength can therefore be attributed to the strength required to separate the charged surfaces in overcoming the Coulombic forces (Lee, 1991; Pocius, 1997; Schultz and Nardin, 1994). This theory has been disputed by others in the past. Studies by Roberts (1977) on rubber adhesion indicated that the contribution of the electrostatic component is usually in the order of 0.1 to 1 percent. A schematic illustration of the formation of an adhesive bond due to charge transfer is presented in Figure 4.

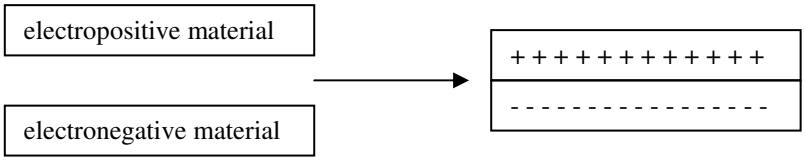

Figure 4. Formation of electric double layer by charge transfer between two surfaces (Pocius, 1997)

More importantly, most surfaces are charged in the presence of water. This is due to the high dielectric constant of water, which makes it a good solvent for ions. Surface charges cause an electric field, which attracts ions. The layer of surface charges and counter ions is called an electric double layer. This concept is illustrated in Figure 5.

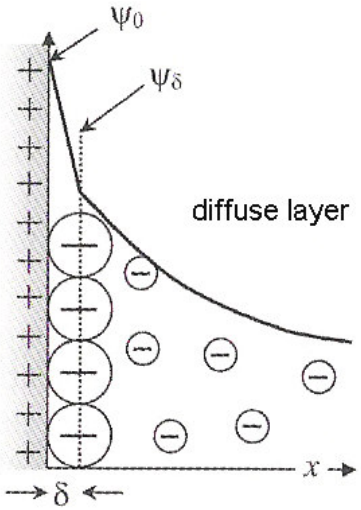

Figure 5. Schematic illustration of the Stern layer with thickness δ (Butt et al. 2003)

Much like a plate capacitor, considered above, the counter ions bind directly to the surface to neutralize the surface charges in the form of a molecular monolayer, referred to as the Helmholtz layer. An extended and more realistic view of this situation is to consider the layer a diffuse layer due to thermal fluctuations, which tends to drive the counter ions away from the surface, also called the Gouy layer. Stern combined the ideas of Helmholtz and Gouy and divided the double layer into two parts, namely the inner part or Stern layer, and the outer part or Gouy (diffuse) layer. The Stern layer consists of one or more layers of ions and liquid molecules adsorbed directly and more or less tightly to the charged surface, therefore immobile. The diffuse layer, on the other hand, consists of mobile ions. Consequently, a shear plane exists which is often not directly at the interface and only at some distance δ do the molecules start to move. The electric potential at this distance is called the zeta potential and can be measured using electrokinetic techniques. The concentration of potential-determining ions (PDI) or pH (log of inverse of hydrogen ion concentration) at which the zeta potential is zero, is defined as the isoelectric point (IEP). The point of zero charge (PZC), on the other hand, is the pH at which the charge at the surface is zero (Butt et al., 2003). The study of charge particles in motion in an electric field is called electrophoreses.

Electrophoreses has been applied to bitumen-aggregate systems in the past to explain moisture damage, or stripping, in these systems (Scott, 1978; Yoon and Tarrar, 1988; Labib, 1992). However, the existence of bulk water, hydrogen bonded to the aggregate surface in the "dry" state, should not be overlooked. Thelen (1958) conducted experiments on quartz to demonstrate how fresh aggregate adsorb a water layer several molecules thick. The data in Figure 6 clearly illustrates the importance of aggregate preconditioning as part of the hot-mix asphalt manufacturing process. Nevertheless, at conventional plant mix temperatures at least a molecular layer of water would remain, requiring about a 1000˚C to drive it completely off the surface.

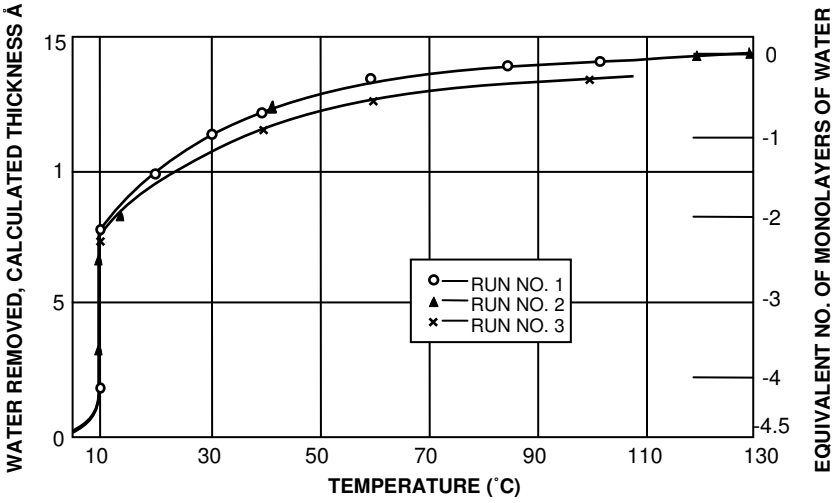

Figure 6. Removal of adsorbed water molecules by heat from quartz (Thelen, 1958)

From the foregoing discussion, pH can be expected to play a role by influencing surface charge. Two aspects should be considered with regard to bitumen-aggregate systems. The first is diffusion of external water to the bitumen-aggregate interface (Fromm, 1974; Nguyen et al., 1992; Cheng, 2002). The pH of this water will differ depending on the environment. Secondly, researchers in the past found that pH of interface water are influenced by the aggregate surface (Yoon and Tarrer, 1988; Labib, 1992; Scott, 1978; Huang et al., 2000). Figure 7 shows typical relationships for the changes of pH values when different aggregate powders are added to water. These relationships reveal that many aggregate surfaces tend to increase the pH of the contacting water. This is not restricted to basic rock types (e.g. limestones), but also occurs with acidic mineral composites (e.g. granites). These phenomena are described in more detail under the section on development of surface charges below.

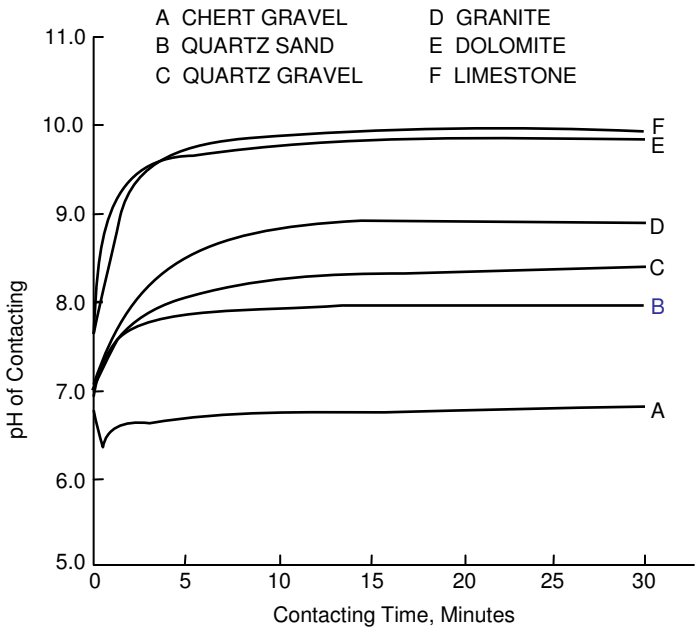

Figure 7. Changes in pH of water in which aggregates were immersed (Yoon and Tarrer, 1988)

If two surfaces approach each other and electric double layers overlap, an electrostatic double-layer force arises (Butt et al., 2003). Labib (1992) developed interaction diagrams between several aggregates and bitumen types based electrokinetic measurements in the form of zeta potential versus pH curves as depicted in Figures 8 and 9. Figure 8 is an interaction diagram for quartz-based granite, SHRP Materials Reference Library code RJ, and four types of bitumen. The isoelectric point for all the bitumen types as well as the granite is around three, i.e. both bitumen and aggregate are negatively charged at pH > 3. This indicates that under dry conditions (pH ≈ 7, proposed by Labib) the propensity for adhesion is low and in wet conditions (pH ≈ 10) both surface types are strongly negative. This condition is expected to lead to repulsion and therefore stripping.

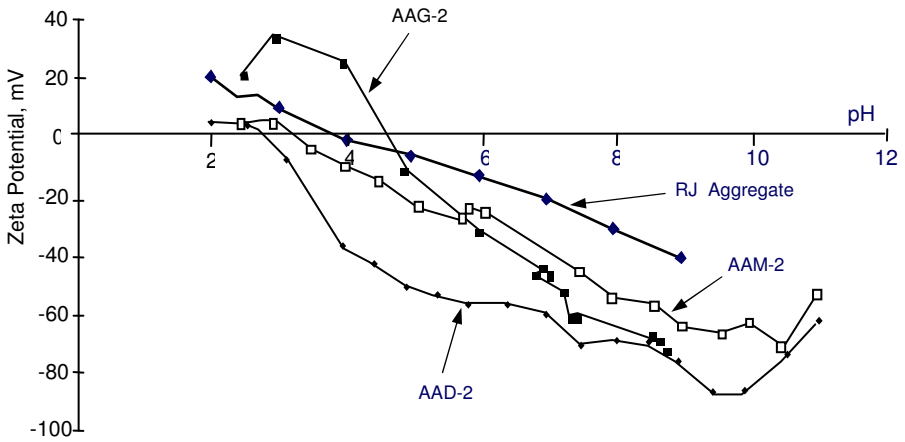

Figure 8. Interaction diagrams for granite aggregate (RJ) with bitumen (Labib, 1992)

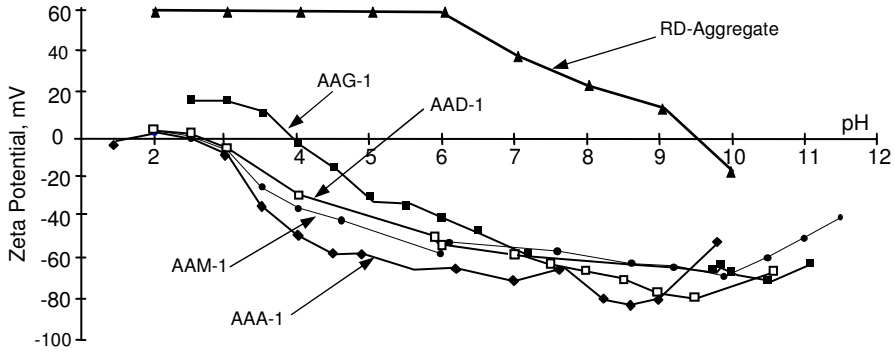

Figure 9. Interaction diagram for limestone aggregate (RD) with bitumen (Labib, 1992)

Figure 9 is an interaction diagram for calcite-based RD limestone and four bitumen types. This diagram reveals that at dry conditions (pH ≈ 7), the bitumen and aggregate surfaces have opposite charges. In the presence of water (pH ≈ 10), the interaction significantly decreases due to negative charges that develop in the aggregate and consequently develop a propensity for repulsion.

Development of Surface Charges

The mechanisms of charge development presented below describe the creation of fundamental forces of adhesion, which also serve as a molecular description for the concept of surface free energy. The chemical groups resulting in charge can also be regarded as function groups (Johnston, 1996), as discussed under Chemical Bonding Theory. The general mechanisms of charge development on aggregate surfaces as discussed by Mertens and Wright (1959) are presented in the following paragraphs.

Limestone, mainly comprised of calcium carbonate (the mineral calcite, $CaCO_3$), is known to have electropositive surface characteristics. When the aggregate is fractured, electrostatic bonds are broken and unsatisfied charges of calcium and carbonate ions occur on the newly formed surfaces. The following simplified reaction describes the fracturing process with the consequent formation of countless unsatisfied charges.

$$Agg - Ca - CO_3 - Ca - Agg \rightarrow \left(Agg - Ca^{+}\right) + \left(Agg - Ca - CO_3^{-}\right)$$

Where *Agg* represents the bulk aggregate structure, with atomic lattice constituting the $CaCO_3$ rhombohedral unit cell, and intermolecular bonds represented by " – ". Water vapor adsorbs instantaneously onto the aggregate to satisfy broken bonds. The hydration reaction that takes place is given by

$$\left(Agg - Ca^{+}\right) + \left(Agg - Ca - CO_3^{-}\right) + H_2O \\ \rightarrow \left(Agg - CaOH\right) + \left(Agg - Ca - CO_3H\right)$$

where unsatisfied calcium ions adsorb hydroxyl groups (OH-groups), and tend to further adsorb carbon dioxide dissolved in surface water ($CO_2 + H_2O \rightarrow H_2CO_3$). An additional reaction takes place.

$$\left(Agg - CaOH\right) + H_2CO_3 \rightarrow \left(Agg - Ca - CO_3H\right) + H_2O$$

Therefore, regardless of the type of charge present immediately after fracture, the final structure on the site of each charge is represented by the right side of the reaction. In the presence of water, this structure dissociates to produce a characteristic electropositive charge on the limestone surface.

$$(Agg - Ca - CO_3H) \rightarrow (Agg - Ca^+) + (HCO_3^-)$$

The following processes are typical for metal oxides. Silica (SiO_2), essentially pure mineral quartz, makes up a large portion of aggregates such as quartzite and granite. Upon fracturing, creation of unsatisfied charges can be presented in a simplified way

$$Agg\begin{Bmatrix} -O \\ -O- \\ -O \end{Bmatrix} Si - O - Si \begin{Bmatrix} O- \\ -O- \\ O- \end{Bmatrix} Agg \rightarrow \left(Agg\begin{Bmatrix} -O \\ -O- \\ -O \end{Bmatrix} Si^+ \right) + \left(Agg\begin{Bmatrix} -O \\ -O- \\ -O \end{Bmatrix} SiO^- \right)$$

where *Agg* represents the bulk aggregate structure, with atomic lattice constituting silicate tetrahedron (Si coordinated to four oxygen atoms) unit cells. As before, a hydration process occurs in response to the unsatisfied charges. Chemical adsorption of water takes place as H_2O is dissociated into H^+ and OH^- during adsorption to form a hydroxilated surface (covered with OH, called silanol groups on these surfaces). Further adsorption of water results in layers of hydrogen-bonded water (as illustrated in Figure 6), of which the outer layer is in equilibrium with water vapor in the air and approximately exhibits the same properties as free water at ambient temperature.

$$\left(Agg\begin{cases} -O \\ -O-Si^{+} \\ -O \end{cases} \right) + \left(Agg\begin{cases} -O \\ -O-SiO^{-} \\ -O \end{cases} \right) + H_2O$$

$$\rightarrow \left(Agg\begin{cases} -O \\ -O-Si-OH \\ -O \end{cases} \right) + \left(Agg\begin{cases} -O \\ -O-Si-OH \\ -O \end{cases} \right)$$

The mechanism that is often associated with the characteristic electronegative charge on silica surfaces is presented below. In this process, charge on these hydroxilated surfaces develops through dissociation of the surface hydroxyl groups, imparting protons to the contacting water.

$$Agg\begin{cases} -O \\ -O-Si-OH \\ -O \end{cases} \rightarrow \left(Agg\begin{cases} -O \\ -O-SiO^{-} \\ -O \end{cases} \right) + H^{+}$$

Examples of other groups on mineral surfaces that dissociate to form charges are carboxyl, sulfate, and amino groups. Adsorption of H^+ and OH^- ions can also lead to charges on these surfaces. The extent to which these reactions proceed depends on the pH of the water in contact with the mineral surface. Water with a high pH (high concentration of OH^- ions) stimulates the dissociation of silanol groups, and therefore causes the surface to become more negatively charged. At low pH levels, silica surfaces can be positively charged (Gast, 1977; Butt et al., 2003). Although the reaction above implies that release of protons into the water should lead to a reduction in pH, Figure 7 suggests that the pH increases with time. Scott (1978) and Yoon and Tarrer (1988) ascribe this phenomenon to hydrolyses of compounds on the aggregate surfaces containing alkaline earth metals such as sodium, potassium, calcium, and magnesium. In the following reaction, the silicate lattice reacts with water to release excess hydroxyl ions.

$$Agg\begin{cases} -O \\ -O-Si-O-Na \\ -O \end{cases} + H_2O \rightarrow Agg\begin{cases} -O \\ -O-SiOH \\ -O \end{cases} + Na^+ + OH^-$$

Mertens and Wright (1959) continue to explain that natural aggregate surfaces contain elements that cause both electropositive and electronegative features. Basalts, diorites and siliceous limestones are examples of intermediate aggregates. Figure 10 classifies aggregates according to surface charge, based on silica and alkaline or alkaline earth oxide content.

Clay minerals have a different mechanism of charge development. Mica, which can be considered a 2:1 clay (one plate of aluminum octahedra sandwiched between two plates of silica tetrahedra), is a common mineral in igneous and metamorphic rocks. The charges on micas generally come from structural imperfections due to ion substitution (called isomorphous substitution) or site vacancies during mineral formation. These surfaces are completely polarizable. Although the charges from a given substitution may theoretically be positive or negative, for the 2:1 clay minerals, ion size limitations generally result in a substitution of cations of lower valence for those of higher valence resulting in a negative net charge on the clay structure (Gast, 1977). Hydroxyl groups are also present on the edges of clay structures, which lead to a pH dependent charge in the presence of water. Most of the charges are associated with the plates and consequent dissolution of cations in the presence of water and replacement by others, depending on the ion exchange capacity of the clay, i.e. depletion of positive charge on the mineral surface. This leads to a relatively constant charge in the presence of water, which is not significantly pH dependent (Butt et al., 2003).

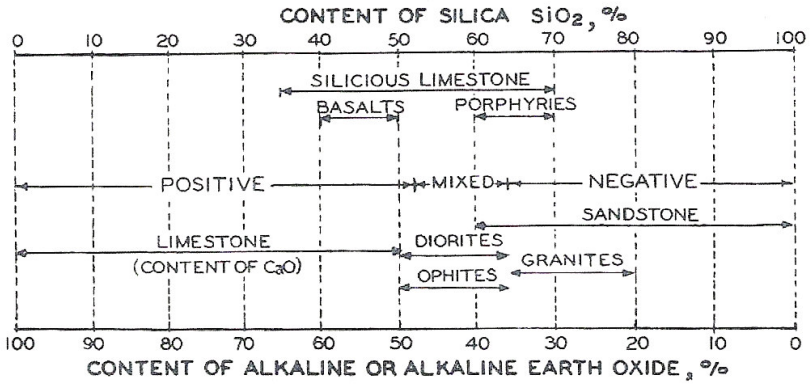

Figure 10. Classification of aggregates (Mertens and Wright, 1959)

In bitumen, carboxylic acid for example (R-COOH, where R represents non-polar hydrocarbon alkane chains) is a chemical functional group that plays an important role in the adhesion process. In the presence of water, the molecule separates into a carboxylate anion ($R\text{-}COO^-$) and the proton (H^+) causing the bitumen surface to have a negative charge. The increase in the pH of the contacting water increases the extent of dissociation of the acid molecules (Yoon and Tarrar, 1988).

CHEMICAL BONDING THEORY

Foregoing discussions on fundamental forces of adhesion introduced the concepts of physical and chemical bonding. Although the processes of chemisorption and physisorption are often characterized based on several features, they are not as distinguishable as it may seem (Kolasinski, 2002; Butt et al., 2003). Broader terms such as primary and secondary interactions are sometimes used to refer to these stronger and weaker interactions, respectively. In this section, the chemical bonding theory will include typical interactions between bitumen and aggregate that are specific in nature, as opposed to non-specific interactions. The traditional view of chemical bonding in

bitumen-aggregate systems that these bonds produce new compounds upon formation (Kiggundu and Robberts, 1988; and Tarrar and Wagh, 1990) is discussed.

Molecular species in bitumen primarily consist of long carbon chains and rings saturated with hydrogen, which are essentially non-polar in character (Little and Jones, 2003). These are the lightweight, oily or waxy fraction in bitumen (Robertson, 2000) called alkanes, paraffins, or aliphatic compounds. The inert character of these molecules stems from the fact that they are saturated, made up exclusively from single C-H and C-C bonds, with relatively balanced electron distributions and therefore little tendency to move around. These non-polar molecules interact mainly through van der Waals forces (McMurry, 2000). Because van der Waals forces are additive, their contribution in these large molecules is significant. While active chemical sites on aggregate surfaces promote bonding of particularly polar species in bitumen, covering of these sites by non-polar hydrocarbons can completely mask their activity (Curtis, 1992). During mixing at high temperatures, however, more polar species should equilibrate with the surface and displace the more weakly adsorbed and non-polar components on the aggregate surface (Petersen et al., 1982).

Bitumen-aggregate interaction chemistry is highly complex and variable among different systems primarily due to the complex and variable composition of the materials involved (Petersen et al., 1982). The polar molecules in bitumen exhibit specific points (sites), which interact with specific sites within the bitumen (Robertson, 2000) and on aggregate surfaces. “Active sites”, is a term used to describe reactivity of macromolecules and also the surfaces of minerals, and implies a process wherein a surface chemical reaction of interest is promoted by a molecular-scale feature on the organic or mineral surface, i.e. surface functional groups (Johnston, 1996). Bitumen and aggregate functional groups are discussed below, followed by a discussion of typical reactions that might take place during bitumen-aggregate bond formation.

Bitumen Functional Groups

Although bitumen is comprised of non-polar hydrocarbons; heteroatoms such as nitrogen (N), sulfur (S), and oxygen (O) may also exist as part of these molecules. Trace amounts of metals are also present and are considered "fingerprints' of the crude source (Robertson, 2000). These atoms introduce polarity into bitumen molecules and although only present in small amounts, have a controlling effect on the properties of the bitumen and its interaction with aggregate surfaces (Petersen et al., 1982). Petersen (1986) has identified polar, strongly associated functional groups in bitumen. Figure 11 shows the chemical structures of important functional groups in natural bitumen including those formed during oxidation.

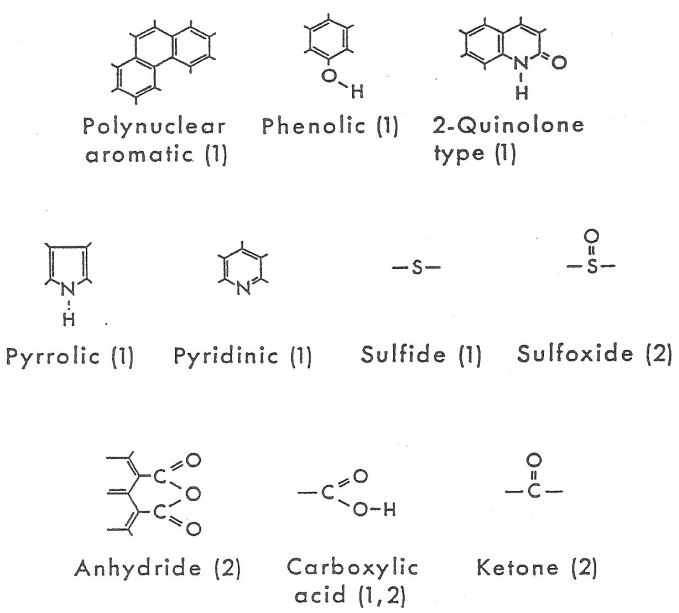

Figure 11. Examples of important chemical functional groups [1] naturally occurring and [2] formed on oxidative aging (Petersen, 1986).

Benzene-like, unsaturated ring structures are common hydrocarbon compounds in crude oil, and along with alkanes, are typical constituents in the molecular make-up of bitumen (McMurry, 2000). According to the historical micellar model, resins and ultimately asphaltenes represent the more polar fractions in bitumen. These fractions are also the higher molecular weight, or larger molecular size fractions. An asphalt (bitumen) model based on non-polar and polar species, derived from molecular size distribution has largely replaced the historic micellar model during Strategic Highway Research Program Research (SHRP) (Robertson, 2000).

Many of the studies on bitumen-aggregate interaction focused on the affinity of different bitumen functional groups for aggregate surfaces. Adsorption of bitumen model compounds, representing specific functional groups in bitumen, has been conducted by researchers including Plancher et al. (1977), Petersen et al. (1982), Curtis et al. (1989), Arderbrant and Pugh (1991a), Brannan et al.(1991), and Park et al. (2000). Relative affinity of functional groups for aggregate surfaces and their relative displacement by water are generally presented in these studies. Although rankings differ depending on the type of aggregate, or sometimes model-aggregate, similar general trends are obtained. Table 1 summarizes selected findings for the average affinity of bitumen functional groups for aggregates, as well as their susceptibility for displacement by water.

The importance of Table 1 is not the exact order, but rather the observation that these groups, which are most strongly adsorbed on aggregate surfaces, are also those displaced most easily by water. This observation emphasizes the fact that the influence of moisture on the durability of bitumen- aggregate bonds should be of primary concern from the starting point. Although minor components in bitumen, it is essentially the acidic components such as carboxylic acids, anhydrides, and 2-quinolone types that are the most highly concentrated in the adsorbed fraction. This is inline with the fact that bitumen generally exhibits an excess amount of acidic compounds compared to the amount of basic organic compounds (Morgan and Mulder, 1995).

Table 1. General affinity of bitumen functional groups for aggregate surfaces

Plancher et al. (1977)[1]	**Petersen et al. (1982)[1]**	**SHRP (Curtis and co-workers)[2]**
Most strongly adsorbed functional groups (decreasing order)		
Carboxylic acids Anhydrides 2-Quinolones Sulfoxides Pyrridine types Ketones	Carboxylic acids Anhydrides Phenols 2-Quinolones Sulfoxides Ketones Pyrridine types Pyrrolic	Carboxylic acids Sulfoxides Pyrridine types Phenolic Pyrrolic Ketones
Susceptibility of adsorbed functional groups for water displacement (decreasing order)		
Carboxylic acids Anhydrides Sulfoxides Pyrridine types 2-Quinolones Ketones	Anhydrides 2-Quinolone types Carboxylic acids Pyrridine types Sulfoxides Ketones Phenolic Pyrrolic	Sulfoxides Carboxylic acids Pyrrolic Ketones Pyrridine types Phenolic
[1] Review by Petersen and Plancher (1998) [2] Reported by Jamieson et al. (1995)		

Petersen and Plancher (1998) state that the two chemical functionalities, carboxylic acids and sulfoxides, account for almost half of the total chemical functionality in the strongly adsorbed fractions. These compounds are both hydrophillic (water loving), with aliphatic structures (zigzag chains as opposed to aromatic ring structures) with no other polar functional groups on the same molecule (mono-functional as opposed to poly-functional). This may contribute to their ease of displacement by water. Poly-functional bitumen molecules are more strongly adsorbed. Typical poly-functional molecules contain ketones, anhydrides, and nitrogen. Certain nitrogen compounds such as pyridine and pyrrolic types, as well as phenolics are strongly adsorbed as suggested by water displacement studies. Desorption by solvents such as pyridine may not always produce reliable extraction of some of these strongly adsorbed chemical functionalities. The significance of adsorbed pyridine on aggregate surfaces was demonstrated by Petersen and Plancher (1998) by thermal desorption experiments. Pyridene could neither

be desorbed at 240˚C, nor be displaced by water. In these studies, pyridine mimicked the basic nitrogen compounds in bitumen as well as the actions of common amine anti-stripping agents. Results suggest that it does matter which functional group bonds with the aggregate surface first. When the carboxylic acid model compound was coated onto the aggregate first, pyridine was readily displaced by water. Jamieson et al. (1995) report that competitive adsorption studies by quadric-component solutions of model compounds did not have a significant effect on the order of rank presented in Table 1.

Aggregate Functional Groups

Aggregates are composed of an assemblage of one or more minerals, which have a definite chemical composition and an ordered atomic arrangement. In these arrangements, or atomic lattices, each atom is bound to neighboring atoms through electrostatic coordination bonds. When aggregates are crushed or cleaved, the new surface atoms are deprived of some of their neighboring atoms and some of the coordination bonds are broken. These atoms seek to form new coordination bonds to replace the old broken ones (Thelen, 1958). This molecular description serves as the basis for development of surface charge, previously described, as well as the concept of surface free energy, discussed subsequently as part of the thermodynamic theory. New coordination bonds can be formed by directing some of the forces inward with consequent orientation adjustment of the crystal lattice as the atoms are pulled closer. Another way to satisfy the broken bonds is to attract contaminants such as water and organics to the surface also serving as bonding sites for functional groups in bitumen.

Functional groups, bonding sites, or active sites on aggregate surfaces have not received as much attention as bitumen by researchers in this field. Silica is the most widely used surface in these studies due to its natural abundance and its association with moisture damage (Curtis et al., 1989; Ardebrant and Pugh, 1991a; Ernstsson and Larsson, 1999; Park et al., 2000). Petersen and Plancher (1998), in their review of the literature, provided insightful reference in this regard. Active sites on these surfaces range from surface hydroxyl groups of varying acidities to hydrogen bonding sites of

high acidity. Strong electropositive Lewis acid bonding sites are typically formed on minerals where metals, such as magnesium, iron and calcium, are present. Oxygen in silica and other minerals can act as Lewis base sites. In addition to providing adsorption sites for many bitumen functionalities, oxide and hydroxyl surface functional groups act as strong adsorption sites for water molecules. In turn, water serves as bonding sites for organic molecules as mentioned above. The latter can be bitumen or organic contaminants that may replace or cover adsorbed water molecules when aggregates are exposed to the environment over time. It has been reported that aggregate stored for long periods were found to resist stripping better than freshly cleaved rock (Endersby et al., 1947; Thelen, 1958).

Jamieson et al. (1995) report that in general, chemical sites on aggregate surfaces associated with high affinity for bitumen include elements such as aluminum, iron, magnesium and calcium. Elements associated with low bonding affinity include sodium and potassium. The role of aggregate physical and chemical properties on net adsorption test results, including eleven aggregates and three bitumen types from the SHRP Materials Reference Library (MRL), was evaluated by stepwise regression analysis. Five aggregate variables were investigated as summarized in Table 2.

Table 2. Physical and chemical properties of aggregates on net adsorption (Jamieson, 1995)

Variable influencing Net Adsorption	**Correlation Coefficient**
Potassium oxide	0.48
Surface Area	0.71
Calcium Oxide	0.75
Zeta Potential	0.87
Sodium Oxide	0.90

The correlation coefficient of 0.9 indicates that the net adsorption is primarily a function of aggregate properties. This is in line with the common finding that adhesion in bitumen-aggregate systems is dominated by the properties of the aggregate. The increased order of impact is therefore, potassium oxide, surface area, calcium oxide, zeta potential, and sodium oxide. While these results corroborate the impact of alkali metals (K and Na) and calcium, it also shows that part of the adsorption-desorption action can be explained by zeta potential, as previously discussed.

The contribution of surface area suggests availability of more active sites per unit mass of aggregate for interaction. In this regard, Petersen et al. (1982) illustrated that surface site density on aggregates is also important. The relationship between aggregate surface area and percentage strongly adsorbed fraction is furnished in Figure 12. Although the Montana and the Colorado aggregates adsorbed almost the same amount of strongly adsorbed functionalities, the Colorado aggregate has a surface area four times that of the Montana aggregate. The researchers conclude that the Montana aggregate has a higher density of adsorption sites. It is mentioned that this may also be observed when adsorption sites are not accessible due to steric hindrance of the bitumen functional groups.

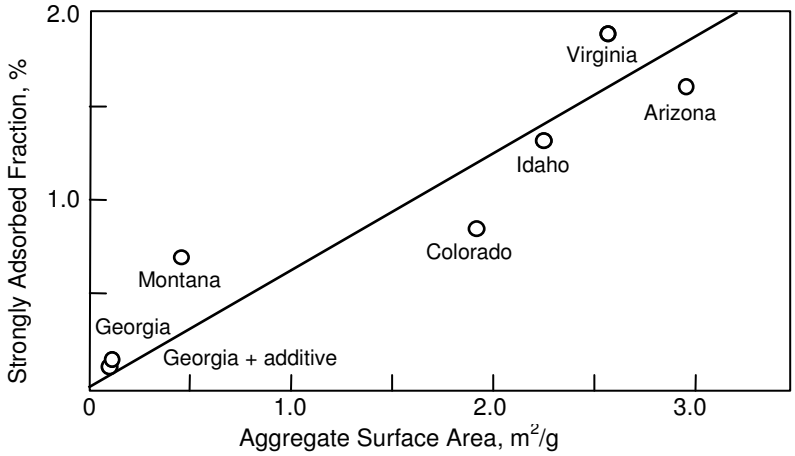

Figure 12. The importance of active site density, in addition to surface area (Petersen at al., 1982).

Bitumen-Aggregate Interaction

Having introduced the key chemical functionalities and prominent research with respect to bitumen-aggregate interaction, our interest in the following paragraphs is to present particular mechanisms of interactions responsible for adhesion between bitumen and aggregate.

As previously stated, the chemical bonding theory holds that reactive components, also termed radicals, in the adhesive and substrate react to form a compound. The concepts of acids and bases was introduced previously. The generalized Lewis acid-base reaction can be represented by,

$$A + : B \rightarrow A: B$$

Where *A* is a Lewis acid, an electron pair acceptor, or generalized acid. *B* is a Lewis base, or electron pair donor, identical to a Brönsted base. The species *A: B* may be called a coordination compound, adduct, or an acid-base complex. Most cations are Lewis acids, and most anions are bases. The salts are therefore automatically acid-base complexes (Pearson, 1968). This is a generic reaction often discussed in literature on adhesive bonds. Hubbard (1938) postulated that the presence of acidic and basic components in bitumen-aggregate systems react to form a water-insoluble compound. As previously discussed, this theory is generally accepted as the chemical reaction or bonding theory in bitumen-aggregate adhesion.

The review of functional groups and their potential significance in bond formation reveals that carboxylic acids play a prominent role. While carboxylic acids often occur only in trace amounts in bitumen, they are usually significant contributors to the strongly adsorbed fraction. Research by the Western Research Institute in Wyoming (USA) under a Federal Highway Administration (FHWA) contract has continued to explore the mechanism of acid-base complex formation and its effect on moisture sensitivity of laboratory-prepared mixes (WRI, 2003a). This study focused primarily on the role of carboxylic acids in moisture damage. Calcium carbonate reacts with carboxylic acids in

bitumen, which are weak acids (Logaraj, 2002). At temperatures at which hot mix asphalt is produced, an insoluble salt of carboxylic acid, water, and carbon dioxide are formed. This process is described by the first reaction presented below.

$$CaCO_3 + 2RCOOH \rightarrow \left(RCOO^-\right)_2 Ca + H_2O + CO_2$$

$$Ca(OH)_2 + 2RCOOH \rightarrow \left(RCOO^-\right)_2 Ca + 2H_2O$$

$$CaO + 2RCOOH \rightarrow \left(RCOO^-\right)_2 Ca + H_2O$$

When hydrated lime (or calcium hydroxide, $Ca(OH)_2$) is present in the absence of carbonates, water is the only reaction product formed. Logaraj (2002) states that when aggregates are exposed to a direct flame in the hot-mix plant, at least for a brief moment, temperatures up to 700˚C can be encountered. Under these conditions, the calcium carbonate surface could decompose into calcium oxide (CaO, or quick lime) and carbon dioxide. Furthermore, calcium oxide, which is a strong base would react instantaneously with acids in bitumen, depicted in the reactions shown above.

Another series of experiments by WRI researchers focused on identification of specific chemical reactions by which acidic components in bitumen (mostly carboxylic acids) and basic components on aggregates produce water-soluble salts. Naturally, the presence of these compounds should promote moisture sensitivity. Sodium and potassium salts, formed from a reaction with carboxylic acids are commonly called "soaps" and are suggested as promoters of moisture sensitivity at the interface. The following reaction describes the formation of alkali metal salts when basic aggregate containing sodium or potassium reacts with carboxylic acid containing bitumen.

$$Na_2CO_3 + 2RCOOH \rightarrow 2\left(RCOO^-Na^+\right) + H_2O + CO_2$$

Similar reactions producing soluble alkali metal salts can be produced by $NaHCO_3, NaOH$ or Na-containing clays. By methodically changing the stoichiometric amounts of bitumen and aggregate reactants in the reactions presented above, results from freeze-thaw experiments on manufactured briquettes confirmed that laboratory performance of these specimens are predictable based on proposed acid-base reactions. Figure 13 and Figure 14 support the hypothesis that the amount of insoluble material produced at the interface is directly dependent on the amounts of chemical reactants present on the aggregate surface and in the bitumen. The combined effect of bitumen AAB-1 treated with increased amounts of stearic acid, and aggregates having different amounts of carbonates, is presented in Figure 13. Figure 14 illustrates the benefits of adding hydrated lime to granite and steric acid to bitumen.

It is well known that hydrated lime, as active filler, changes the physical properties of a mix through chemical interaction with the bitumen. Numerous studies have reported on the benefit of adding lime to bitumen to mitigate moisture sensitivity of asphalt mixes. In their review of the literature, Little and Jones (2003) report that hydrated lime ties up carboxylic acids and 2-quinolones in the bitumen, with the formation of insoluble calcium organic salts, which prevent these functionalities from reacting with a siliceous surface to form water sensitive bonds. This leaves important active sites on the siliceous surface to form strong water resistant bonds with nitrogen groups in bitumen.

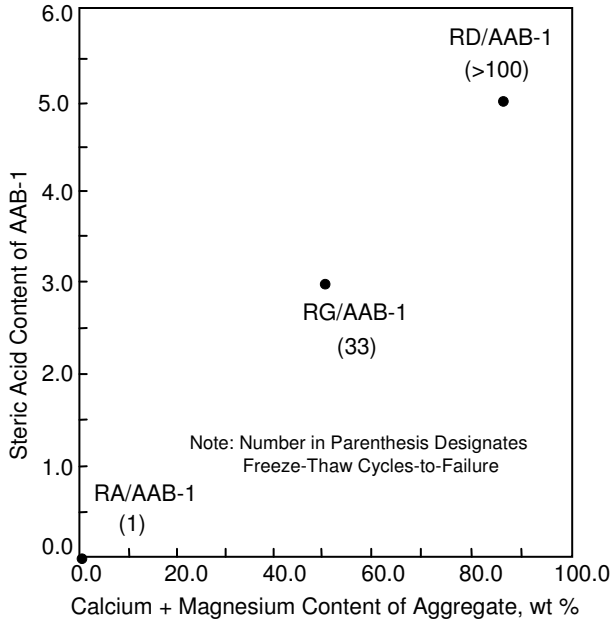

Figure 13. Effect of stearic acid content of bitumen and carbonate content of aggregate on freeze-thaw-cycles to failure (WRI, 2003a).

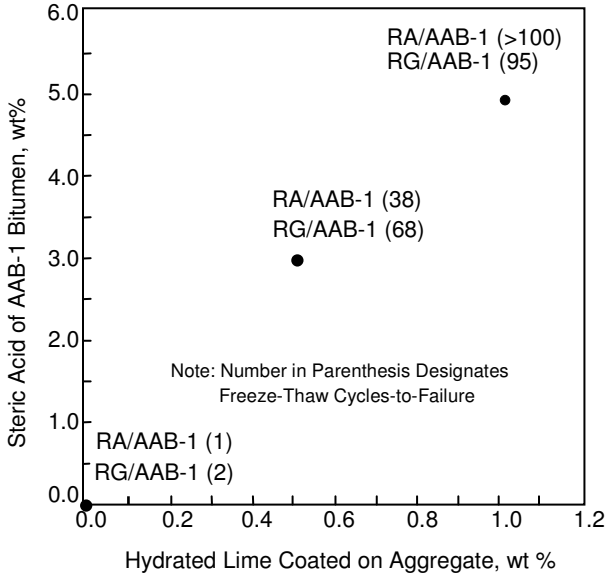

Figure 14. Effect of stearic acid content of bitumen and hydrated lime treatment on freeze-thaw-cycles to failure (WRI, 2003a).

The importance of metal oxides as functional groups on mineral surfaces, and their hydrolysis to form hydroxyl groups was previously discussed. Electron donor or acceptor sites on these surfaces can be explained by the amphoteric nature of these functional groups, as they act as either an electron donor or an acceptor. Weak acidic silanol groups dominate silica surface chemistry. Ernstsson and Larsson (1999) estimated four to five OH groups per nm^2 on the surface plane of crystalline silica. The interactions of surface hydroxyls with organic acid or basic functional groups are discussed in the following paragraphs. It should be noted that although the interactions presented here are specific to siliceous minerals, similar interactions can occur with other metal oxides such as iron oxides in basalts for example.

The fact that carboxylic acids readily bond with siliceous aggregate surfaces, but that they are also easily displaced by water has been established experimentally by a number of researchers as previously discussed. Simmons and Beard (1987) describe generic interactions between hydrated metal oxide surfaces with organic acids and bases, and the influence of water on these bonds.

Ardebrant and Pugh (1991a) discuss these interactions with reference to bitumen-aggregate interactions and show how carboxylic acids and a tertiary amine will interact with metal hydroxyl groups. The interaction between a silanol group and a carboxylic acid is depicted in the reaction shown below. These interactions between the mineral functional group and the organic functional group can range from completely covalent to completely ionic. Bond energy increases as the equilibrium shifts to the right and the bond becomes more ionic. Maximum strength exists when the surface hydroxyl group acts as a strong base and the organic functionality act as a strong acid.

$$-SiOH + RC(=O)-OH \rightleftharpoons -SiO\Lambda\, HO-C(=O)R \rightleftharpoons -SiOH_2^{+}\,{}^{-}O-C(=O)R$$

Where "···" denotes hydrogen bonding. Due to the lone pair electrons on the oxygen (O) of the silanol group, a partial negative dipole exists and an attraction to the partial

positive dipole on the hydrogen of the carboxylic acid occurs. For the situation where these partial polarities are similar, the O donates these electrons to the covalently bonded H without bond transfer, thereby accepting a hydrogen bond. The strength of the acid is determined by the length and type of R group. Strong acids tend to donate a proton (deprotonize) more readily. It is known that carboxylic acids in bitumen are weak acids, meaning they are not easily dissociated to form ionic species, and the right side of the reaction is less likely to occur. Hydrogen bonds, however, are susceptible to displacement or interruption by water according to the following reaction,

$$-SiO\Lambda\ \overset{H}{\underset{|}{HO}}-\overset{O}{\underset{||}{CR}}+2H_2O \rightleftharpoons -SiO\Lambda\ \overset{H}{\underset{|}{HOH}}+H_2O+\overset{O}{\underset{||}{RC}}-OH$$

In this hydrolyses reaction, water, acting as either a base or an acid, forms a stronger hydrogen bond with the silanol group than the hydrogen bond between the functional group and the silanol group.

The addition of adhesion promoters to bitumen is common practice and numerous research papers and reviews have been published on different compounds used and the effects of anti-strip agents on performance of asphalt mixes. Basic, amine anti-strip agents are generally used to improve adhesion of bitumen with siliceous aggregates. Logaraj (2002) states that the two main characteristics of anti-strip additives are (a) they have a polar amine end group which will chemically bond with the siliceous aggregate surface, and (b) they have a hydrocarbon chain with similar properties to that of the bitumen so that they will interact and become part of the bitumen. A primary amine (RNH_2) and tertiary amine (NR_3) are schematically illustrated in Figure 15.

The number of amine groups and length of the chains can greatly influence the adhesion of the bitumen, while optimum performance is typically achieved with 14 to 18 carbon chain amines with one or two amine groups (Tarrar and Wagh, 1992).

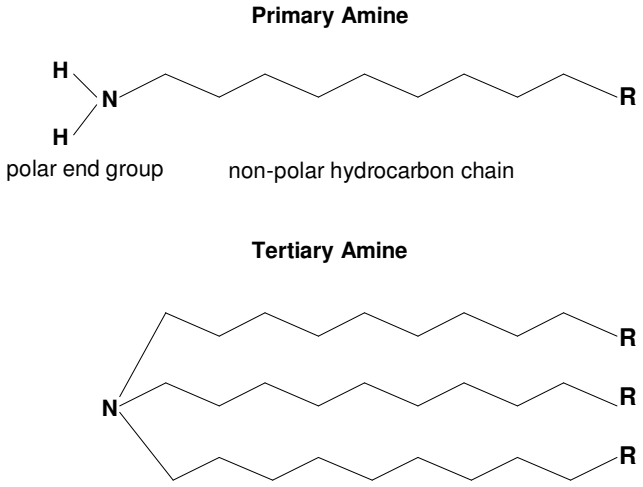

Figure 15. Schematic illustration of typical amine groups

Similar to the interaction described above, Ardebrant and Pugh (1991a) presented the interaction between a tertiary amine and a metal hydroxyl group. The following interaction shows the interaction of these basic molecules with surface silanol groups.

$$-SiOH + R_3N \rightleftharpoons -SiOH\,\Lambda\, NR_3 \rightleftharpoons -SiO^{-}{}^{+}HNR_3$$

In this interaction, the lone pair electrons on the nitrogen of the amine cause a partial negative dipole over the nitrogen and an attraction to the partial positive hydrogen dipole on the silanol group occurs. As before, the strength of the basic amine is determined by the type and length of the R groups. For strong bases, protonation of the amine occurs leaving the ionic species as shown on the right hand side of the reaction. Titova et al. (1987) showed that a tertiary amine with three ethyl (CH_2CH_3) groups, Triethylamine, interacts with a silanol group to form an insoluble silica-Triethylamine compound that is stable at temperatures greater than 900˚F. It therefore appears that hydrogen bonding would be less likely to occur with this reaction.

Species of lower basicity in bitumen might form hydrogen bonds, which would then again be susceptible to water disruption or displacement. In general, the hydrolysis reaction for organic bases that form hydrogen bonds with silanol groups is shown in the following equation,

$$-SiOH\,\Lambda\ XR + 2H_2O \rightleftharpoons -SiO\Lambda\ OH_2 + HOH\,\Lambda\ XR$$

where X denotes some O or N-containing basic functional groups. Therefore, if water acts as a base or an acid and forms a stronger hydrogen bond with the surface hydroxyl or with the basic functional group than the existing hydrogen bond, displacement of this functionality occurs.

The pH of water at the interface is also expected to affect the hydrogen bonds formed between metal hydroxyl groups on aggregate surfaces and basic or acidic functionalities in bitumen. Two general cases are presented below.

For an organic acid,

$$-MOH + {}^{+}HXR \rightleftharpoons -MO\Lambda\ H\,\Lambda\ XR \rightleftharpoons -MO^{-} + HOH + XR$$

$[H^+]$ Increased pH ⟵ ⟶ $[OH^-]$ Decreased pH

And for an organic base,

$$-MOH_2^{+} + HXR \rightleftharpoons -M-\overset{H}{\underset{|}{O}}\Lambda\ H\,\Lambda\ XR \rightleftharpoons -MOH + HOH + {}^{-}XR$$

$[H^+]$ Increased pH ⟵ ⟶ $[OH^-]$ Decreased pH

where M represents a metal atom, and X denotes oxygen, sulfur, or nitrogen. The pH range over which these bonds would be expected to retain adhesion is a function of the acidity of the surface hydroxyl groups and the functional groups in the adhesive, bitumen (Simmons and Beard, 1987).

The generation of covalent bonds at interfaces has become an industry of its own. Coupling agents are chemicals used to "couple" an organic and inorganic phase through covalent bonding, producing durable adhesive bonds in adverse environmental conditions. Silane coupling agents, or organofunctional silanes, form the largest and most successful group of these materials (Walker, 1994; Pocius, 1997). The silane molecule is generally comprised of a silicone (Si) atom at the center, with an organic chemical functional group (R) compatible with the organic matrix, and (R') which is a hydrolyzable group. The coupling mechanism consists of three steps: hydrolysis, coupling, and condensation. Hydrolysis takes place when the organofunctional silane is brought into contact with moisture to generate active silanol groups (SiOH), and usually an alcohol. This process is described by the following reaction.

$$RSi(OR')_3 + H_2O \rightarrow RSi(OH)_3 + 3R'OH$$

Silane Trisilanol Alcohol

Silanol molecules then hydrogen bond with the hydroxylated metal oxide surface (MOH). In addition, similar reactions will occur between silanol groups themselves (not shown), to form hydrogen bonds.

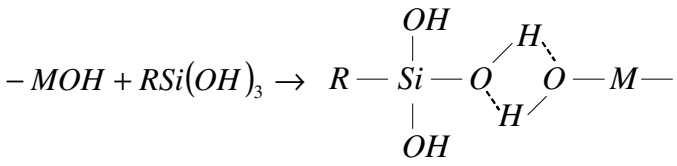

Upon heating or drying, these hydrogen bonds are condensed (or collapse) to produce H_2O and a covalently bonded metallosiloxane (MOSi) and a crosslinked siloxane (SiOSi) film structure over the surface.

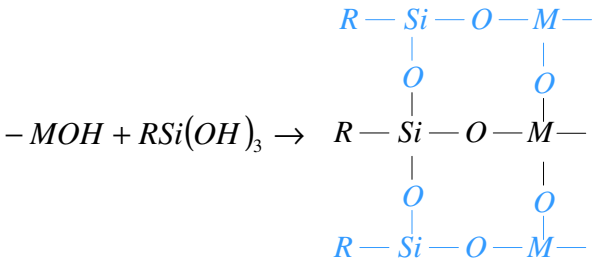

Research on the treatment of aggregates with organosilane coupling agents to promote resistance against water susceptibility of the bitumen-aggregate bond has been conducted in the past. Divito et al. (1982) compared aggregates treated with silanes to aggregates treated with commercial amine anti-strip agents. Their results showed that silane treated aggregates have greater resistance to water damage than aggregates treated with commercial amine anti-strip agents. Graf (1986) conducted a study where he demonstrated how silane treatment increased hydrophobic bonding between crushed glass and bitumen. Perry and Curtis (1992) investigated the effect of aggregate modification by organosilanes on the adsorption behavior of bitumen model compounds and bitumen. They found no relationship between the increased adsorption amounts and resistance to water and conclude that these interactions are highly dependent on the specific bitumen, or model compound, and aggregate involved.

THERMODYNAMIC THEORY

This theory, also called adsorption theory, is the most widely used approach in adhesion science as indicated by most comprehensive references on this subject, such as the one by Schultz and Nadrin (1994). Thermodynamic theory is based on the concept that an adhesive will adhere to a substrate due to established intermolecular forces at the interface provided that intimate contact is achieved. The magnitude of these fundamental forces can generally be related to thermodynamic quantities, such as surface free energies of the materials involved in the adhesive bond. The orientation of polar molecules in bitumen as part of the process to minimize the free energy at the

interface has been recognized and discussed in previous reviews on stripping in bitumen-aggregate systems (Rice, 1958; Hicks, 1991; Kiggundu and Robberts, 1988; Little and Jones, 2003). In order to appreciate the material presented in this section, elementary thermodynamic concepts are reviewed.

Thermodynamics is the study of energy changes. A spontaneous process is one that occurs on its own, without external assistance. Such a process occurs due to an imbalance between two natural tendencies. The first tendency is the spontaneous conversion of potential energy into work and heat, known as enthalpy. The second tendency is the spontaneous increase in randomness of the system, known as entropy (77). In order to relate enthalpy and entropy, the Gibbs free energy (G) is defined so that, at constant temperature (kelvin) and pressure (atm),

$$\Delta G = \Delta H + T\Delta S \qquad (1)$$

Gibbs free energy therefore represents the difference between the initial and final energy state of a system and predicts whether a process, carried out at the defined constant temperature and pressure conditions, can occur or cannot occur.

Enthalpy (ΔH) is the total heat given off or absorbed during this process. Consider the interaction between two chemical entities, such as two ions. The potential energy of attraction between two isolated ions with opposite charge will decrease as they approach each other at a temperature of absolute zero. This change in energy as a function of separation distance is illustrated in Figure 16.

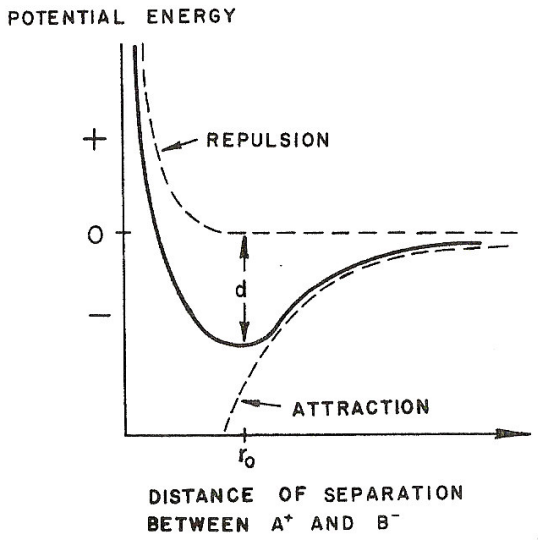

Figure 16. Potential energy as a function of separation distance at a temperature of absolute zero (Kittrick, 1977).

A negative sign indicates that energy is given off in the process. When the two entities are sufficiently close, their electron clouds overlap and cause potential energy of repulsion to increase rapidly. The resultant of the attractive and repulsion curves indicates the existence of a state of minimum energy, where the entities will reside in a more stable, equilibrium state. The equilibrium distance (r_o) is therefore indicated by the position of the "potential energy well", while the energy given off is given by the depth (d) of the well.

For $\Delta G < 0$, the energy will be released to perform work and the process will occur spontaneously. If, on the other hand $\Delta G > 0$, then energy will have to be absorbed from the environment and cannot occur on its own. For $\Delta G = 0$, the process is in equilibrium. Equation (1) indicates that the absolute temperature, T, must be specified due to temperature dependency of entropy. Fortunately, the magnitudes of H and S do not vary much over a limited temperature range. The free energy, however, may vary

considerably with temperature unless S is very small. At relatively low temperatures, such as room temperature, ΔH usually dominates while ΔS become more important at high temperatures (Kittrick, 1977).

The Gibbs free energy is an important thermodynamic parameter in quantifying adhesive bonding. It should be pointed out that the Gibbs free energy in this context is the excess free energy of the system associated with the surface or interface. A detailed account of the derivation of thermodynamic parameters related to surfaces is presented by Adamson and Gast (1997). It is common to refer to the Gibbs free energy as the free energy of adhesion or, when applicable to the binding between similar phases, the free energy of cohesion.

The relationship between the Gibbs free energy, work of adhesion and surface energy are presented below. The molecular description of surface (free) energy was previously introduced. The surface energy, γ, in a thermodynamic sense is the reversible work required to create a unit area of new surface. While researchers such as Good and van Oss (1991) base their theory on the definition of the Gibbs free energy, the work of adhesion (W_a) is more commonly used in the literature pertaining to the thermodynamic theory of adhesion. Although equal in magnitude, the work of adhesion and the Gibbs free energy of adhesion should be interpreted as follows,

$$W^a = -\Delta G^a \tag{2}$$

Consider a brittle material of unit cross sectional area subjected to a tensile force. Then, if the material is completely brittle, the work done on the sample is dissipated only through propagation of a crack, thereby creating two new surfaces. The total work expended per unit of surface area in forming the two surfaces (W_a) is then equal to twice the surface energy per unit of surface area, of the material under consideration. Under these conditions,

$$W^c = 2\gamma \tag{3}$$

or, $$\Delta G^c = -2\gamma \quad (4)$$

When two dissimilar materials form an interface by being in intimate contact, a tensile force can be applied to split the materials into dissimilar parts. For a completely brittle interface of unit cross sectional area, the energy expended should be the sum of the individual surface energies for the two materials involved. However, because the dissimilar materials are separated, some of the intermolecular forces present during intimate contact, are now missing. That is, an interfacial energy may have exited before separation, which should be accounted for by subtracting it from the energy done to create the two new surfaces (Pocius, 1997). Dupré, in 1867, postulated the following relationship, which plays a central role in the study of adhesion.

$$W^a = \gamma_1 + \gamma_2 - \gamma_{12} \quad (5)$$

or, $$\Delta G^a = \gamma_{12} - \gamma_1 - \gamma_2 \quad (6)$$

where γ_i is the surface energy of the i^{th} material and γ_{12} is the interfacial energy between the two materials in contact.

The terms wetting, spreading, and contact angle have become synonymous with adhesion. The shape of a liquid drop on a surface, usually described through the contact angle between them, provides information on the intermolecular forces of the individual phases involved as well as the interfacial forces between them. Although the great utility of contact angle measurements stems from their interpretations based on thermodynamic considerations, they can also be used to provide a measure of wetting and spreading on a macroscopic scale. Wetting of a surface (or spreading of the liquid over the surface) is the process where the adhesive comes into intimate molecular contact with the surface and establishes fundamental forces of adhesion. Wetting is a prerequisite for good adhesion. For complete spreading, the contact angle equals zero

and the adhesive spreads spontaneously over the surface (Myers, 1991). Naturally, wetting and spreading depends also on the viscosity of the liquid, roughness and heterogeneity of the solid surface involved. From a thermodynamic point of view, wetting and spreading depends on the competition between adhesive forces and cohesive forces, which can be used to define a spreading coefficient, S.

$$S = W^a - W^c \tag{7}$$

Thus, the higher and more positive the value of S, the greater the work of adhesion is compared to the cohesive energy of the adhesive. A negative value of S represents a finite contact angle and zero corresponds to final equilibrium (Shanahan, 1992). Figure 17 conceptually illustrates the relationship between surface energy (or surface tension), wetting and spreading.

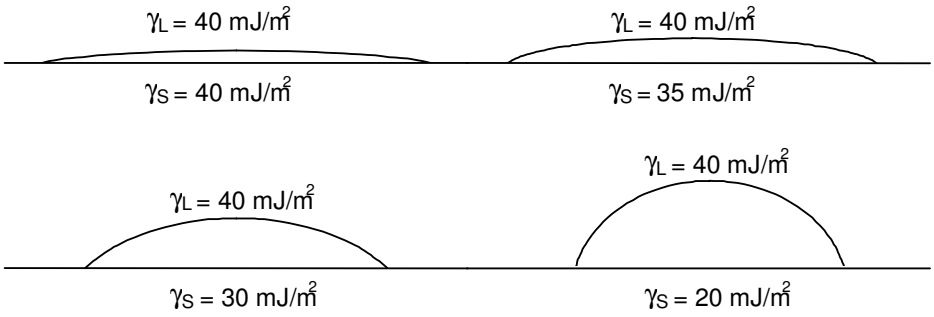

Figure 17. Conceptual relationship between spreading, wetting and surface energy [adapted from Pocius (1997)]

The properties of interfaces can normally be described as triple junctions, or a three-phase boundary. Young, in 1805, proposed an equation to obtain surface tension from

the contact angle formed when a drop of liquid is placed on a perfectly smooth, rigid solid. A schematic of the contact angle experiment is presented in Figure 18, where θ is the contact angle between the solid-liquid (SL) interface and the tangent of the liquid-vapor (LV) interface. If water is the liquid under consideration, the case on the left side would be an example of an hydrophilic (water-loving) surface, evident from the drop that tends to spread over the solid due to favorable interaction between interfacial forces. The contact angle on the right side, however, is greater than 90º indicating that water does not spread readily over this surface, and is thus hydrophobic (water-hating).

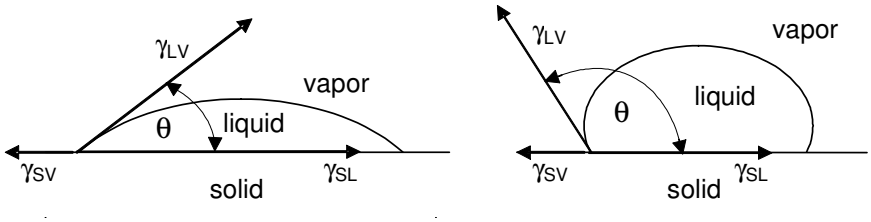

Figure 18. The three-phase boundary of a liquid drop on a solid surface in vapor

To each interface, forming the triple line, a surface or interfacial free energy or tension can be attributed. Thus, γ_{SV} is the surface free energy of the solid in equilibrium with the saturated vapor of the liquid, γ_{LV} is the surface tension of the liquid in equilibrium with the solid, and γ_{SL} is the solid-liquid interfacial free energy. Young's equation is the result of the triple line in equilibrium (tension in force per unit length).

$$\gamma_{SV} = \gamma_{SL} + \gamma_{LV} \cos\theta \qquad (8)$$

Although this equation was originally based on a mechanical (tension) definition, it has since been verified by rigorous thermodynamic derivations based on minimizing the

overall free energy (Pocius, 1997). The solid-vapor interfacial energy in this equation, however, is not the true surface free energy of the solid. When vapor is adsorbed onto the surface of the solid, its free energy is reduced so that,

$$\gamma_{SV} = \gamma_S - \pi_e \tag{9}$$

where γ_S is the surface free energy of the solid only in contact with its own vapor, and π_e the equilibrium spreading pressure which is a measure of energy released during vapor adsorption. Although equilibrium spreading for the liquid phase should also be possible, this value has historically been assumed equal to zero. It has been shown that π_e is negligible for high-energy liquids on low-energy solids, which is usually the case for contact angle measurements on polymeric surfaces (Good and van Oss, 1991). Equations (5) and (8) can therefore be combined in the following way to obtain the Young-Dupré equation.

$$W_a^{LS} = \gamma_{LV}(1 + \cos\theta) \tag{10}$$

The Young-Dupré equation is the starting point for any method that utilizes contact angles to obtain surface free energies by relating the contact angle to the work of adhesion. This is also the way to tie contact angles back to adhesion.

Fowkes (1964) suggested that surface energy is comprised of a polar and non-polar component. Since that time, several models were proposed for the calculation of the work of adhesion based on surface energy components. Several researchers and practitioners from different sectors of the adhesion science community report that the theory developed by van Oss, Chaudhury, and Good (1988) is the best available at the time (Adão et al., 1998; Woodward, 2000). Although the theory also received much critique during the past decade (Kwok, 1999), its application has not always been well-understood (Della Volpe and Siboni, 2000).

Following the form suggested by Fowkes (1964), the surface energy of a single phase is given by,

$$\gamma_i = \gamma_i^{LW} + \gamma_i^{AB} \tag{11}$$

where LW denotes Lifshitz-van der Waals, and AB denotes acid-base. The Lifshitz theory was introduced conceptually in the section addressing fundamental forces. The London, Keesom, and Debye components together form the apolar (LW) component of attraction. Based on the Lifshitz theory, Chaudhury and Good (1991) showed that the contribution of the Keesom and Debye van der Waals forces are small relative to the London forces. The acid-base component represents polar, or specific, interactions primarily due to hydrogen bonding (Good and van Oss, 1991).

It follows that the free energy of cohesion and adhesion likewise constitutes two components. Therefore, the Gibbs free energy of cohesion is,

$$\Delta G_i^c = -2\gamma_i = \Delta G_i^{cLW} + \Delta G_i^{cAB} \tag{12}$$

and the Gibbs free energy of adhesion is,

$$\Delta G_{ij}^a = \gamma_{ij} - \gamma_i - \gamma_j = \Delta G_{ij}^{aLW} + \Delta G_{ij}^{aAB} \tag{13}$$

The van der Waals forces represent the interaction between two symmetric molecules and its treatment can be traced back to first principles. For the LW component, the Berthelot geometric mean rule therefore holds,

$$\Delta G_{ij}^{aLW} = -2\sqrt{\gamma_i^{LW}\gamma_j^{LW}} \tag{14}$$

The acid-base component, however, cannot be treated in the same fashion, although some theories assume that the geometric mean rule holds for this component as well. These interactions are specific and are only possible between interaction partners with complimentary acid-base properties. The relationship describing the AB component of free energy was derived empirically by van Oss et al. (1988),

$$\Delta G_{ij}^{aAB} = -2\left(\sqrt{\gamma_i^+ \gamma_j^-} + \sqrt{\gamma_i^- \gamma_j^+}\right) \tag{15}$$

Van Oss and his co-workers presented the full version of the Young-Dupré equation by inserting ΔG^{LW} and ΔG^{AB},

$$-\Delta G^a = W^a = \gamma_L^{Tot}(1+\cos\theta) = 2\left(\sqrt{\gamma_L^{LW}\gamma_S^{LW}} + \sqrt{\gamma_L^+\gamma_S^-} + \sqrt{\gamma_L^-\gamma_S^+}\right) \tag{16}$$

where L represents a liquid and S the solid under consideration. Equation (16) implies that if the contact angles of three liquids with different and known polarities are measured on an unknown surface, then the three unknown surface energy components can be solved. These polarities have been defined as monopolar basic, monopolar acidic, bipolar (basic and acidic), or apolar (only van der Waals forces). In addition, the use of this equation is not restricted to contact angle measurements, but can be applied with any technique able to quantify the work of adhesion between the unknown surface and probe substances with known surface energy components. An important practical application of this theory is that it can be used to predict the work of adhesion between two materials if their surface energy components are known. Similarly, the work of cohesion can be predicted within the bulk phase of a material. By adapting the Dupré equation for the interaction between two condensed phases, 1 and 2, within a liquid, 3,

$$\Delta G_{132}^a = \gamma_{12} - \gamma_{13} - \gamma_{23} \tag{17}$$

and with the components of the free energy of interfacial interaction additive,

$$\Delta G_{132}^{a} = \Delta G_{132}^{aLW} + \Delta G_{132}^{aAB} \tag{18}$$

van Oss et al. (van Oss et al., 1988; Good and van Oss, 1991) proposed the following form for the interaction between two materials, 1 and 2, submersed in a polar liquid, 3.

$$\Delta G_{132}^{a} = 2\begin{bmatrix} \sqrt{\gamma_1^{LW}\gamma_3^{LW}} + \sqrt{\gamma_2^{LW}\gamma_3^{LW}} - \sqrt{\gamma_1^{LW}\gamma_2^{LW}} - \gamma_3^{LW} \\ + \sqrt{\gamma_3^{+}}\left(\sqrt{\gamma_1^{-}} + \sqrt{\gamma_2^{-}} - \sqrt{\gamma_3^{-}}\right) \\ + \sqrt{\gamma_3^{-}}\left(\sqrt{\gamma_1^{+}} + \sqrt{\gamma_2^{+}} - \sqrt{\gamma_3^{+}}\right) \\ - \sqrt{\gamma_1^{+}\gamma_2^{-}} - \sqrt{\gamma_1^{-}\gamma_2^{+}} \end{bmatrix} \tag{19}$$

When the liquid is water, this interaction is called the "hydrophobic interaction" where $\Delta G_{132}^{a} < 0$. For $\Delta G_{132}^{a} > 0$, the interaction between 1 and 2 becomes repulsion, which is the driving force for phase separation of adhesives in aqueous media (van Oss et al., 1988)

Thermodynamic concepts have been used by many researchers to elucidate adhesion between bitumen and aggregate materials. Ensley at al. (1984) determined the heat of immersion using microcalorimetry. Curtis et al. (1992) determined Gibbs free energies from adsorption isotherms. Lytton (2004) utilized surface energies measured on bitumen and aggregates surfaces to calculate free energies of adhesion and cohesion by applying modern surface energy theories as discussed in the forgoing paragraphs.

These concepts, especially surface energy, have played an important role in discoveries of the rules governing the microfracture and healing in bitumen-aggregate mixtures (2000). Thermodynamic theory lends itself to quantifying the relationship between fundamental adhesion and practical adhesion. Since real materials are not completely brittle, especially polymer-like materials such as bitumen, energy dissipation can result from molecular chain disentanglement and stretching, and conformational

changes (rotation about flexible intermolecular bonds) under applied loads, i.e. viscoelastic effects, as well as plastic deformation. Merril et al. (1991) report that the apparent or practical work of adhesion is much larger than the fundamental work of adhesion based on adhesive peel test experiments. However, the experiments showed that the practical work of adhesion is a multiplication of some dissipation factor with the fundamental work of adhesion. From fracture mechanics, the well-known Griffiths crack growth criterion suggests that for a completely brittle material, the energy necessary to break a adhesive (or cohesive) bond is equal to the fundamental work of adhesion, W_a. This energy can be considered the minimum amount of practical adhesion that one can expect from a bond. If other modes of dissipating energy exist, then this minimum value increases (Pocius, 1997). Schapery (1984) extended this crack growth theory to viscoelastic materials based on the fundamental laws of fracture. Schapery (1989) and Lytton et al. (1998) developed similar relationships for healing. Healing is the opposite of fracture and is pronounced when longer rest periods are introduced between applied loads, manifested in extended fatigue life. Lytton et al. (1998) applied these fundamental relationships of fracture and healing to asphalt mixtures.

The fundamental law of fracture for viscoelastic materials is presented in Equation (20). This expression essentially describes an energy balance between the energy required for fracture and the energy released, expended in crack propagation and extension. An expression similar to this equation exists for healing.

$$W = E_R D(t_\alpha) J_R \tag{20}$$

Where W is the work of adhesion (W^a) or cohesion (W^c) per unit of each crack surface area created, i.e. the minimum energy required to cause fracture. The term on the right side is termed pseudo-strain energy because the energy required in overcoming non-linear and viscoelastic effects is eliminated. The reference modulus E_R, is an arbitrary value used during this correction; $D(t_\alpha)$ is the viscoelastic creep compliance over a period t_α, the time required for a crack to move a distance equal to the length (α)

of the process zone ahead of the crack tip; and the J-integral J_R, the pseudo-strain energy release rate, i.e. the change of available energy per unit crack area, from one load cycle to the next. For the situation where the pseudo-strain energy released is greater than the required minimum energy for bond breakage, crack extension occurs.

From Equations (2) and (12), the work of adhesion (W) for a dry interface is given by,

$$W_{12}^{a} = -\left(\Delta G_{12}^{aLW} + \Delta G_{12}^{aAB}\right) \tag{21}$$

Where ΔG_{12}^{aLW} and ΔG_{12}^{aAB} the Lifshitz van der Waals and acid-base components of the free energy of interfacial interaction, respectively, between materials one and two.

Lytton (2000) demonstrated that the rate of healing can be separated into a short-term healing rate and a long-term healing rate, which are distinguishable based on their relations with the Lifshitz van der Waals surface energy component and the acid-base surface energy component of the material, respectively. The relationships presented in Figures 19 and 20 show that short term healing is inversely related to the Lifshitz van der Waals component of surface energy, while long term healing is directly related to the acid-base component.

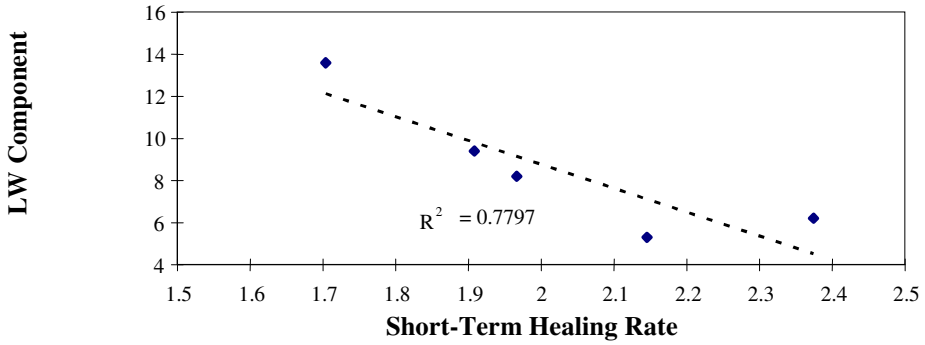

Figure 19. Relationship between Lifshitz van der Waals surface energy and short term healing rate (Lytton, 2000)

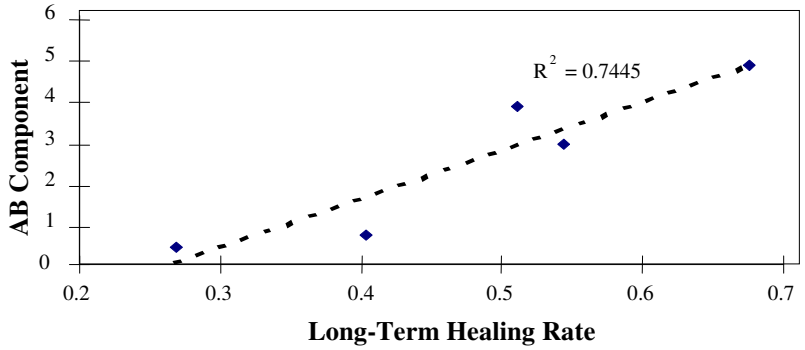

Figure 20. Relationship between acid-base surface energy and long term healing rate (Lytton, 2000)

Upon fracture, the non-polar forces on the crack faces forms a "skin" due to their additive nature and in an attempt to minimize the free energy created, thereby preventing the required close contact for potential van der Waals interaction between the faces. In contrast, acid-base interactions are specific, acting over a longer distance to heal microcracks through hydrogen bonding over time.

Surface free energies measured on various bitumen types using the Wilhelmy plate technique(Elphingstone, 1997; Cheng, 2002; Cheng et al., 2002), and on aggregates (Li, 1997; Elphingstone, 1997; Cheng, 2002, Cheng et al., 2002) using a vacuum static sorption technique, served as inputs to the van Oss- Chaudhury-Good models to predict free energies of interaction. A summary of this work was recently presented by Lytton (2004) and selected results are furnished in Table 3. Lytton and his colleagues postulated that the advancing (wetting) contact angles and receding (dewetting) angles obtained from hysteresis during contact angle measurements on bitumen, corresponds to healing and fracture in asphalt mixtures, respectively. The work of adhesion for fracture (W_f) and healing (W_h) were calculated accordingly.

An important observation from the values reported is that all bitumen-aggregate combinations produce negative bond strengths in the presence of water. While larger

positive numbers indicate resistance to fracture and an ability to heal, larger negative numbers suggest that water has a greater affinity for the aggregate surface than bitumen and therefore promotes adhesive fracture. Negative healing bond strength indicates that water prevents healing of the adhesive bond.

Table 3. Effect of bitumen and aggregate on dry and wet adhesive bond strength (Lytton, 2004)

Aggregate	Bitumen	Fracture	Healing	
		W_f	W_h^{LW}	W_h^{AB}
Adhesive Bond Strength in the Dry state (mJ/m^2)				
Georgia Granite	AAD	152.9	88.6	15.7
	AAM	198.6	46.2	61.8
Texas Limestone	AAD	141.8	71.4	2.0
	AAM	250.2	37.2	88.1
Rhine River Gravel	AAD	210.0	89.9	9.2
	AAM	304.5	46.9	132.2
Adhesive Bond Strength with Water present (mJ/m^2)				
Georgia Granite	AAD	-48.3	-11.4	-47.0
	AAM	-30.0	-36.7	-22.5
Texas Limestone	AAD	-66.9	-7.7	-89.2
	AAM	-30.9	-24.7	-24.7
Rhine River Gravel	AAD	-120.3	-11.7	-181.0
	AAM	-53.2	-37.6	-79.7

Mechanisms that contribute to stripping under traffic loading include pore pressure effects and hydraulic scouring (Fromm, 1974). Lytton and his co-workers proposed a phenomenological model that relates the compressive strength reduction in dry and wet conditions during cyclic loading, to work of adhesion and the percentage of the aggregate surface area that has been exposed to water at that time (Cheng et al., 2002; Lytton, 2004).

The percentage of the surface area of an aggregate that has been exposed to water (P) can be used as an index to quantify the level of adhesive fracture.

$$\Delta W = W_{12}^{a}(1-P) + W_{132}^{a}P \tag{22}$$

Where ΔW^{a} is the net work of adhesive fracture; W_{12}^{a} is the work of adhesion in the absence of water; (1-P) is the percentage of the aggregate surface area that is not exposed to water; W_{132}^{a} is the work of adhesion in the presence of water, and P is the percentage of the aggregate surface area that is exposed to water.

Under cyclic compression loads, the reduction in stiffness at loading cycle N, under wet conditions, can be computed as the ratio of the net work of adhesive fracture in the presence of water and the work of adhesion in the dry state.

$$\frac{E_{wet}}{E_{dry}} = \frac{(\sigma/\varepsilon)_{wet}}{(\sigma/\varepsilon)_{dry}} = \frac{\varepsilon_{dry}}{\varepsilon_{wet}} = \frac{W_{12}^{a}(1-P) + W_{132}^{a}P}{W_{12}^{a}} \tag{23}$$

Where E_{wet} and E_{dry} are the compressive stiffness in the wet and dry conditions, respectively; σ is the compressive stress; ε is the permanent strain, induced either in wet or dry conditions; and other terms as defined above.

Figure 21 illustrates the aggregate-water-exposure phenomenon for the asphalt mixtures under cyclic loading. The initial P-values imply that the mixtures undergone premature damage due to diffusion of water through the bitumen to the interface during moisture preconditioning. The data indicates that the P-value generally increases with increase in number of load cycles. The P-value for the AAD mixture remains higher than for the AAM mixture throughout the test. Figure 21 indicates that a point exists on the wetting line where a sudden increase in the slope occurs. This point (or knee) on the wetting line corresponds to the number of cycles to accelerated damage, or adhesive fracture. The slope of the line represents the rate of adhesive fracture. The approach

presented here offers great potential to evaluate stripping quantitatively by combining mechanical testing with thermodynamic parameters.

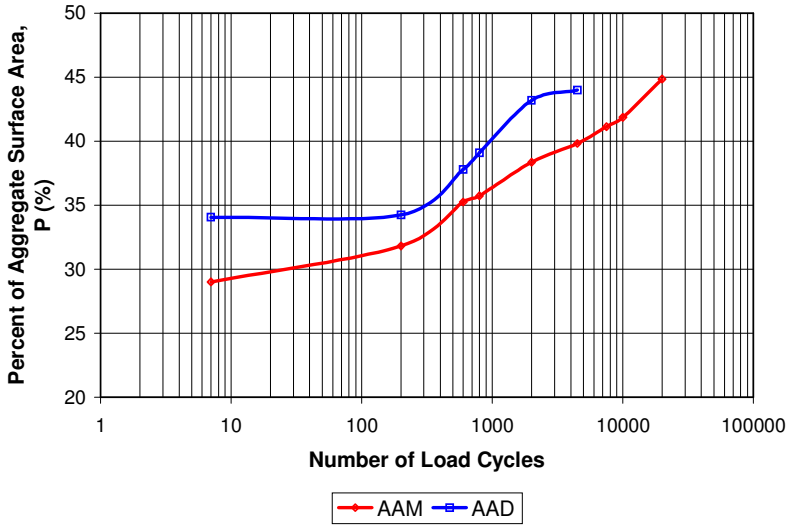

Figure 21. Percent of aggregate surface wetted by water as a function of number of load cycles for bitumen AAM and AAD mixed with limestone, respectively (Cheng et al., 2002; Lytton, 2004).

CONCLUSIONS

Theories and associated mechanisms of adhesion were reviewed and presented with specific reference to bitumen-aggregate systems. The theories identified for application to bitumen-aggregate systems include theory of (weak) boundary layers, mechanical theory, electrostatic theory, chemical bonding theory, and thermodynamic theory.

The first two theories remind us of the importance of physical characteristics of the aggregate to adhesion. Although surface morphology can promote adhesion, it can also have the potential to cause weak boundary layers if selective absorption occurs. The characteristics of water in contact with the aggregate as well as the aggregate's ability to

act as catalyst to oxidative aging can contribute to formation of cohesively weak boundary layers.

Wetting of the aggregate remains an important prerequisite for good adhesion and does not only rely on good mixing conditions, but also on cleanliness of the aggregate surface. Wetting is required to obtain intimate contact between the materials, and thereby establish fundamental forces ultimately responsible for adhesion. Without wetting, it is unlikely that the beneficial effects of surface texture through mechanical adhesion could be established.

Electrostatic theory shows that electric double layers develop on material surface in the presence of water. Overlapping of these layers leads to important electric double layer forces that can either enhance or work against adhesion. The pH of the contacting water forms an integral part of this phenomenon and can dictate the stability of adhesive bonds. Electric double layer effects together with pH of the water at the interface are important considerations in developing models to predict water damage in bitumen-aggregate mixes.

A review of adsorption-desroption studies confirms that adhesion in bitumen-aggregate systems cannot be adequately addressed without special assessment of these bonds under wet conditions: Bitumen functional groups responsible for adhesion in the dry state are also the ones most easily displaced in the presence of water. Research shows that surface chemistry of the aggregate dominates the bitumen-aggregate adhesive bond strength. Not only surface area, but also the density of bonding sites on aggregate surfaces plays important roles.

In environmentally adverse conditions, insoluble stable complexes and covalent bonds should be provided on the bitumen-aggregate interface. This can be achieved by proper selection of the bitumen-aggregate pair or by applying selected additives.

Although separate discussions of theories and associated mechanisms help to clarify our ideas, stimulating development of new concepts, and defining future research, they can rarely be separated completely from each other. The fact that thermodynamic theory is the most widely applied in the adhesion science community is not surprising. The

energy approach makes it universal, creating the opportunity to incorporate different fundamental chemical processes that drive adhesive bonding, as well as physical processes induced by dynamic loading. It offers the potential to quantify adhesion through the surface energies of the materials involved. An important and direct application of this approach is to assess the compatibility of various bitumen-aggregate combinations. In addition, these parameters can be incorporated together with other material properties into holistic, fundamental hot-mix performance prediction models.

While the current form of thermodynamic theory presented finds application in bitumen-aggregate adhesion due to the importance of non-covalent hydrogen bonding and van der Waals interactions in these systems, this review indicates that complex formation on the interface can also occur in some bitumen-aggregate combinations. Nevertheless, the merits of this approach have been shown among other applications, in prediction of stripping potential.

CHAPTER III

ASSESSMENT OF TECHNIQUES FOR SURFACE ENERGY CHARACTERIZATION

INTRODUCTION

The synthesis presented in Chapter II revealed that the thermodynamic theory is the most widely applied approach in quantifying adhesive bonding and offers numerous advantages. Following the theory proposed by van Oss et al. (1988), this approach relies on determining the surface energies of both materials, as well as surface energy components. In the context of measurement of these quantities, it is important to reiterate the difference between liquid and solid surfaces.

The terms surface "tension" and surface "energy" are interchangeable for liquids, are dimensionally equivalent, and numerically equal. Since the surface energy of a liquid is equal to surface tension, it can be readily obtained through direct mechanical means, such as detachment. Other methods are based on measurement of contact angles, and shapes of bubbles and drops. Adamson and Gast (1997) describe several classic techniques including the Capillary Rise method, the Wilhelmy Plate method, the Maximum Bubble Pressure method, the du Nöy Ring method, the Drop Weight method, the Pendant Drop method, and the Sessile Drop method.

For solids, however, the application of the surface tension concept becomes less clear and surface energy and surface tension are not necessarily equal. Solid surface characteristics such as reduced mobility of atoms and molecules, and varying surface morphology give rise to a heterogeneous, or direction dependent, solid surface tension phenomenon, which is not easy to convey. The concept of surface energy is therefore more appropriate to solid surfaces (Myers, 2002). Stretching of solids not only involves a large expenditure of work associated with elastic and sometimes plastic deformation, but also changes the surface structure. Direct mechanical measurement of solid surface

energy has therefore been limited to a few solids like mica and diamond where surface stretching is avoided during cleavage, and the work of cleaving yields surface energy. Surface "tension" values for solids have also been derived from empirical relationships with their liquid phase surface tensions (Adamson and Gast, 1997). Modern texts on adhesive science suggest that techniques for determining surface energies of solids can generally be divided into direct and indirect methods (Pocius, 1997). Indirect methods are by far the most popular and involve measurement of a surface related property, such as contact angle, which is then related to surface energy based on an appropriate thermodynamic function.

It was previously pointed out that this theory can be used with any technique capable of quantifying the work of adhesion between a surface and at least three other probe substances, liquids or gasses, with known surface energy properties. The objective of this chapter is to present a review of techniques previously used to determine surface energies and its components for both bitumen and aggregate, as well as to identify and assess other potential techniques. Broad categories identified include contact angle techniques, vapor sorption techniques, force microscopy, and microcalorimetry.

CONTACT ANGLE TECHNIQUES

In this section, three different techniques of determining solid surface energies from contact angles are presented. The approach of dipping a plate into a liquid, first proposed by Wilhelmy in 1863 (Adamson and Gast, 1997), was used by Elphingstone (1997) and later by Cheng (2002) to obtain the surface energies of bitumen coated onto a glass plate. Thelen (1958) proposed a test to determine the contact angles of asphalt drops on smooth aggregate surfaces. A lamp and lens system was used to project an image of the drop onto a screen where the contact angle could be measured with a straight edge and protractor. This method, generally known as the sessile drop method, is widely used in the field of adhesion science and technological advanced imaging systems are commercially available today. Ardebrant and Pugh (1991b) used the sessile drop approach to obtain contact angles on aggregates, while Bose (2002) obtained

contact angles on bitumen films. The wicking method is a technique often used in the field of powder technology to obtain contact angles on these particulate materials utilizing capillary rise.

Wilhelmy Plate Method

The Wilhelmy Plate method is based on kinetic force equilibrium when a thin plate, suspended from a highly accurate balance, is immersed or withdrawn from a liquid at very slow and constant speed (Adamson and Gast, 1997). The dynamic contact angles that develop between the bitumen coated glass plates and liquids are obtained. The basic principle is schematically illustrated in Figure 22. The dynamic contact angle measured during the immersion process is called the advancing contact angle (a wetting process), while the dynamic contact angle measured during the withdrawal process is called the receding contact angle (a de-wetting process).

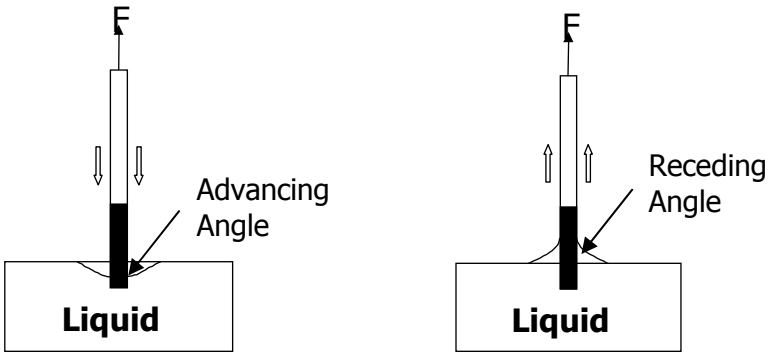

Figure 22. Schematic illustration of Wilhelmy plate technique

The Dynamic Contact Angle (DCA) system commercially used by Cheng (2002) is shown in Figure 23. On the left side is the Wilhelmy Plate sample chamber in which the asphalt coated glass plate is suspended from the Cahn Balance, and on the right is the

data acquisition and processing system using the DCA software. The DCA software directly acquires force data from the Cahn Balance and automatically calculates the advancing and receding contact angles.

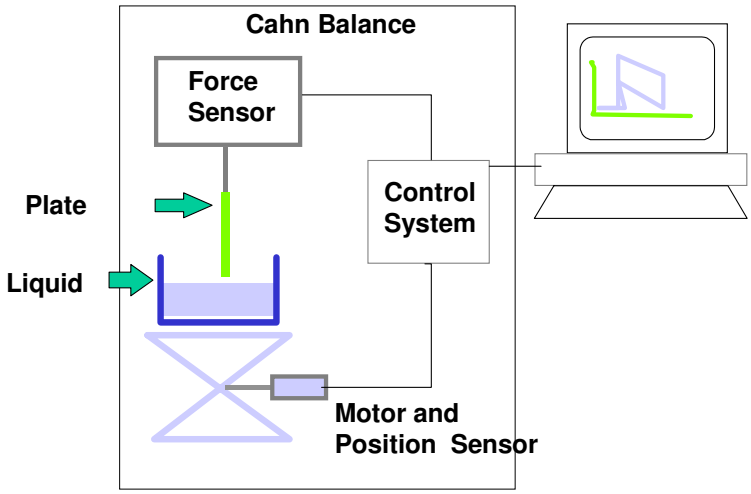

Figure 23. The Cahn Dynamic Contact Angle Analyzer (Thermo Cahn Instruments, 2002)

A typical output of the DCA experiment is shown in Figure 24. The advancing stage is represented by the bottom part of the hysteresis loop. When the plate advances to the liquid surface and touches it, a meniscus forms and the force increases substantially. As the plate is immersed, the advancing angle builds up with a corresponding decrease in mass due to buoyancy. As the direction of travel is reversed, the receding angle is measured and again, a slope due to buoyancy is observed.

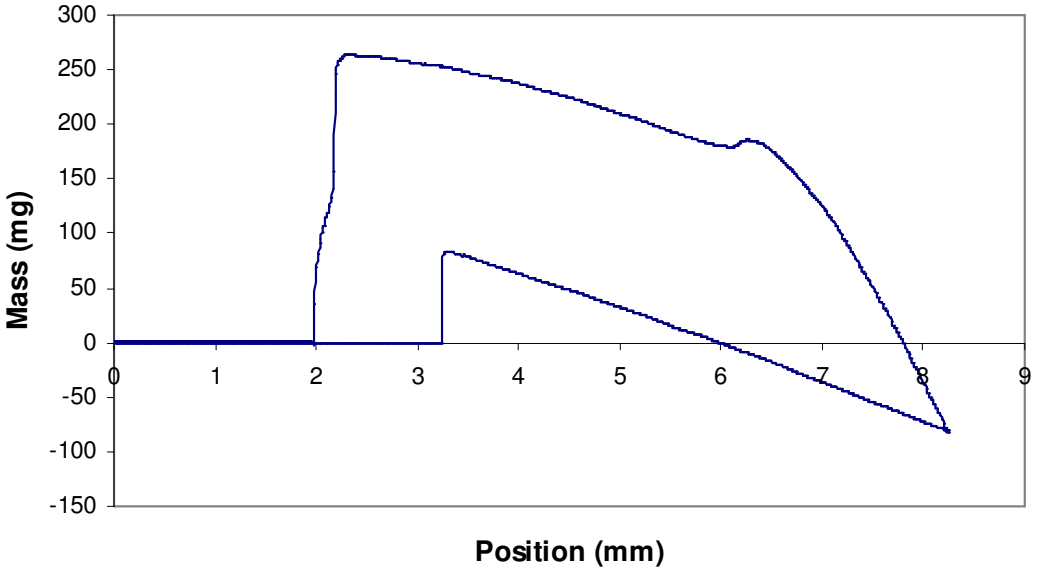

Figure 24. Typical contact angle hysteresis loop

The theory for calculating the contact angle from force measurements is presented below. When a plate is suspended in air, Equation (24) is valid.

$$F = Wt_{plate} + W_{bitumen} - V.\rho_{air}.g \qquad (24)$$

Where F is the force measured by the Cahn Balance, which includes the force required to hold the plate. Wt_{plate} and $Wt_{bitumen}$ are the weights of the glass plate the bitumen film respectively, V is the volume of the bitumen coated plate, ρ_{air} is the density of air, and g is the local acceleration of gravity.

When a plate is partially immersed in a liquid, the balance measures the force using Equation (25).

$$F = Wt_{plate} + Wt_{bitumen} + P_t\gamma_L \cos\theta - V_{im}\rho_L g - (V - V_{im})\rho_{air} g \qquad (25)$$

Where, P_t is the perimeter of the bitumen coated plate, γ_L is the total surface energy of the liquid, θ is the dynamic contact angle between the bitumen and the liquid, V_{im} is the volume immersed in the liquid, and ρ_L is the density of the liquid. By subtracting Equation (24) from Equation (25), Equation (26) is obtained.

$$\Delta F = P_t \gamma_L \cos\theta - V_{im}\rho_L g + V_{im}\rho_{air} g \tag{26}$$

Equation (27) is obtained by rearranging terms in Equation (26), and the contact angle can be calculated from all the parameters on the right hand side, which are determined during testing.

$$\cos\theta = \frac{\Delta F + V_{im}(\rho_L - \rho_{air})g}{P_t \gamma_L} \tag{27}$$

The relationship between the work of adhesion, expressed as a function of contact angle through the Youn-Dupré equation, and the surface energy components of the materials involved was introduced in Chapter II. According to the theory of van Oss et al. (1988),

$$\gamma_{Li}(1+\cos\theta_i) = 2\sqrt{\gamma_S^{LW}\gamma_{Li}^{LW}} + 2\sqrt{\gamma_S^-\gamma_{Li}^+} + 2\sqrt{\gamma_S^-\gamma_{Li}^-} \tag{28}$$

where γ_{Li}, γ_{Li}^+ and γ_{Li}^- are the known surface energy characteristics of the i^{th} liquid. The term θ_i can be measured using the Wilhelmy plate method. The three unknowns for the bitumen in this equation are: γ_S^{LW}, γ_S^+ and γ_S^-. These unknowns are the three components of asphalt surface free energy: Lifshitz-van der Waals, Lewis acid and Lewis base, respectively. To solve for the above parameters, at least three liquids with known surface energy components must be used to produce three simultaneous

equations. Elphingstone (1997) used water, formamide, glycerol, and ethylene glycol, while Cheng (2002) used water, glycerol, and formamide.

Sessile Drop Method

The Sessile Drop method is based on direct measurement of the contact angle of a known liquid on the surface of the material being tested. This approach is widely reported in the literature. While the plate technique measures a dynamic contact angle in a quasi-equilibrium state, the sessile drop approach measures a static contact angle. As in the case of Wilhelmy plate method, the three unknown surface energy components of the solid under investigation can be calculated using Equation (28) once the contact angles of each of the known liquids on this substrate is measured.

The test equipment for measuring the contact angle using this method, typically consists of a pre-aligned fixed optical system that is capable of capturing and analyzing the image of a sessile drop. A sessile drop (about 2 to 3mm in diameter) of the probe liquid is dispensed on a horizontal, flat surface of the material being tested using a syringe. The syringe tip can be replaced to generate the required drop volume and the syringe itself is operated by a computer controlled micro pump that can be adjusted to dispense a predetermined volume of the probe liquid. Once an image of the sessile drop is captured by the optical system, image analysis software is used to calculate the contact angle of the drop on the material being tested. The angle measurement can also be made manually using a print of the image shadow (Little et al. 2003). A schematic showing the set up of the test equipment is shown in Figure 25.

Bitumen and aggregate can be tested using this method. In the case of aggregate, the sample is polished to attain a flat smooth surface. This is not ideal, since the surface does not represent a natural crushed state. Since each measurement is made using a single drop that covers only an area of about 2 to 3 mm in diameter, the application of this test on aggregate surfaces containing relatively large minerals is questionable. In addition, conventional application of this approach on these high-energy surfaces is not possible since complete wetting occurs, i.e. a zero contact angle. Nevertheless,

researchers such as Ardebrant and Pugh (1991b) have used this approach on aggregates. In their work, the measurements were made in the presence of another immiscible liquid, thereby attaining a finite contact angle. This technique can be readily applied to bitumen by coating it onto a plate using a solvent cast approach. Measurement of the receding angle using the sessile drop technique is however difficult, if not impossible, because it requires a reverse action of the micro pump causing the drop to be sucked back into the syringe.

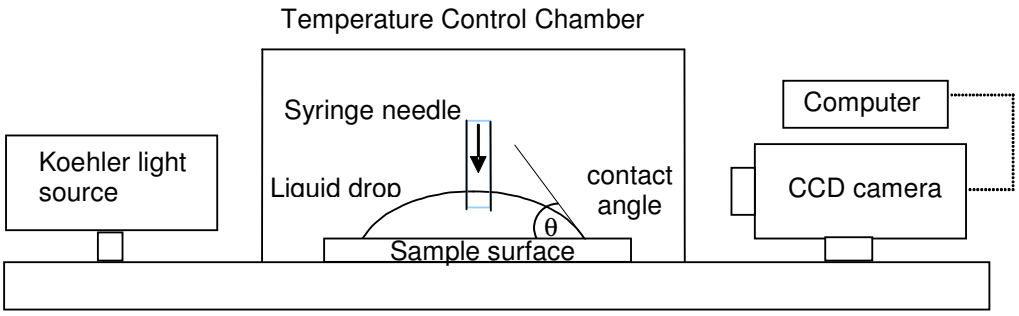

Figure 25. Schematic illustration of a sessile drop set-up (Adapted from Bose, 2002)

Wicking Method

Direct measurement of contact angles on flat surfaces is not feasible for particulate materials, such as powders. These materials exhibit surface roughness that leads to erroneous results. However, the rate of capillary rise of a liquid through a column packed with such particles can also yield the contact angle of the liquid with respect to the particle surface. The "wicking" approach uses the Washburn equation to obtain $\cos\theta$:

$$h^2 = \frac{tR\gamma_L \cos\theta}{2\eta} \tag{29}$$

Where h is the height that the column of liquid L has reached by capillary rise in time t, R the average radius of the pores, θ the contact angle, and η the viscosity of liquid L.

A value for R is obtained by first determining the wicking rate for a number of low energy, non-polar liquids, i.e. normal alkanes such as hexane and octane. These liquids spread over the surface of the high-energy surface so that $\cos\theta = 1$. With R known, contact angles of the selected probe liquids can be obtained and the surface energy characteristics of the solid particles determined using Equation (28).

In the column wicking approach, however, unreliable values can be obtained if columns are not uniformly packed, or if the particles are of irregular size or shape. These particle characteristics can cause strongly asymmetrical rise of the liquid in the packed column (van Oss, 1994; van Oss and Giese, 2003). An alternative approach is thin-layer wicking, which is similar to thin layer chromatography. In this method, particles are deposited onto a glass slide from a liquid suspension, and then air-dried. Van Oss et al. (2003) present detail information on sample preparation and testing using this approach. They also use thin layer wicking to determine specific surface areas (SSAs) of powders and compared the results obtained to conventional SSAs determined from conventional sorption techniques.

In conclusion, this approach only applies to aggregate in powder form, or fillers. Effective preconditioning of these samples may be a problem, since suction is required to hold the particles onto the slide. Some unconventional approaches, such as double-sided sticky tape has also been used (Chen, 2004).

VAPOR SORPTION TECHNIQUES

Vapor sorption techniques can be classified into two broad categories: 1) techniques that rely on the development of a vapor sorption isotherm, i.e. the amount of vapor adsorbed, or desorpbed, on the solid surface at a fixed temperature and partial pressure; and 2) techniques that rely on the volume of 'carrier' gas required to facilitate an adsorption-desorption interaction of the probe vapor with the surface when eluted through a column. The first category is sometimes called 'static' sorption and the

second ‘dynamic’ sorption. In this research, both the static and dynamic vapor sorption techniques will be considered under the first category, while the second category is reserved for inverse gas chromatography.

Different varieties of techniques are available to obtain sorption isotherms. Static sorption techniques are routinely used in industry to obtain the specific surface area of particles. A gravimetric static sorption technique was used by Li (1997) and later by Cheng et al. (2002) at Texas A&M University to obtain the surface energies of different aggregates. While volumetric based static sorption devices are also available and frequently used in the pharmaceutical and other industries, they are generally restricted to the use of inert gases. Dynamic sorption techniques differ from static techniques in that no vacuum is required in this process. Dynamic vapor sorption options that can accommodate organic vapors are commercially available nowadays (SMS, 2004). The gravimetric static sorption method is discussed in the following paragraphs.

In addition, Inverse gas chromatography is introduced. This is a well-established technique used for many decades, which received renewed interest in recent years for studying the surface energetics of solid particles.

Universal Sorption Device (USD)

This is a gravimetric static sorption technique, used to measure the sorption characteristics of selected vapors on aggregate surfaces. These quantities can then be used to calculate the surface energy parameters of aggregate. Sorption methods are particularly suitable due to their ability to accommodate the peculiarity of sample size, irregular shape, mineralogy, and surface texture associated with aggregates. In the method used by Li (1997) and Cheng et al (2002), an aggregate fraction between the No.4 (4.75 mm) and No.8 (2.36 mm) sieve size is suspended in the sample chamber, in a sample container manufactured from aluminum mesh. The chamber is vacuumed and the solute is injected into the system. A highly sensitive magnetic suspension balance is used to measure the amount of solute adsorbed on the surface of the aggregate at predetermined increasing levels of relative pressure. The surface energy of the aggregate

is calculated after measuring the adsorption of three different solutes with specific characteristics.

Static gravimetric sorption devices are generally custom built and comprise a number of components. A schematic of the main components of this setup is illustrated in Figure 26. A Mettler balance is securely established on a platform with a hang-down Rubotherm magnetic suspension balance and sample chamber beneath it. This balance has the ability to measure a sample mass of up to 200 g with accuracy of 10^{-5} g, which is sufficient for precise measurement of mass increase due to gas adsorbed onto aggregate. The USD also contains a temperature control unit, a mechanical vacuum pump, temperature and pressure transducers, and three vapor cylinders in an insulated chamber.

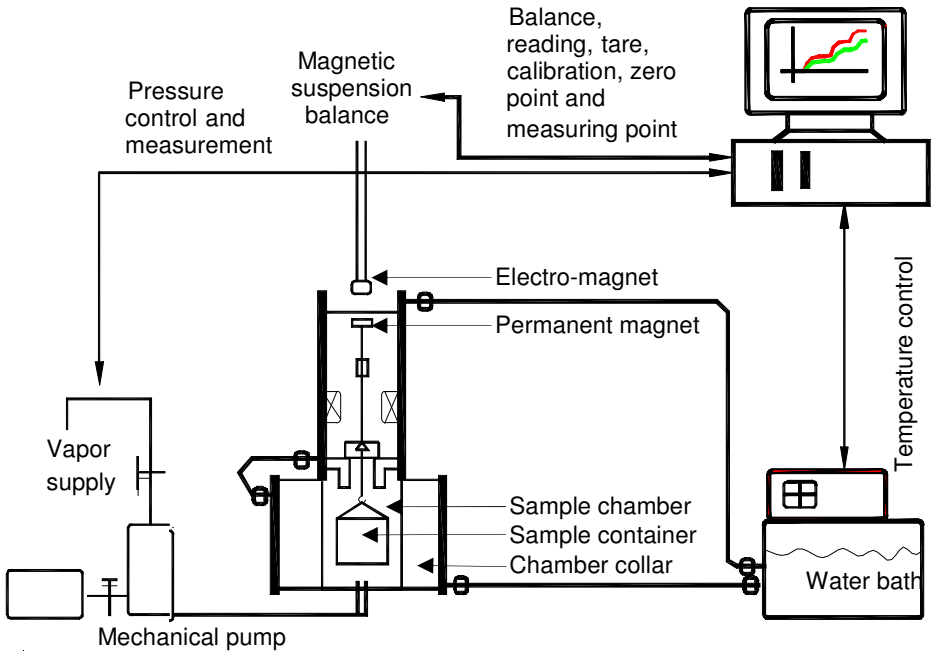

Figure 26. Schematic illustration of the Universal Sorption Device (Adapted from Cheng, 2002)

In a typical experiment, the saturation vapor pressure of the solute under consideration is arbitrary divided into 8 to 10 parts. Vapor is then introduced into the system to obtain the first pressure set point. This set point is maintained until equilibrium mass is reached. The USD at Texas A&M is fully automated and predetermined pressure set-points can be programmed before operation starts. These set points are automatically triggered when the captured balance readings reach equilibrium.

The resulting output is the amount of mass adsorbed at each of these pressure set points up to the maximum value, which is the saturation vapor pressure of the solute. This data can be used to construct an isotherm of amount adsorbed versus relative pressure at constant temperature. An example of a typical isotherm is presented in Figure 27.

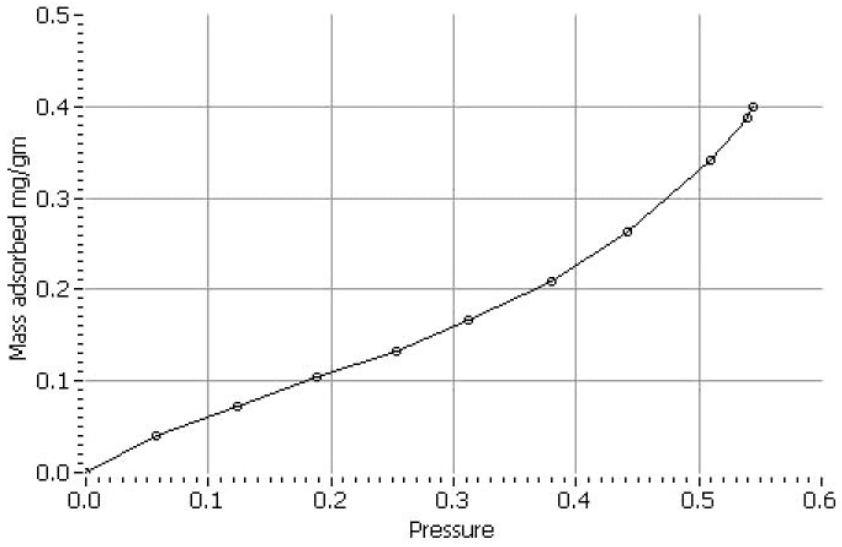

Figure 27. Typical adsorption isotherm (Little et al., 2004)

The two-parameter BET (Brunauer, Emmett, and Teller) model is applied to the isotherm data to obtain the specific surface area of the aggregate sample for the three gasses adsorbed. According to the BET theory, adsorption can be represented by the following linear equation,

$$\frac{P}{n(P_0 - P)} = \left(\frac{c-1}{n_m c}\right)\frac{P}{P_0} + \frac{1}{n_m c} \qquad (30)$$

where, P_0 is the saturated vapor pressure of the solute, P is the vapor pressure, n the specific amount adsorbed on the surface of the absorbent, n_m is the monolayer capacity of the adsorbed solute on the absorbent, and c the parameter theoretically related to the net molar enthalpy of adsorption. For the type of isotherms associated with the pressure conditions in these experiments, n_m can be obtained from the slope and the intercept of the straight line that fits the plot *P/n(P-Po)* versus *P/Po* best as illustrated in Figure 28.

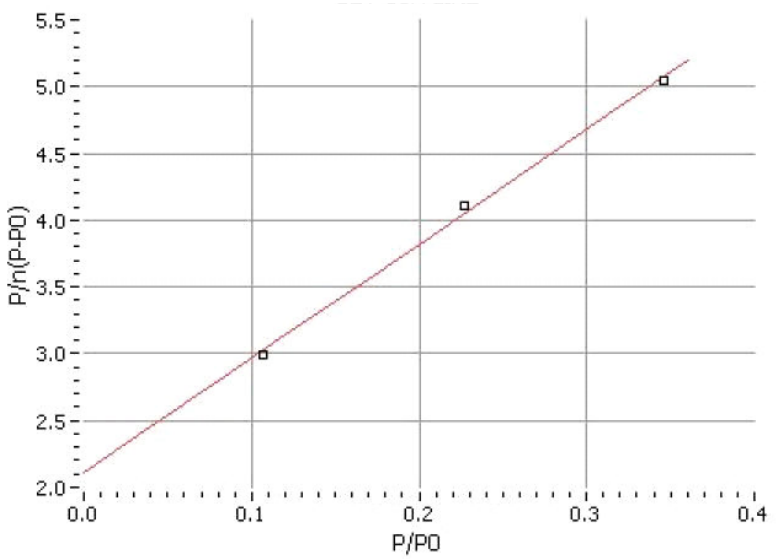

Figure 28. Plot for determining monolayer capacity, n_m (Little et al., 2004)

The specific surface area, *A*, of the aggregate can be calculated through the following equation,

$$A = \left(\frac{n_m N_o}{M} \right) \alpha \tag{31}$$

where α is the projected area of a single molecule, which can be calculated by the hexagonal close-packing model,

$$\alpha = 1.091 \left(\frac{M}{N_o \rho} \right)^{2/3} \tag{32}$$

In Equation (32), ρ is the density of the adsorbed molecule in liquid at the adsorption conditions, *M* is the molecular weight and N_o is Avogadro number.

The result from the BET equation is used to calculate the spreading pressure at saturation vapor pressure, π_e, for each solvent using the following form of the Gibbs equation,

$$\pi_e = \frac{RT}{A} \int_0^{p_0} \frac{n}{P} dP \tag{33}$$

where π_e is the spreading pressure of the solute at saturation vapor pressure, *R* is the universal gas constant, *T* is the absolute temperature, and A the specific surface area of absorbent calculated previously.

The work of adhesion of a liquid on a solid, W_a , can be expressed in terms of the surface energy of the liquid, γ_L , and the equilibrium spreading pressure of adsorbed vapor on the solid surface, π_e , as shown in Equations (34) and (35):

$$W_a = \pi_e + 2\gamma_L \tag{34}$$

Equation 16, proposed by van Oss et al. (1988), therefore becomes:

$$\pi_e + 2\gamma = 2\sqrt{\gamma_S^{LW}\gamma_L^{LW}} + 2\sqrt{\gamma_S^{+}\gamma_L^{-}} + 2\sqrt{\gamma_S^{-}\gamma_L^{+}} \quad (35)$$

The unknown surface energy components of the solid (S) can be solved if three solutes with known surface energy components are used. A non-polar solute, such as n-hexane, enables solving for the Lifshitz van der Waals component first. Equilibrium spreading pressures for the mono-polar and bi-polar solutes are subsequently used to determine the remaining acid and base components. Li (1997) and Cheng (2002) used n-hexane, the mono-polar basic liquid methyl propyl ketone (MPK), and distilled water.

Inverse Gas Chromatography (IGC)

Gas chromatography is a simple technique for the separation of solutes in a mixture. Each solute has a different interaction with a known material (stationary phase) in the chromatographic column, this results in different travel times for different solutes carried by an inert gas through the column. The retention time of each of the solutes depend on the nature of the stationary phase and the nature of the solute.

In inverse gas chromatography (IGC), solutes or probe molecules, with known properties are carried by an inert gas through a column packed with the material under investigation (Gutierrez et al., 1999). The retention time allows determination of characteristic thermodynamic properties of the column packing under investigation. Davis and Petersen (1966; 1967), Barbour et al. (1974), and Kim et al. (1997) used a similar approach, called inverse liquid-gas chromatography (IGLC) to investigate oxidative aging of bitumen. In this approach, dissolved bitumen was coated onto Teflon particles which where then packed into a column. Later, Barbour and his colleagues (WRI, 2003a; 2003b) modified this approach and coated the bitumen solution as a lining into a capillary column. The assessment was qualitative based on relative interaction coefficients calculated for different bitumen types.

Literature on this subject suggests that the simplicity, convenience of experimentation, and control of test conditions inspired the use of this technique in many industries, and proved to be effective in characterizing the surface energies of various

materials such as polymers, fibers, minerals, and pigments. IGC is a dynamic sorption technique. One of the main limitations of static sorption techniques, such as the USD, is the long time needed to obtain a complete adsorption isotherm, for some materials it may take days. Degassing to obtain a vacuum environment is not a requirement in IGC experiments (Charmas and Leboda, 2000).

The net retention volume (V_N) is the quantity from which the desired thermodynamic parameters can be determined, and is that volume of the carrier gas needed to push the probe molecule through the chromatographic column containing the solid of interest. If the solute concentration is sufficiently small (known as an infinitely diluted system), then V_N of an adsorbing probe can be computed form the flow rate of the carrier gas (D_c) and the measured net retention time (t_N) (Brendlé and Papirer, 1997a),

$$V_N = D_c t_N \tag{36}$$

The free energy of adsorption (ΔG_a) of a probe is related to V_N through Equation (37).

$$-\Delta G_a = RT \ln(V_N) \tag{37}$$

where R is the universal gas constant, and T the temperature. On the basis that the contributions of the non-specific components (mainly due to London, or dispersive forces) and specific components (mainly due to acid-base interactions) to the free energy of adsorption are additive, it follows that,

$$\Delta G_a = \Delta G_a^D + \Delta G_a^{SP} \tag{38}$$

As illustrated in Figure 29, the free energies of adsorption of different non-polar solutes, or normal alkanes, are usually linear with their associated molecular descriptors, e.g. the number of carbon chains. The free energy of adsorption of a polar probe with the same molecular descriptor value as a hypothetical alkane should be located above the "alkane reference line". The contribution of the non-specific (acid-base) interaction is

then given by subtracting the dispersive interaction at a representative point on the alkane line (Brendlé and Papirer, 1997b).

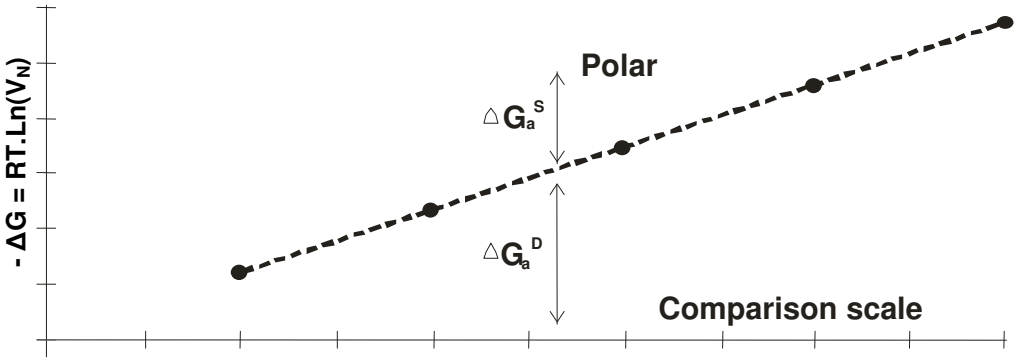

Figure 29. Principle of determining the dispersion and non-specific components of ΔG_a (Brendlé and Papirer, 1997b)

The free energy of adsorption of a single CH_2 group, ΔGa(CH2), is given by the slope of the n-alkane line. This value can then be used to calculate the dispersive component of surface energy of the solid, γ_S^D,

$$\gamma_S^D = \frac{1}{4\gamma_{CH2}}\left(\frac{\Delta G_a(CH_2)}{N \cdot a_{CH2}}\right)^2 \qquad (39)$$

where γ_{CH2} is the surface energy of a solid entirely made up of CH_2 (polyethylene), N is Avogardo's number, and a_{CH2} the cross-sectional area of an adsorbed CH_2 group (Brendlé and Papirer, 1997a).

Although the dispersive component of surface energy is commonly calculated from data obtained from IGC experiments, the quantitative evaluation of the acid-base

interaction parameters for solid surfaces is generally based on the enthalpy of specific interaction, ΔH_{AB}, between two molecules A and B. An extension of the so-called Gutmann equation is generally used where ΔH_{AB} between an amphoteric (exhibits both acid and base interaction capacities), and an amphoteric solid surface, is given by,

$$-\Delta H_a^{SP} = AN \cdot K_D + DN \cdot K_A \tag{40}$$

where AN (electron-acceptor number) and DN (electron-donor number) are the Gutmann numbers used to classify the probes as acidic, basic, or as amphoteric. K_A and K_D are the Acceptor and Donor numbers of the solid surface, respectively. The values for the solid surface are graphically determined by plotting ΔG^{SP} /AN vesus DN/AN. The slope of the line gives K_A, while the intercept gives K_D (Gutierrez et al, 1999; Uhlmann and Schneider, 2002).

Although the approach using the Gutmann numbers to quantify the acid-base interactions is widely used, it is not directly applicable to the theory adopted in this research. Goss (1997) applied the approach proposed by van Oss et al. (1988) to obtain the Lifshitz-van der Waals, acid and base components using IGC. The specific free energies are related to the acid and base components through,

$$\Delta G_{12}^{AB} = -Na2\left(\sqrt{\gamma_1^+\gamma_2^-} + \sqrt{\gamma_1^-\gamma_2^+}\right) \tag{41}$$

where N, Avogardo's constant, and a the area covered by one molecule, hence expressing ΔG as energy per mol in this instance, and surface energy components previously defined. The unknown surface energy components can therefore be determined by using monopolar acid and base probe molecules. This approach has the potential to characterize the surface energy components of bitumen and aggregates.

FORCE MICROSCOPY

With the advent of scanning tunneling microscopy (STM) in the 1980s, a whole family of related techniques were developed which, together with STM, may be classified in the general category of scanning probe microscopy (SPM) techniques. Of these later techniques, the most important is undoubtedly that of atomic force microscopy (AFM), also called scanning force microscopy (SFM) (Kolasinski, 2002; Niemantsverdriet, 2000). AFM uses a fine tip to measure surface morphology and properties through an interaction between the tip and surface. In this technique, a tip (30 to 50 nm) is attached to a non-rigid cantilever, and the force experienced by the tip when brought near the surface causes bending of the cantilever (Kolasinski, 2002).

This deflection is detected by reflection of a laser beam off the cantilever as illustrated in Figure 30.

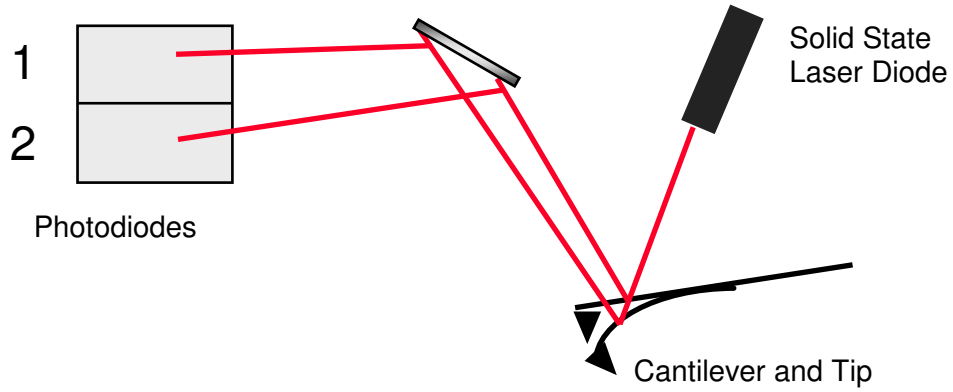

Figure 30. General AFM tip deflection measurement

The reflected laser beam strikes a position-sensitive photo detector consisting of two side-by-side photodiodes. The difference between the photodiode signals defines the position of the laser spot on the detector and thus the angle of deflection of the

cantilever. Figure 30 illustrates this reflection of the focused laser to two diodes, 1 and 2, when the tip is attracted or repelled by the sample. If the tip bends towards the surface, photodiode 2 receives more light than 1, and the difference in intensity between 1 and 2 is a measure of the deflection of the cantilever (Niemantsverdriet, 2000). Double photodiodes detect bending, quadrant diodes can detect bending, sideways deflection, and torsion simultaneously.

Digital Instruments (1998) classifies AFM operation into three modes, namely contact mode (CM), TappingMode^{TM},(TM), and non-contact mode (NM). Force-distance curves and friction forces can be obtained in CM, while TM and NM are used for imaging. A typical force-distance curve is presented in Figure 31.

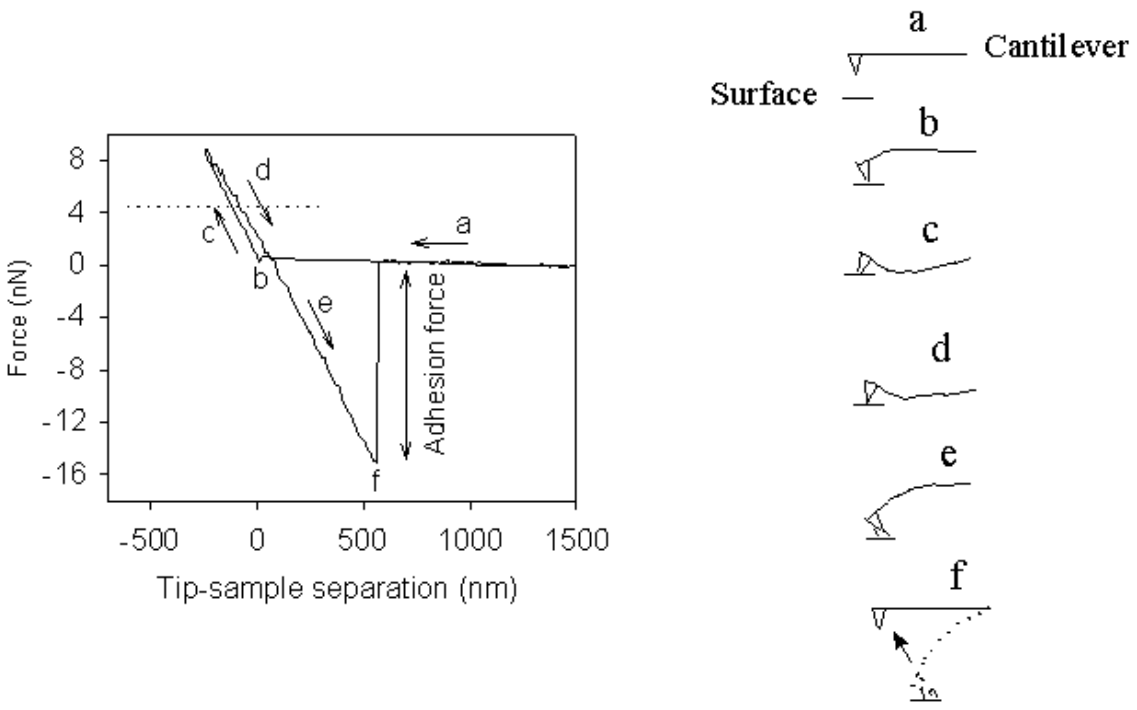

Figure 31. Typical force-distance curve obtained by AFM in contact mode (Digital Instruments, 1998)

The sample is moved by the piezoelectric scanner in the z-direction towards the cantilever (a). When the tip is sufficiently close to the surface, the interaction between the tip and substrate is large enough to overcome the force constant of the cantilever, and the tip "jumps into contact" with the substrate (b). The tip is then pressed against the substrate (c), retracted (d), through the point of zero deflection or force, and through (e). At point (f), the adhesive force between the tip and substrate is exceeded and the tip is pulled off the substrate.

The measured adhesive force, or pull-off force, is the key parameter for calculating the work of adhesion, W_a. A prerequisite, however, for converting the measured force to work of adhesion is to know the contact area between the cantilever tip and the substrate. This contact area cannot be measured and is usually predicted employing contact mechanics models. Beach et al. (2002) describe the Hertz model, the Derjagun-Muller-Toporov (DMT) model, and the Johnson-Kendal-Roberts (JKR) model. The DMT and JKR models are commonly used. The DMT model is applicable to smaller particles that are rigid, and with low surface energies, while the JKR model is applicable to larger particle radii, more compliant materials with high surface energies. The JKR model, which considers only short-range surface forces, explicitly treats the effect of adhesive bonding. The DMT model, which includes long-rang interactions, does not accurately assess adhesion-controlled compliance effects (Thomas et al., 1995). The following forms of these models are used to obtain the work of adhesion from adhesion force values.

$$\text{DMT model:} \quad F_a = 2\pi RW \tag{42}$$

$$\text{JKR model:} \quad F_a = \frac{2}{3}\pi RW \tag{43}$$

F_a is the adhesion force, or measured pull-off force, R is the particle radius, and W is the work of adhesion (Beach et al., 2002). Johnson, Kendal and Roberts reported that their model underestimates the work of adhesion but reasonably predicts the contact area at pull-off. Derjagun, Muller and Toporov, in contrast, reported that their model

accurately estimates the work of adhesion but predicts a zero contact area at pull-off (Thomas et al., 1995).

Pauli and his colleagues (WRI, 2003a) used a Digital Instruments MultiMode™ Scanning Probe Microscope to measure force-distance curves for eight Strategic Highway Research (SHRP) "core" bitumen types. In this technique, bitumen is solvent-cast onto a glass substrate to obtain a smooth surface. The process to calculate the surface energy is summarized below. The pull-off force just before separation of the cantilever tip and bitumen substrate is given by,

$$F(@\ D=0) = k\Delta z \tag{44}$$

where k is the known spring constant, and Δz is the deflection which defines the adhesion force. At equilibrium the work of adhesion between the cantilever (c) and substrate (s), is defined as,

$$W_{sc}(@\ D=0) = 2\sqrt{\gamma_c \gamma_s} \tag{45}$$

Employing the DMT model, the work of adhesion is related to the "measured" force by,

$$W_{sc}(@\ D=0) = \frac{F(@\ D=0)}{2\pi R} \tag{46}$$

where R is defined as the radius of curvature of the cantilever tip sphere. The surface energy of the substrate can be obtained in two different ways depending on the type or condition, of the tip used during force measurement. For purely adhesive interactions, the surface energy of the substrate material is given by,

$$\gamma_s = \frac{1}{\gamma_c}\left(\frac{k\Delta z}{4\pi R}\right)^2, \tag{47}$$

and for cohesive interactions, surface energy of the material is given by,

$$\gamma_s = \frac{k\Delta z}{4\pi R} \tag{48}$$

The researchers observed that at the initial contact of a new cantilever with a fresh film of bitumen, the tip is found to coat with bitumen by a capillary effect. The cohesive form, Equation 48 was therefore applied.

Figures 32 and 33 show typical force-distance curves obtained for bitumen by Pauli and his collegues (WRI, 2003a). Figure 32 represents bitumens of lower molecular weight, associated with more brittle behavior. Bitumens studied from the material reference library (MRL) in this group include codes AAD-1, AAG-1, AAA-1, and AAK-1. The linear relationship between deflection (or force) and retraction distance as well as the more or less sharp point at pull-off is typical for brittle materials. Figure 33 in contrast, represents higher molecular weight bitumens which typically exhibit more ductile behaviour. MRL bitumens tested in this group includes AAB-1, AAM-1, and AAC-1. The non-linear relationship between deflection and retraction distance and the less adrupt failure at pull-off is evidence of the viscoelastic nature of these materials.

The curves presented here also indicate that the pull-off force varies with applied variation in sampling frequency of the cantelever which is more pronounced for the more ductile bitumens. Apart from frequency, other parameters such as the applied loading force and tip size can also influence the magnitude and variability of pull-off force, and thus calculated surface energies significantly.

With this technique it would be possible to manufacture or purchase functionalized cantilever tips, i.e. precoated with substances comprising selected chemical species (non-polar, acid, and basic), in order to determine surface energy components (Thomas et al., 1995). Possible contamination of these tips with bitumen may, however, undermine the effctiveness of this approach to bitumen. The small scale on which these measurements are performed, make its application to aggregates unpracticle due to inhomogeneity of these materials. In addition, aggregate surfaces would have to be polished to obtain smooth substrates required for force microscopy.

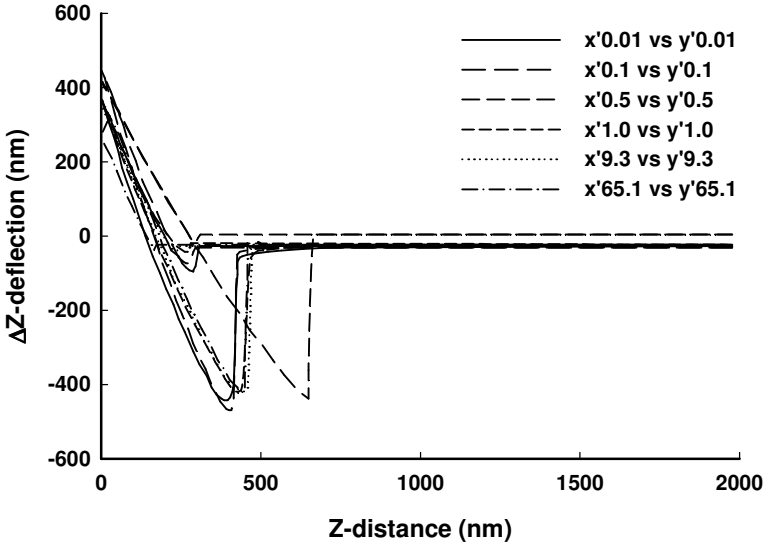

Figure 32. AFM force curve of SHRP core bitumen AAD-1 measured as a function of contact rate at constant loading (WRI, 2003a)

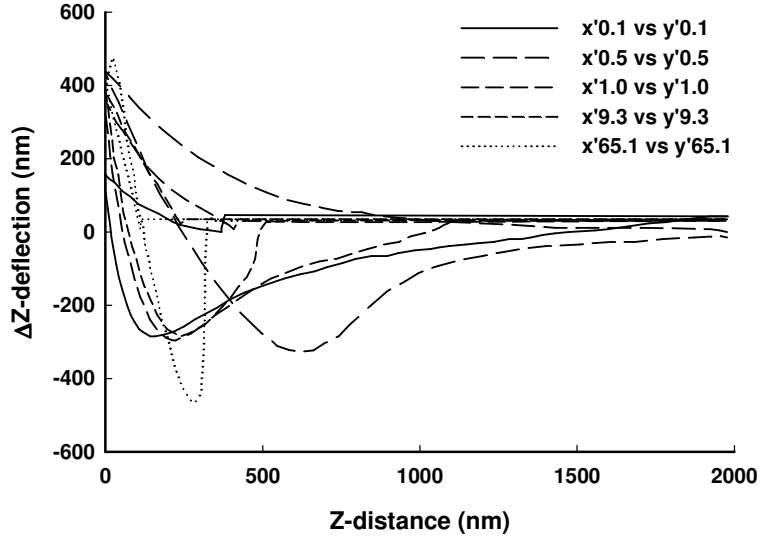

Figure 33. AFM force curve of SHRP core bitumen AAM-1 measured as a function of contact rate at constant loading (WRI, 2003a)

MICROCALORIMETRY

Two types of microcalorimetric methods are available, namely immersion and flow microcalorimetry. Only the former type will be considered in this discussion to illustrate how these thermo-analytical methods have been applied to obtain surface energies of talc and swelling clay minerals as described by Médout-Marére et al. (1998) and Malandrini et al. (1997). Two experiments can be performed. In wetting calorimetry, the initial surface state of the solid is different, i.e. there is a third phase involved, the vapor phase. This state is described by the Young equation for a triple phase system. In this simple experiment, the solid is immersed in a liquid at constant temperature and constant (usually atmospheric) pressure. In immersion calorimetry a solid, which is maintained under vacuum, is immersed directly into a liquid phase. The solid is maintained under vacuum in a closed glass bulb, immersed into the liquid and then the glass bulb is broken. Thermal effects are attributed primarily to the disappearance of the solid-vacuum interface and to the formation of a solid-liquid interface.

A schematic of part of the differential conduction microcalorimeter set up, specifically a Tian-Calvet microclaorimeter, is illustrated in Figure 34.

Both of the experiments described above can be performed with this instrument. This calorimeter cell is approximately 100 mm long and the total length of the calorimeter is approximately 1200 mm. Different components of the system as shown in Figure 34 are the thermopiles (1), dead volume of the cell (2), the glass rod (3), dead volume of the bulb (4), bulb (5), powder sample (6), and liquid (7).

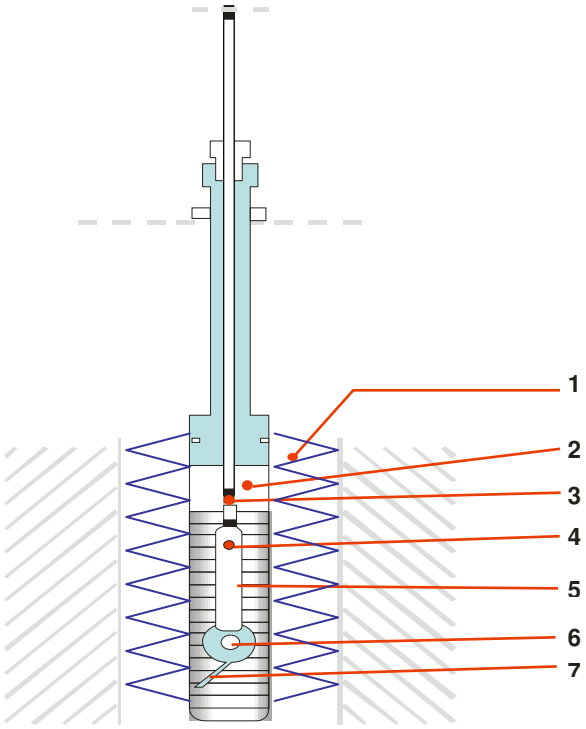

Figure 34. Immersion microcalorimeter (Adapted from Médout-Marére et al., 1998)

In order to consider this as a candidate technique, it is important to evaluate the possible use of the measured sorption heats to obtain surface energy and its components. The wetting experiment is considered first. Fundamentally, the thermodynamic relation between the Gibbs free energy (G) and enthalpy (H), entropy (S) and temperature (T) was previously introduced in Chapter II, Equation (1).

$$\Delta G = \Delta H - T\Delta S \tag{1}$$

The enthalpy of adhesion is expressed as:

$$\Delta H = \Delta G + T\Delta S = \Delta G - T\left(\frac{\partial G}{\partial T}\right) \tag{49}$$

Young's equation, introduced in the previous chapter, states:

$$\gamma_{LV}\cos\theta = \gamma_{SV} - \gamma_{SL} \tag{50}$$

where γ_{SV} is the interfacial free energies between the solid (S), vapor (V), and liquid phases (L). In the wetting experiment, the free energy of immersion is given by the following relationship:

$$\Delta G_i = \gamma_{SL} - \gamma_{SV} \tag{51}$$

Therefore, if Equation (51) is substituted into (49),

$$\Delta H = \gamma_{LV}\cos\theta - T\left(\frac{\partial(\gamma_{LV}\cos\theta)}{\partial T}\right) \tag{52}$$

Equation (52) can also be expressed in terms of the three surface energy components by replacing the free energy term with the acid-base interaction part of the van Oss-Chaudhury-Good equation. Equation (52) implies that one would be able to either calculate the contact angle from wetting immersion calorimetry, or the enthalpy of adhesion. However, the eventual measurement of contact angles at different temperatures is required to evaluate the role of the entropic term (Della Volpe and Siboni, 2000, Yildirim, 2001).

Malandrini et al. (1997) show how "surface enthalpy components" can be determined by immersion calorimetry using the acid-base theory but applied enthalpy instead of the Gibbs free energy. The following relationship between enthalpy and Gibbs free energy at constant temperature can be used to obtain surface energies from microcalorimetry.

$$\Delta H = f\Delta G \tag{53}$$

where

$$f = 1 - T\left(\frac{\Delta S}{\Delta H}\right) \tag{54}$$

The value of f has been evaluated by obtaining values for ΔG and ΔH from gas adsorption experiments and from immersion calorimetry, respectively (Malandrini et al., 1997; Médout-Marére et al.,1998).

The microcalorimetry method is attractive in that the measurement of sorption heats is relatively simple. The wetting experiment is fast but introduces an additional factor that needs to be considered, i.e. entropy in Equation (1). A procedure, which would require the measurement of contact angles of the aggregate at different temperatures would be neither practical nor efficient and cannot be considered as a feasible candidate technique. The second immersion experiment described above requires measurement of sorption heats in a vacuum. The experimental preparation is similar to the current USD procedure and requires degassing at an elevated temperature. In addition to calorimetry experiments, vapor sorption experiments would need to be performed to obtain the factor f to account for entropy.

CONCLUSIONS

Potential techniques to characterize surface energies of both bitumen and aggregate were introduced in this chapter. Practicality for routine testing and the ability to use these techniques to produce surface energies and its related components according to the theory by van Oss et al. (1988) were discussed. Table 4 summarizes the techniques presented with the measured parameters and the most conceivable applications in terms of bitumen and aggregate characterization.

Contact angle techniques are relatively simple and widely used in adhesion science. Bitumen surface energies have been determined using the Wilhelmy plate technique at Texas A&M University in the past. In contrast to the WP technique, the sessile drop technique measures static contact angles that are closer to the assumption of equilibrium conditions. This approach has recently been used on bitumen at the University of Rhode Island. Bitumen surface energies have also been characterized by atomic force microscopy (AFM) at the Western Research Institute (WRI) in Wyoming. While contact angle approaches produce macroscopic parameters, AFM works on a microscopic level,

which makes it a powerful tool for research purposes. The applicability for routine work in asphalt laboratories is, however, questionable.

Table 4. Summary of techniques for surface energy characterization

Technique	Parameter	Materials
Wilhelmy Plate Method	Contact angle indirectly	Bitumen
Sessile Drop Method	Contact angle directly	Bitumen
Wicking Method	Contact angle indirectly	Aggregate powder
Universal Sorption Device	Equilibrium spreading pressure	Aggregate
Atomic Force Microscopy	Adhesion force	Bitumen
Inverse Gas Chromatography	Retention time	Bitumen and aggregate
Microcalorimetry	Enthalpy	Aggregate

Inverse gas chromatography (IGC) is an attractive technique due to its simplicity and speed. This technique became popular in recent years for characterization of the energetics of solid particles. Oxidative aging of bitumen has been assessed since the 1960's using IGC. This was accomplished by coating bitumen from solution onto particles which were then packed into a column. Recently, this methodology was improved by coating bitumen from solution onto the walls of a capillary column. This technique is a strong candidate for characterization of surface energies of bitumen. Static vapor sorption techniques on the other hand, are not particularly suitable for use with bitumen due to absorption of vapors into the bulk and ability of these compounds to dissolve bitumen under static conditions.

Macroscopic heterogeneity, texture and shape of aggregates present a complexity associated with these surfaces that limit the applicability of many of the aforementioned

techniques for surface energy characterization. In addition, manufacturing of smooth sample surfaces are a prerequisite for direct contact angle measurements and AFM. Contact angles can be obtained indirectly on powdered particles by a wicking approach, but reliability of this technique is questionable due to an uneven capillary front produced when particles of uneven size and shape are used. Although IGC has been used extensively to characterize solid particles, heterogeneity of road building aggregates may be an important determining factor in the applicability of this technique to these materials.

Static vapor sorption techniques have been used in the past and appear to be one of the few suitable techniques for aggregate surface energy characterization. The universal sorption device, essentially a highly sensitive magnetic suspension balance, is a sophisticated device and not particularly suitable for routine work in conventional asphalt laboratories. Nowadays, however, more user-friendly "off-the-shelve" vapor sorption equipment exists that are compatible with different organic vapors and which can produce the same data.

Microcalorimetry is a relatively quick and simple technique that is commonly used to obtain enthalpy values. Supplementary testing is however required to utilize this technique in determining surface free energies of the materials under consideration. This aspect of the microcalorimetry approach makes it difficult to compete as a candidate test.

CHAPTER IV

SURFACE ENERGY CHARACTERIZATION OF BITUMEN AND AGGREGATE

INTRODUCTION

The concepts and theories of existing and potential techniques to determine surface energies of bitumen and aggregate were presented in Chapter III. The objectives of this chapter are to: 1) assess and refine methodologies for existing techniques; 2) introduce alternative technique(s) and 3); characterize bitumen and aggregates representing a range of chemical compositions.

In Chapter II, it was pointed out that the theory presented by van Oss et al. (1988) received much critique in the past. It was stated that recent work by Della Volpe and Siboni (2000) suggests that the root of these apparent problems should be sought in the application of the theory to contact angle data. These considerations and other refinements of the contact angle approach using the Wilhelmy plate method are addressed in this chapter. Literature on inverse gas chromatography indicates that this technique has been used successfully to characterize the surface energetics of different materials such as polymers and minerals. The Western Research Institute (WRI, 2003a; 2003b) developed a protocol to assess oxidative aging of bitumen using an inverse gas-liquid chromatography approach. Inverse gas chromatography is proposed as an alternative technique for surface energy characterization of bitumen. Finally, surface energy characteristics of aggregates are determined by an improved methodology with the universal sorption device. The results presented in this chapter pave the way for prediction of adhesion between bitumen and aggregate in the presence of water.

MATERIALS

Five bitumen and five aggregate types were obtained from the Materials Reference Library (MRL) in Reno, Nevada. These materials were primarily used during the Strategic Highway Research Program (SHRP) and a wealth of information therefore exists, which could be beneficial to interpretation of results obtained during this research. Table 5 summarizes the MRL codes, source, physical and chemical properties of the selected bitumen types. The functional group composition is based on infra-red analysis and only for tank bitumen, not aged.

Table 5. Source and description of bitumen types (SHRP, 1993)

Code	Source	Physical	Chemical (Functional groups), mol/liter						
			CA	A	Q	K	PH	S	P
AAB-1	Wyoming Sour	AC-10 PG58-22	< 0.005	0.000	0.012	< 0.005	0.06	0.064	0.140
AAD-1	California Coast	AR-4000 PG58-28	0.015	0.000	0.027	< 0.005	0.130	0.036	0.190
AAF-1	West Texas Sour	AC-20 PG64-10	< 0.005	0.000	0.007	< 0.005	0.010	0.050	0.140
AAM-1	West Texas Inter	AC-20 PG64-16	< 0.005	0.000	0.013	< 0.005	0.070	0.023	0.170
ABD	California Valley	AR-4000 PG58-10	0.025	0.000	0.015	< 0.005	0.077	0.024	0.376
Legend: CA: carboxylic acid; A: anhydride; Q: quinolones; K: ketones; PH: phenols; S: sulfoxides; P: pyrroles									

Table 6 summarizes the MRL codes, origin, description and major minerals present in the selected aggregates. These mineral quantities are the totals over different rock types that may have formed part of the quarry, or gravel pit as part of the primary descriptive aggregates. Note that RL is a mixed gravel, consisting primarily of siliceous aggregate, but also contains carbonaceous aggregate.

Table 6. Description, origin, and major mineralogical composition of aggregates (SHRP, 1991)

Code	Description and Origin	Major Minerals, %						
		C	Q	P	K	O	B	A
RA	Lithonia granite: Grayson, Georgia	0	55	14	25	1	6	0
RD	Limestone: White Marsh, Maryland	83	3	0	0	0	0	0
RG	Sandstone: Connellsville, Pennsylvania	49	47	0	3	1	0	0
RK	Basalt: Hermiston, Oregon	1	4	34	1	36	0	12
RL	Gulf Coast gravel: Sullivan City, Texas	15	65	1	2	11	0	0
Legend: C: calcite; Q: quartz; P: plagioclase feldspar; K: potassium feldspar; O: opaques; B: biotite; A: augite								

CONTACT ANGLE EXPERIMENTS

The Wilhelmy plate technique was used to characterize bitumen surface energies. General theory and concepts are presented in Chapter III. Detailed test methodologies and analysis procedures used in this research are presented in the following paragraphs.

Wilhelmy Plate Method

Microscope glass slides (24mm×60mm, No.1.5) are used as substrates for preparation of bitumen films. A coated slide can only be tested once and the number of liquids therefore, dictates the number of slides prepared. In this research, three replicate measurements were made. A set of five liquids therefore required at least fifteen slides. A tin with an approximate capacity of 50g, pre-filled with bitumen, is placed in an oven at the mixing temperature of the bitumen under consideration. The tin with bitumen is removed from the oven after about one hour, stirred, and placed on a hot plate to maintain the desired temperature during the coating process. The end of the glass slide

intended for coating is passed six times on each side through the blue flame of a propane torch to remove any moisture. The handheld slide is dipped into the molten bitumen to a depth of approximately 15 mm. Excess bitumen is allowed to drain from the plate until a very thin (0.18 to 0.35 mm) and uniform layer of at least 10 mm remains on the plate. It should be emphasized that a thin coating is required to reduce variability of the results. The plate is then turned with the uncoated side downwards and carefully placed into a slotted slide holder. If necessary, the heat-resistant slide holder, with all the coated slides can be placed in the oven after coating for 15 to 30 seconds to obtain the desired smoothness. The bitumen-coated plates are placed in a desiccator overnight.

A DCA 315 microbalance and WinDCA software from Thermo Chan Instruments were used to perform the test, acquire force data, and calculate contact angles. Balance calibration was performed with a 500 mg weight according to the manufacturer's specification. Five probe liquids (HPLC grade, Sigma-Aldrich) including distilled water, glycerol, formamide, ethylene glycol, and methylene iodide (diiodomethane) were used in these experiments. Important method parameters include the surface tension of the probe liquids, local gravitational force, plate speed, and penetration depth. A speed of 20μm and penetration depth of 5 mm was used in these experiments. A low speed is required to ensure quasi-equilibrium conditions, which approaches the assumption of equilibrium. A glass beaker is filled with the test liquids to a depth of at least 10 mm and placed on the balance stage. A dark beaker is used for methylene iodide since this liquid is light sensitive. Liquid surface tension data suggests that a fresh sample be used for each set comprising of three replicate slides. One coated slide is removed from the desiccator at a time. The width and thickness are measured to an accuracy of 0.01 mm for calculation of the slide perimeter. A clip (crocodile clamp) -hook assembly (Thermo Chan Instruments) is clipped onto the slide as close as possible to the center and at right angles with the slide edge. The slide is suspended onto the measuring hook, and the stage adjusted to a height where the liquid surface is in close proximity to the bottom of the slide, without touching.

After data acquisition, manual analysis of the force-distance data is performed. Buoyancy correction based on slide dimensions and liquid density can introduce unwanted variability into the resulting contact angles. To eliminate these effects, a regression analysis of the buoyancy line and extrapolation to the force at zero depth is performed. In this procedure, it is important to select a representative area of the line for regression analysis as illustrated in Figure 35.

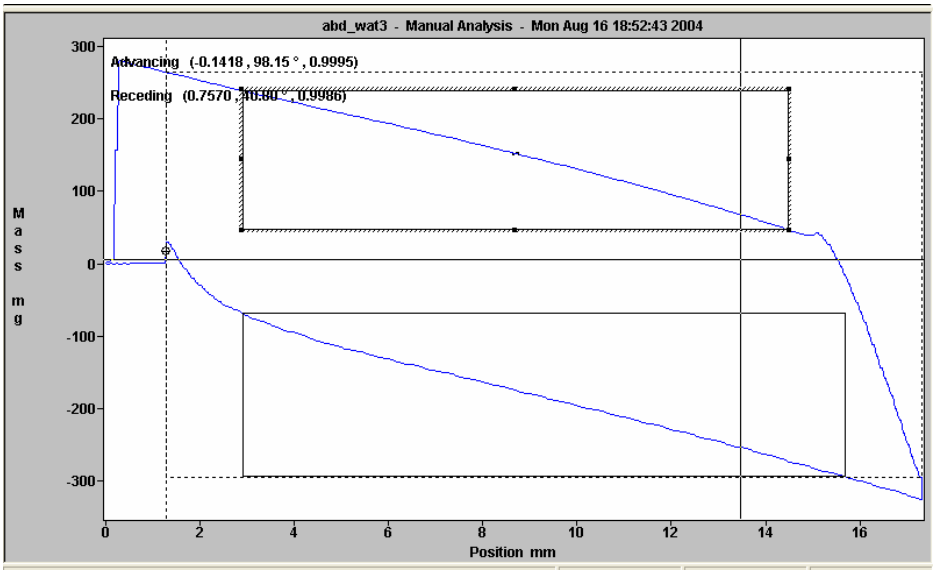

Figure 35. Selection of representative area for regression analysis (Captured from WinDCA Software).

Analysis

The van Oss-Chaudhury-Good theory has been applied widely during the 1990s to determine the surface energy components of solid surfaces from contact angle data. Contradicting results have, however, been published and some authors have questioned the practical use of this theory. Della Volpe and Siboni (1997, 2000) conducted

pioneering work in their effort to resolve these problems. They show that the theory itself is perfectly legitimate but its results must be considered with care. Problems arising from the application of this theory to the calculation of surface energies of low energy surfaces (polymers and polymer-like materials) from contact angle data and proposed solutions are briefly presented in the following paragraphs.

The Scale Problem

Analyzed results show basic components systematically greater than acid components. The van Oss-Chaudhury-Good equation (Equations 16 and 32) is essentially non-linear if neither one of the two coefficient sets, representing the two materials under consideration, are considered as parameters. If, however, one set of coefficients is known, they become parameters and the function becomes linear in the unknown coefficients. With this non-linearity unmasked, a best-fit solution of this model implies the existence of an infinite number of solutions. The only way to solve this problem is to choose convenient reference values for a suitable liquid, e.g. water. The original scale selected by van Oss and co-workers assumes the γ^+ / γ^- ratio of water to be equal to unity at 20˚C, i.e. each component contributes 25.5 mJ/m^2. Chemists generally consider atmospheric water to be a stronger Lewis acid than base. Although at this point it is not known what the true ratio for water is, Della Volpe and Siboni propose that it is greater than one and the interval 3.2 to 5.5 can be considered reasonable. The original scale, however, does allow relative comparisons of the acid and base components for different materials. This means that comparison of the acid and base component of the same material is not allowed. In addition, the chosen scale does not affect the total surface energy and work of adhesion quantities (van Oss, 1994; Dela Volpe and Siboni, 1997, 2000). Although other scales have been proposed, much work is required to obtain a definitive solution to this problem. Furthermore, these scales have mostly been developed for liquids suitable for contact angle experiments and values for polar compounds used in gas sorption experiments are presently unavailable.

Selection of a Liquid Set

The choice of the liquid set dictates the results. This tendency is due to ill-conditioning of the related set of equations. This is a mathematical feature, intrinsic to the chemical nature of the selected liquid set. The effect can be eliminated, or reduced by selecting a proper set of liquids that represent different chemical properties. The condition number (CN) is able to provide information on the ill-conditioning of a matrix and is associated with any particular operation that could be done on it, e.g. inversion. Ill-conditioning means that a slight change in the coefficients of the equations result in a large modification of the solution. A large condition number (generally greater than about 10) means a strong sensitivity of solutions to data errors.

The Negative Square Root Problem

While the unknowns are practically the roots of the surface energy components, they sometimes assume negative values. This effect is reduced with the selection of a large and proper liquid set, and measurement and analyses of contact angles in a suitable way. In many cases where these solutions occur, the standard deviation of a negative component is typically greater than the component itself. Negative coefficients are therefore a consequence of measurement uncertainty combined with possible ill-conditioning of the equation set. Della Volpe and Siboni state that other contributory effects, and even origins of these solutions in some cases, cannot be excluded. In addition, singular value decomposition (SVD) is a powerful numerical procedure that deals with sets of equations or matrices that are either singular or numerically very close to singular. It is therefore appropriate to utilize this technique when solving for the surface energy components through a linear least squares best-fit approach. Despite taking all of these precautions, negative square roots can still show up. Apart from the fact that these components are usually close to zero, a negative root implies that the component can be either negative or positive. Setting these values equal to zero is therefore the best approach under these conditions.

The SVD approach and calculation of condition number is mathematically defined below. SVD is based on the following linear algebra theorem: "Any M × N matrix **A** whose number of rows M is greater or equal to its number of columns N, can be written as the product of an M × N column-orthogonal matrix **U**, an N × N diagonal matrix **W** with positive or zero elements, and the transpose of an N × N orthogonal matrix **V**" (Press et al., 1989). Consider the following form of the model proposed by van Oss, Chaudhury and Good with all the terms as previously defined.

$$\sqrt{\gamma_{Li}^{LW}\gamma_{S}^{LW}}+\sqrt{\gamma_{Li}^{+}\gamma_{S}^{-}}+\sqrt{\gamma_{Li}^{-}\gamma_{S}^{+}}=\frac{1}{2}\gamma_{Li}^{Tot}\left(1+\cos\theta_{i}\right)=\frac{1}{2}W^{a} \tag{55}$$

The set of over determined linear equations to be solved in order to find the least squares solution can be given as:

$$\begin{pmatrix}\sqrt{\gamma_{L1}^{LW}} & \sqrt{\gamma_{L1}^{+}} & \sqrt{\gamma_{L1}^{-}}\\ \mathrm{M} & \mathrm{M} & \mathrm{M}\\ \mathrm{M} & \mathrm{M} & \mathrm{M}\\ \sqrt{\gamma_{Lm}^{LW}} & \sqrt{\gamma_{Lm}^{+}} & \sqrt{\gamma_{Lm}^{-}}\end{pmatrix}_{M\times 3}\cdot\begin{pmatrix}\sqrt{\gamma_{S1}^{LW}}\\ \sqrt{\gamma_{S1}^{-}}\\ \sqrt{\gamma_{S1}^{+}}\end{pmatrix}=\frac{1}{2}\begin{pmatrix}\gamma_{L1}\cos\theta_{1}\\ \mathrm{M}\\ \mathrm{M}\\ \gamma_{Lm}\cos\theta_{m}\end{pmatrix}_{M\times 1} \tag{56}$$

or, $$\boldsymbol{A}\cdot\boldsymbol{x}=\boldsymbol{b} \tag{57}$$

and therefore, $$\boldsymbol{x}=\boldsymbol{A}^{-1}\cdot\boldsymbol{b} \tag{58}$$

According to the SVD theorem, decomposition of the matrix **A** takes the following form with terms defined above.

$$\boldsymbol{A}=\boldsymbol{U}\cdot\boldsymbol{W}\cdot\boldsymbol{V}^{T} \tag{59}$$

U and **V** therefore enter the SVD decomposition of **A**. This decomposition is always possible and "almost" unique. In addition, the condition number (CN) of a matrix is formally defined as the ratio of the largest of the w_j's to the smallest of the w_j's of the diagonal matrix **W**. From Equation (59) it follows that the inverse of **A** is:

$$\boldsymbol{A}^{-1} = \boldsymbol{V} \cdot [diag\ (1/w_j)] \cdot \boldsymbol{U}^{\boldsymbol{T}} \tag{60}$$

thus,

$$\boldsymbol{x} = \boldsymbol{V} \cdot [diag\ (1/w_j)] \cdot \boldsymbol{U}^{\boldsymbol{T}} \cdot \boldsymbol{b} \tag{61}$$

The object of the least squares problem is to obtain the best parameters, a_k, that minimize the goodness-of-fit measure, χ^2, which can be written as:

$$\chi^2 = |\boldsymbol{A'} \cdot \boldsymbol{a} - \boldsymbol{b'}|^2 \tag{62}$$

The solution to the least squares problem, Equation (61), then becomes:

$$\boldsymbol{a} = \sum_{i=1}^{M} \left(\frac{\boldsymbol{U}_{(i)} \cdot \boldsymbol{b}}{w_i} \right) \boldsymbol{V}_{(i)} \tag{63}$$

Errors due to the measured contact angles and the surface tension of the liquids are taken into account by $\mathbf{A'}$ and $\mathbf{b'}$, defined as follows (Bhasin, 2004):

$$\boldsymbol{A'} = \begin{pmatrix} \frac{\sqrt{\gamma_{L1}^{LW}}}{\sigma_1} & \frac{\sqrt{\gamma_{L1}^{+}}}{\sigma_1} & \frac{\sqrt{\gamma_{L1}^{-}}}{\sigma_1} \\ \mathrm{M} & \mathrm{M} & \mathrm{M} \\ \frac{\sqrt{\gamma_{Lm}^{LW}}}{\sigma_m} & \frac{\sqrt{\gamma_{Lm}^{+}}}{\sigma_m} & \frac{\sqrt{\gamma_{Lm}^{-}}}{\sigma_m} \end{pmatrix}_{M \times 3} \tag{64}$$

and,

$$\boldsymbol{b'} = \begin{pmatrix} \frac{\gamma_{L1} \cos\theta_1}{\sigma_1} \\ \mathrm{M} \\ \frac{\gamma_{Lm} \cos\theta_m}{\sigma_m} \end{pmatrix}_{M \times 1} \tag{65}$$

Where the propagated error σ_x, with $x = 1$ to m, are the propagated errors calculated as follows (Bhasin, 2004):

$$\sigma_x^2 = \sigma_u^2\left(\frac{\partial x}{\partial u}\right)^2 + \sigma_v^2\left(\frac{\partial x}{\partial v}\right)^2 \tag{66}$$

with σ_u the error in the total surface tension of the probe liquid, and σ_v the error in the measured contact angles with the probe liquid under consideration. From Equation (55),

$$\frac{\partial x}{\partial u} = \frac{1}{2}\gamma_L \tag{67}$$

and,

$$\frac{\partial x}{\partial v} = -\frac{1}{2}\gamma_L \sin\theta \tag{68}$$

Finally, the variance of the parameters of $\boldsymbol{x}$, a_j (with j = 1 to 3), can be estimated from the following expression:

$$\sigma^2(a_j) = \sum_{i=1}^{m}\left(\frac{V_{ij}}{w_j}\right)^2 \tag{69}$$

Where a_j represents the square roots of the surface energy components of the solid under investigation. Average contact angles and standard deviations of each liquid can therefore be used to obtain the corresponding surface energy statistics. This approach conveniently addresses the fact that each contact angle measurement has to be performed on a new surface.

Surface energy characteristics of the probe liquids used in contact angle experiments and analyses are summarized in Table 7. These values are referenced to water and based on the original 1:1 scale proposed by van Oss and his colleagues.

Table 7. Surface energy characteristics of probe liquids at 20˚C, mJ/m^2 (van Oss, 1994)

Liquid	γ^{Total}	γ^{LW}	γ^{+}	γ^{-}
Water	72.8	21.8	25.5	25.5
Glycerol	64.0	34.0	3.92	57.4
Formamide	58.0	39.0	2.28	39.6
Ethylene Glycol	48.0	29.0	1.92	47.0
Methylene Iodide[1]	50.8	50.8	0.0	0.0
Note: [1] also known as Diiodomethane				

Results and Discussion

Advancing and receding contact angle measurements on five MRL bitumen types are furnished in Tables 8 and 9, respectively. Since controversy exists in the surface science community about the use of receding contact angles, some discussion on this subject is in order. As introduced previously, the receding contact angle manifests through hysteresis between the two modes (advancing and receding) of measurement, i.e. $\theta_a - \theta_r$. Hysteresis is usually positive, indicating complete or at least partial wetting of the surface. Surface roughness can also contribute to this phenomenon. Although rare, negative hysteresis can occur and is usually associated with a change of the surface properties by the liquid, or one of the components of the liquid (van Oss, 1994). In the Wilhelmy plate method, hysteresis is automatically part of the measuring process. The advancing contact angle is commonly used for surface energy calculations and it is almost considered "scandalous" to calculate these values from receding angles. It is a fact that scientists do not agree on the applicability of surface energies determined from receding contact angles (van Oss, 1994; Della Volpe and Siboni, 2000; Chibowski, 2003). In principle, surface energies calculated from receding angles are just as correct as those calculated from the advancing angles are (Della Volpe and Siboni, 2000). In addition, it has been postulated that receding angles could be related to the fracture mode of damage in asphalt mixes as discussed in Chapter II. Jacobasch et al. (1995) describe

the use of receding contact angles as a better index of high-energy surfaces and support the idea that advancing angles are not adequately sensitive to characterize the acidic or basic character of these surfaces. Chibowski (2003) incorporated both the receding and advancing angle as an expression of equilibrium spreading pressure to calculate total surface energy.

Table 8. Advancing contact angle (θ_a)[1] data from Wilhelmy plate technique

Bitumen	Water		Methylene Iodide		Ethylene Glycol		Glycerol		Formamide	
	Avg.	s	Avg.	s	Avg.	s	Avg.	s	Avg.	s
AAB-1	108.5	1.5	89.2	1.6	67.8	0.3	97.7	0.6	94.0	0.1
AAD-1	110.1	1.0	78.1	0.3	69.6	1.2	101.3	0.5	96.6	0.8
AAF-1	102.7	2.0	73.7	1.0	64.7	0.3	94.7	0.3	92.3	1.0
AAM-1	107.9	0.9	67.3	3.3	58.5	1.6	92.0	0.5	89.9	0.7
ABD	99.2	1.0	54.2	2.0	61.5	0.0	85.1	0.6	81.8	1.5
AAB-1+L	102.8	5.8	79.7	2.8	62.9	1.3	90.5	1.6	89.3	0.2
AAM-1+L	94.1	4.5	77.5	1.0	53.0	0.1	85.1	0.2	80.0	1.6
ABD+L	100.6	0.7	55.0	1.5	62.5	1.2	87.3	0.1	82.3	0.2

Legend:
Avg: average; s: standard deviation; L: amine liquid anti-strip agent (Akzo Nobel C-450)
Note:
[1] All contact angles in degrees

A coefficient of variation range between 0.1% and 3.8% is typical with a few exceptions. Standard deviations in the order of 1˚ are considered excellent and attainable, while values up to 3˚ are not uncommon in the literature.

Table 9. Receding contact angle (θ_r)[1] data from Wilhelmy plate technique

Bitumen	Water		Methylene Iodide		Ethylene Glycol		Glycerol		Formamide	
	Avg.	s	Avg.	s	Avg.	s	Avg.	s	Avg.	s
AAB-1	81.2	0.5	41.1	1.0	57.3	0.6	63.2	2.8	63.4	0.3
AAD-1	86.1	1.5	42.1	1.1	65.0	0.2	70.2	0.1	74.1	1.0
AAF-1	86.7	0.6	41.7	0.2	58.8	0.2	67.5	0.5	67.0	0.4
AAM-1	45.8	1.5	43.4	6.4	51.1	0.5	21.3	5.7	41.6	2.9
ABD	47.9	0.7	43.5	0.6	51.5	1.5	34.5	1.3	40.1	1.4
AAB-1+L	72.3	1.6	43.4	1.7	52.1	0.7	58.8	1.4	59.0	0.4
AAM-1+L	41.2	1.3	40.2	0.5	49.9	0.2	20.6	3.2	31.0	2.1
ABD+L	45.3	0.7	46.0	0.4	50.5	0.2	22.6	4.9	33.5	0.9

Legend:
Avg.: average; s: standard deviation; L: amine liquid anyi-strip agent (Akzo Nobel C-450)
Note:
[1] All contact angles in degrees

Reproducibility in terms of standard deviation of the contact angles was used as a measure of precision of the technique. The pooled standard deviations for both the receding and advancing angles for each probe liquid was estimated under the assumption of common precision for different materials. This statement is presented in Table 10 and is valid for conditions of one operator and one laboratory.

Table 10. Pooled standard deviations (Sp) for contact angles obtained from Wilhelmy plate technique

Mode	Water	Methylene Iodide	Ethylene Glycol	Glycreol	Formamide
θ_a (degrees)	2.4	1.9	0.9	0.7	0.9
θ_r (degrees)	1.1	2.4	0.7	3.1	1.5

With the exception of ABD, all bitumens tested exhibited a jagged pattern in the measured hysteresis loops. A typical example is presented in Figure 36 (p. 114). The effect is pronounced in advancing contact angle measurements. These patterns are associated with a "slip-stick" phenomenon, which is attributed to the failure of the solid surface to meet the assumptions of Young's equation. The surface must be smooth, homogeneous and non-interacting with the probe liquid. On advancement, the liquid "sticks" to the high-energy regions, wets the low energy regions and "slips" when forced to proceed. In measurements on bitumen, this pattern is attributed to both chemical and physical heterogeneity on a microscopic scale. Figure 3 (Chapter II) presents evidence of these features established by Atomic Force Microscopy (AFM). Despite these patterns, regression fits of the buoyancy line is generally good which is manifested in reproducible measurements as indicated in Tables 8 to 10. The selection of a large, representative area to perform the regression fit is therefore essential for consistent and unbiased results.

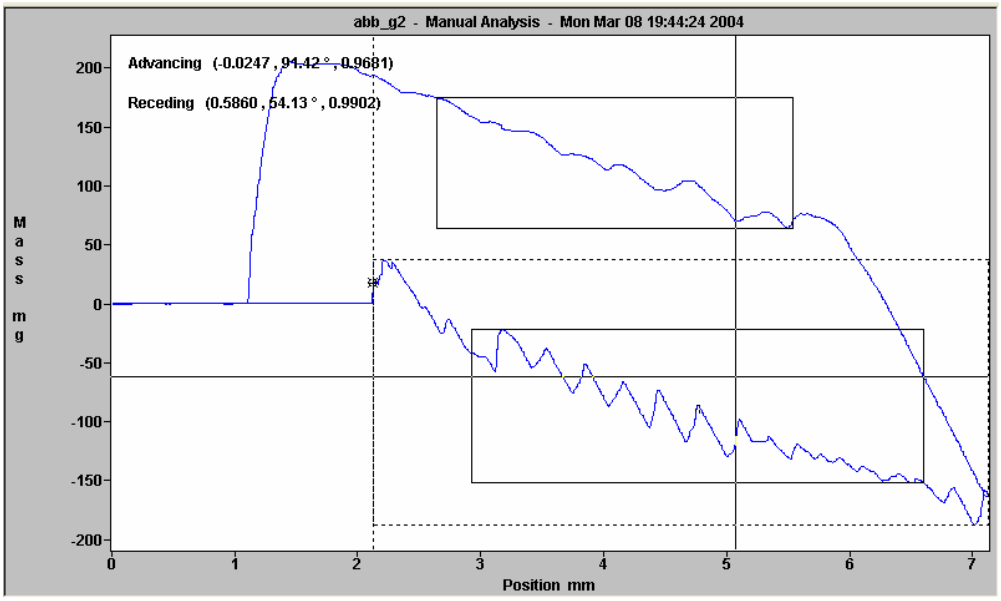

Figure 36. Slip-stick phenomenon exhibited by bitumen AAB-1

An important consideration in contact angle measurement and subsequent surface energy calculations is the selection of appropriate probe, or reference liquids. The concept of condition number was introduced previously. Since ABD was the only bitumen that did not show any signs of slip-stick, this bitumen was used as an example to illustrate the application of condition number in Table 11.

Table 11. Effect of different liquid sets on surface energies calculated for ABD

Liquid Set	CN	γ^{Total}	γ^{LW}	γ^{+}	γ^{-}
3 × 3					
W /MI/ EG	4.89	32.1	31.9	0.5	1.5×10^{-4}
W/ MI/ G	4.47	31.9	31.9	7.1×10^{-4}	0.7
W/ MI/ F	5.17	31.9	31.9	-0.7 (2)	2.4
W/ G/ F	18.66	14.9	10.2	3.2	1.8
W/ G/ EG	139.16	619.8	619.8	-13.7	0.0
3 × 4					
W/ MI/ F/ EG	4.9	30.5	30.3	0.6	1.5×10^{-2}
W/ MI/ G/ EG	5.0	32.4	32.4	0.4	-4.4×10^{-4}
W/ MI/ G/F	5.3	31.1	31.1	-3.2×10^{-2}	0.9
3 × 5					
W/ MI/ G/ EG /F	5.5	30.9	30.9	0.6	-3.7×10^{-2}

Legend:
CN denotes condition number; γ : Surface energy; LW: Lifshitz van der Waals; +: acid (electron acceptor); -: base (electron donor)
Note:
Negative values are shown to complement interpretation of data. These components can be set to zero as indicated by an γ^{AB} value of 0.

A number of observations can be made from the data presented in Table 11. It should be emphasized that condition number only relies on the surface energy characteristics of the probe liquids. Calculated surface energy values agree well for any set of liquids that produce a relatively low condition number, generally less than 10. The importance of including a non-polar liquid to achieve this is evident from the table.

Methylene iodide is the only non-polar liquid (with known surface energy components) that could be used without dissolving the bitumen. An oily layer on the liquid surface was, however observed after tests and restriction of the sample to one test (three replicates) was therefore imperative with the use of this liquid.

Despite computation using the SVD algorithm, negative square roots in the solutions are evident in a number of cases. This can be introduced by measurement error and is pronounced when the components are close to zero. A combination of both these factors, which is in part related to these materials, implies that larger liquid sets are not necessarily beneficial. One may also be tempted to point out that in this table, formamide forms part of most sets that produce negative components.

Kwok and Neumann (2003) illustrated how liquids that exhibit anomalous behavior in contact angle measurements can be determined by plotting $\gamma_L \cos\theta$ versus γ_L. An example of anomalous behavior may be a liquid that is more prone, or sensitive, to the slip-stick phenomenon. The authors showed that an acceptable set of liquids follow a smooth curve or line. Any liquid that deviates substantially from this line is associated with anomalous behavior. Little et al. (2004) recently applied this approach to the contact angle data from a number of MRL bitumen types. They report that with the exception of one case, formamide substantially deviates from the fitted curve. An example of this approach is depicted in Figure 37 for bitumen AAF-1. In this plot, formamide deviates substantially from the fitted line.

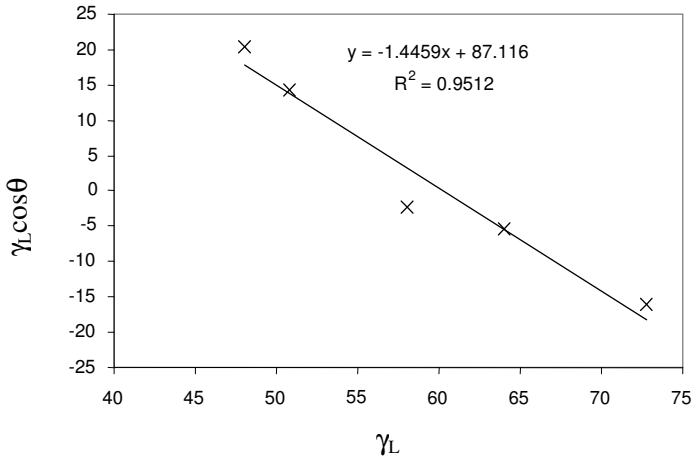

Figure 37. Plot of $\gamma_L\cos\theta$ vs. γ_L for AAF-1 (Little. et al. 2004)

Little et al. (2004) investigated this phenomenon more closely by calculating the squared errors associated with each liquid. Table 12 includes the errors calculated for both advancing and receding contact angle data. The errors calculated from advancing angles illustrate the finding that formamide tends to deviate from the fitted line. Although the errors produced for methylene iodide are in some cases relatively high, the contribution of this liquid to complete the set is imperative as illustrated in Table 11.

In addition, it is important to use a consistent set of liquids when different bitumen types are compared, since some liquids tend to accentuate one or the other component. For example, ethylene glycol has a tendency to produce higher acidic numbers. It should be noted that the total surface energy as well as Lifshitz-van der Waals component does not change significantly with different liquid sets and the influence on the components are small, provided the condition number is low and measurement errors small. For the purpose of surface energy calculations from advancing angles, the liquid set consisting of distilled water, methylene iodide, and glycerol (CN = 4.89) was selected.

The errors obtained when attempting to follow the same approach for the receding angles are cumbersome and may corroborate some of the criticism associated with this parameter. It is interesting that in this case, formamide turns out to be the best liquid to

include into a set. The set selected, based on these considerations include distilled water, methylene iodide, and formamide (CN = 5.17).

Table 12. Squared errors calculated from $\gamma_L \cos\theta$ vs. γ_L plots

Bitumen	W	MI	EG	G	F
Advancing Angles					
AAB-1	0.0	49.2	41.5	4.8	2.8
AAD-1	3.8	0.4	5.0	0.1	19.6
AAF-1	4.4	0.3	7.7	0.0	30.9
AAM-1	0.1	0.7	1.3	12.2	28.2
ABD	0.9	43.0	20.4	7.0	14.3
Receding Angles					
AAB-1	22.7	43.0	60.9	43.7	0.4
AAD-1	10.2	118.5	79.5	36.9	23.4
AAF-1	23.8	54.5	71.4	46.4	0.8
AAM-1	45.4	0.1	15.0	109.3	0.0
ABD	24.3	0.4	17.0	36.2	5.8
Legend: W: distilled water; MI: methylene iodide; EG: ethylene glycol; G: glycerol; F: formamide					

From Table 13, it is evident that the main contribution to the total surface energy is the Lifshitz-van der Waals component. This is in line with the knowledge gained in Chapter II, which suggests that bitumen is primarily a non-polar material and that these forces are expected to play an important part in the adhesion process. The variation or lack of variation between different bitumen types are therefore also attributed to this component. A glance at the data indicates that the advancing angles seem to distinguish better between the different material types. This is also the case if one considers the total surface energy parameter. The acid components (γ^+) derived from both advancing and receding angles are small, negligible in most cases, while the base components (γ^-) are generally higher, but still small for the advancing derived surface energy component.

Table 13. Surface energies calculated from contact angle measurements, mJ/m^2

Bitumen	γ^{Total}		γ^{LW}		γ^{+}		γ^{-}	
	Avg.	s	Avg.	s	Avg.	s	Avg.	s[1]
Advancing								
AAB-1	14.3	0.8	13.1	0.2	0.4	0.2	0.9	0.5
AAD-1	18.5	0.2	18.5	0.0	0.0	0.1	0.8	0.3
AAF-1	20.8	0.6	20.8	0.1	2.0	0.7	0.0	0.2
AAM-1	24.5	1.9	24.4	0.4	0.0	0.3	0.0	0.3
ABD	31.9	1.2	31.9	0.2	0.0	0.2	0.7	0.4
AAB-1+L	19.1	2.1	17.6	0.3	0.5	0.6	1.1	2.0
AAM-1+L	21.7	1.5	18.8	0.1	0.5	0.4	3.8	1.5
ABD+L	31.4	0.9	31.4	0.2	0.0	0.1	0.6	0.2
Receding								
AAB-1	39.1	0.6	39.1	0.1	0.0	0.1	7.4	0.2
AAD-1	38.5	1.0	38.5	0.1	0.0	0.3	8.7	0.5
AAF-1	38.7	0.3	38.7	0.0	0.0	0.1	4.6	0.2
AAM-1	43.9	5.4	37.9	0.5	0.2	0.7	36.6	0.6
ABD	45.4	1.3	37.8	0.1	0.4	0.2	32.4	0.3
AAB-1+L	37.9	1.2	37.9	0.1	0.0	0.2	13.9	0.5
AAM-1+L	50.2	1.6	39.5	0.0	0.8	0.3	35.0	0.3
ABD+L	49.0	0.9	36.5	0.0	1.3	0.1	31.1	0.2

Legend:
γ : Surface energy; LW: Lifshitz van der Waals; +: acid (electron acceptor); -: base (electron donor)
Avg.: average; s: standard deviation; L: liquid anti-strip agent (Akzo-Nobel C-450)
Note:
[1] Negative surface energy values set equal to zero. Standard deviation associated with these values are only reported for completeness.

The base components derived from receding angles are more sensitive to distinguish among different materials, corroborated by statistical analyses, and in line with observations by Jacobasch et al. (1995). The fact that the base components are higher does not mean that the material is basic, but is a manifestation of the scale assumption previously discussed. Bitumen with zero acidic character is not realistic and these values should rather be interpreted as an indication of acidic character much weaker than that of water.

An interesting and significant test for characterization of surface energy of bitumen using any technique is the ability to reflect the influence of a surface-active agent (surfactant). In this research, a fatty amine (C-450) from Akzo Nobel was used at a 0.5% dosage. The results presented in Table 13 do not consistently show any significant effect. One would expect the base component to increase due to the addition of the basic amine groups. This is the case for treated AAM-1, derived from advancing angles. Although the receding angle shows a difference, which is statistically significant, it is practically insignificant with an unexpected change to a lower base value. Bitumen AAB-1 appears to be the closest to what one would expect with a significant increase in the base component derived from receding contact angle values. Further influenced by some differences between the Lifshitz van der Waals components, the only statistical different treated and untreated pair based on total surface energy is AAB-1, based on advancing contact angles, and AAM-1, based on receding contact angles. Treatment of ABD with 0.5% liquid anti-strip agent is not significant based on these measurements.

A series of boil tests were conducted on asphalt mixtures with untreated bitumen types AAB-1 and ABD with granite RA, respectively, following Tex-530-C. Tests on mixtures manufactured with these binders containing different percentages of liquid anti-strip agent (C-450, Akzo Nobel) were also performed. Results indicated that without liquid anti-strip agent, less than 5 percent bitumen was retained in both cases. The tests also revealed that only 0.25% of amine anti-strip agent is required to increase the percentage retained after 10 minutes of boiling to more than 95%. This finding is significant and demanded further investigation into the ability of the current technique to characterize surface energies of bitumen.

INVERSE GAS CHROMATOGRAPHY

The feasibility of using IGC generated retention times to calculate surface energies was illustrated from the literature and presented in Chapter III. Scouting experiments were conducted on aggregate particles using a packed column approach. Short 180 mm to 300 mm stainless steel and glass columns with inner diameters ranging from 2 mm to

6 mm were used and the mass of the sample varied until both polar and non-polar hydrocarbon probe signals were detected. The validity of the approach was assessed by testing amorphous silica (silica gel 60). The Lifshitz-van der Waals component of surface energy calculated from this experiment compared well with values from the literature. Testing with aggregates followed. A balance between the non-polar, and the polar and non-polar (with high molecular weight) probes had to be attained. Peak broadening occurred when polar or higher molecular weight non-polar probes were injected which was attributed to intrinsic heterogeneity, high surface area or porosity, and high-energy surfaces of the samples. In addition, the sample mass that allowed signal detection for polar probes was too small to obtain sufficient separation of non-polar peaks. These factors undermined the reliability of this approach for aggregate testing. For some aggregates, such as RK basalt with a specific surface area of approximately $10 m^2/g$, including high energy sites such as iron oxides, elution of even the non-polar probes of moderate molecular weight, was difficult. Barbour et al. (1974) used a 3.8 m by approximately 6 mm inner diameter column in an attempt to measure retention times of vapors through a column packed with limestone. They report that most of the polar compounds interacted so strongly that they did not exit the column. Despite its simplicity and potential speed, it was decided to abandon this technique for aggregate characterization. Surface energy characterization using IGC should therefore be restricted to minerals, which are relatively homogeneous materials.

As indicated in the previous chapter, IGC has been applied to characterize oxidative aging of bitumen (Davis and Petersen, 1966; Barbour et al., 1974; Kim et al., 1997). In these methodologies, bitumen was coated from a solution onto Teflon particles and then packed into a column. More recently, Barbour and co-workers (WRI, 2003a; 2003b) adapted the original method to a more user-friendly and time efficient approach where a fused silica capillary column (30m×0.53mm) is coated with bitumen from a toluene solution. The methodology followed in the current research was adapted from the capillary IGLC technique developed at the Western Research Institute under a FHWA contract (WRI, 2003b).

IGC Method

Untreated Fused silica columns with configuration 15m×0.25mm (Sigma-Aldrich, Suppelco), were used in these experiments. Approximately one gram of bitumen is diluted in 10 ml toluene to produce a 10% solution. A rinsing kit (Sigma-Aldrich, Suppelco) consisting of a 25 ml plastic coated (pressure safe) glass reservoir with a screw-on stainless steel inlet-outlet unit is the key apparatus in the coating process. The solution is transferred to the 25 ml vial and one end of the column inserted into the solution. The solution is pushed through the column with dry nitrogen by applying a pressure of approximately 35 kPa. The column rinsing assembly is illustrated in Figure 38. With about 6 to 7 coils of the transparent capillary column filled, the inlet of the column is pulled out of the solution and the plug of bitumen solution pushed through the column by the nitrogen pressure. This process is repeated two more times to ensure adequate coating of the column walls. No significant coloring of the column occurs due to the thin film produced. After the final plug is pushed through, the pressure is increased to approximately 200 kPa and the water bath turned on. This initial drying process is allowed to continue for 60 minutes at 40˚C.

A HP5890 Series II Gas Chromatograph (GC) equipped with Electronic Pressure Control (EPC) and a flame ionization detector (FID) was used in this study. ChemStation software was used for experimental set-up, control, and data capturing. The inlet and outlet temperatures were set to 175˚C and 250˚C, respectively. The bitumen column was installed in the GC oven and conditioned for an hour at 130˚C before testing. A temperature program lowered the temperature to the test temperature of 25˚C after conditioning. The column flow set to 1.5 ml/min, corresponded to a column head pressure in the order of 70 kPa, and the total flow (or injection-spit flow) was set to 15 ml/min. Operating in split mode allowed injection of minute amounts with a syringe by removing some of the injected sample before elution through the column, thereby increasing peak resolution.

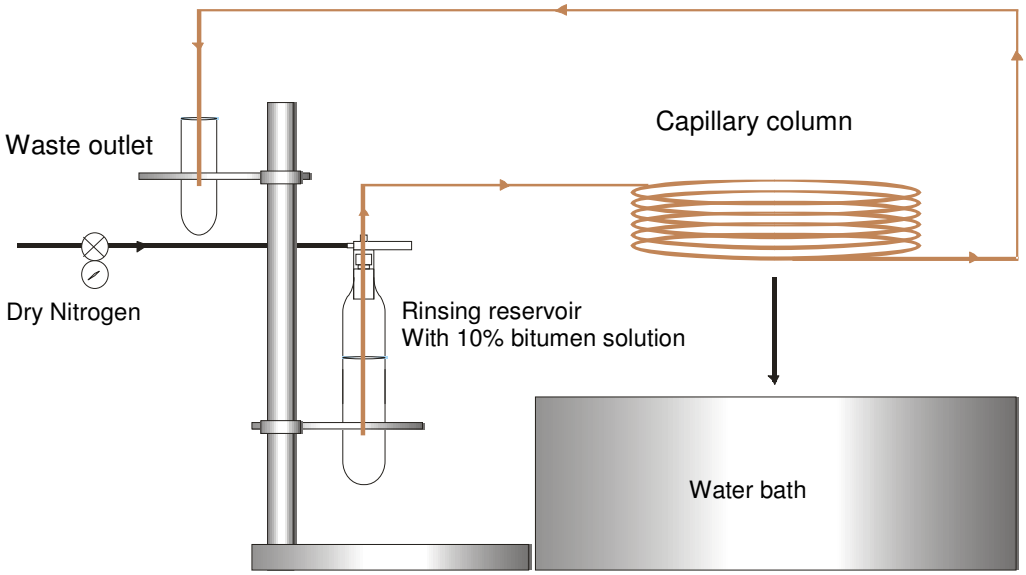

Figure 38. Column rinse assembly

Injection of the probe molecules was carried out manually with gas tight glass micro syringes (Sigma-Aldrich, Hamilton). All the chemicals were HPLC grade supplied by Sigma-Aldrich. A mixture of normal alkanes, including normal pentane, hexane, heptane, octane and nonane were made with methane as the reference probe. Approximately 0.1µl of the mixture in liquid form was injected. Methane is considered an inert hydrocarbon and its retention time serves as a measure of the dead volume of the column. While the same series of n-alkanes were used as in the original oxidation experiments, polar probes with known surface energy components were required in these experiments. Two probes with acidic character, namely chloroform and dichloromethane, and two probes with basic character, namely toluene and ethyl acetate were selected. One replicate consisted of a sequence of the n-alkane mixture followed

by individual injections of each of the polar probes. A five-minute conditioning at 130˚C was sufficient between sequences to remove all excess gas from the system.

Figure 39 shows a typical retention time output obtained for an n-alkane mixture, including methane (0.731 min.) to nonane (8.156 min.). Retention time was defined as the time corresponding with the maximum peak height.

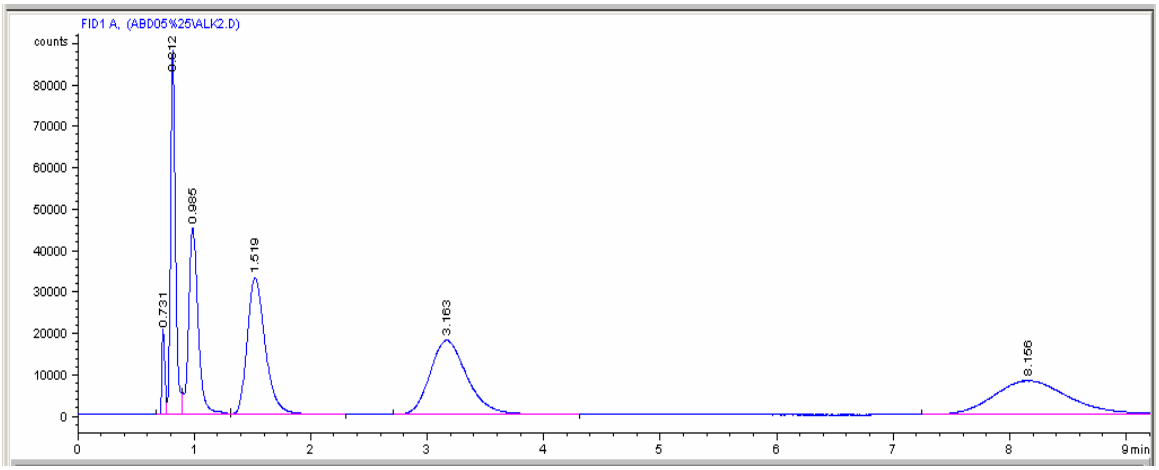

Figure 39. Typical IGC output for an n-alkane mixture (Captured from ChemStation Software)

Analysis

An important assumption in the application of IGC to study adsorption processes is that the solute equilibrium conditions are achieved between the mobile and stationary phase. These conditions are achieved at infinite dilution of the vapor or adsorbate, therefore zero coverage of the surface. Under these conditions, the vapor can be considered to behave as an ideal gas, which becomes important in the following approach to the analysis (Charmas and Leboda, 2000). The retention time, t_R, of the

adsorbates interacting with the surface allows one to determine the net retention volume, V_N. This quantity is obtained from the following relationship (Skoog and Leary, 1992).

$$V_N = j/m \cdot F \cdot (t_R - t_M) \cdot \frac{T}{273.15} \tag{70}$$

Where, t_M is the dead time, accounting for column characteristics, or essentially any volume other than that of the sample. The latter is usually determined by an "inert" hydrocarbon, usually methane, through the column. Some researchers use air and record an air peak. The difference $t_R - t_M$ is therefore the net retention time, t_N. The flow-rate of the carrier gas (F), usually helium, the test temperature (T), and sample mass (m) are also provided for in this equation. The variable, j, is the dimensionless James-Martin compressibility factor, correcting for the pressure drop in the column, expressed by,

$$j = \frac{3}{2} \cdot \frac{(p_i / p_0)^2 - 1}{(p_i / p_0)^3 - 1} \tag{71}$$

Where p_i and p_o represent the column input and outlet pressures, respectively. V_N is the quantity from which all thermodynamic quantities can be determined. A common relationship between this volume and the Gibbs free energy of adsorption (ΔG in kJ/mol) is provided by the following relationship.

$$\Delta G = RT \ln(V_N) \tag{72}$$

In order to obtain the Lifshitz-van der Waals (apolar, London or dispersive) component of surface energy, non-polar vapors need to be eluted through the column. Each of the retention times obtained for these solutes are used to calculate the free energy utilizing Equation (72). For the series of n-alkanes with progressive increase in molecular weight, plotting of the free energies against some molecular descriptor of the solutes (e.g. molecular weight, partial pressure etc.) enables one to obtain a straight line. The slope of this line is associated with the LW component of the surface energy (γ^{LW}). This relative approach makes it possible to simplify Equation (70) and therefore

Equation (72) so that only the retention time is required as an input, plotting $RTln(t_N)$ against the molecular descriptor. For the theory adopted in this research, the LW component of the free energy (ΔG^{LW} in mJ/m^2 or ergs/m^2) is expressed by the Berthelot geometric mean as introduced in Chapter II.

$$\Delta G^{LW} = 2\left(\gamma_L^{LW}\right)^{\frac{1}{2}}\left(\gamma_S^{LW}\right)^{\frac{1}{2}} \tag{73}$$

Where *L* and *S* traditionally represents liquid (vapor in this case) and solid, respectively. And if expressed in kJ/mol,

$$\Delta G^{LW} = aN_A 2\left(\gamma_L^{LW}\right)^{\frac{1}{2}}\left(\gamma_S^{LW}\right)^{\frac{1}{2}} \tag{74}$$

where a is the cross-sectional area of the solute, and N_A is Avogardo's number (6.0221 x 10^{23} species per mol). Hence, $a\left(\gamma_L^{LW}\right)^{\frac{1}{2}}$ were used as the molecular descriptor in this research. The LW component of surface energy in mJ/m^2 is then given by,

$$\gamma_S^{LW} = \left(\frac{slope}{2N_A}\right)^2 \tag{75}$$

Elution of monopolar basic and monopolar acid vapors enable determining the acid and the basic surface energies, respectively. When a polar molecule interacts with the surface, specific interactions (mainly due to acid-base interactions) and non-specific interactions (mainly due to London forces), take place simultaneously. It is therefore assumed that the LW and acid-base (AB) contributions to the total free energy is additive as introduced in Chapter II.

$$\Delta G = \Delta G^{LW} + \Delta G^{AB} \tag{76}$$

This subtraction takes place at a position above the alkane line where the molecular descriptor of the polar molecule corresponds to that of a hypothetical n-alkane as

illustrated in Figure 29, Chapter III. The difference is equal to the free energy of specific interaction, i.e. acid or base due to the use of monopolar probes.

$$\Delta G_{AB} = RT \ln\left(\frac{t_N^p}{t_N^n}\right) \tag{77}$$

Where t_N^n is the net retention time for the hypothetical n-alkane, and t_N^p is the net retention time for the polar molecule under consideration. Figure 40 shows a typical analytical plot obtained for bitumen; in this case ABD. It is essential that a good fit is obtained for the alkane line. Decane was abandoned because a good fit could not be established with this high molecular weight n-alkane.

Using the approach by van Oss, Good and Chaudhury, the acid-base contribution of the free energy can be expressed in terms of the known surface energy components of the solute and that of the surface under consideration.

$$\Delta G^{AB} = aN_A 2\left[\left(\gamma_l^+ \gamma_s^-\right)^{\frac{1}{2}} + \left(\gamma_l^- \gamma_s^+\right)^{\frac{1}{2}}\right] \tag{78}$$

If the acid (+ , electron acceptor) and base (- , electron donor) properties of the two monopolar solutes are known, and either γ^+ or γ^- equals zero in each case, then the unknown surface energy components can be calculated alternately.

Relevant characteristics of the probe molecules are presented in Table 14. The cross-sectional areas (a) of the n-alkanes were calculated by assuming that each CH_2 group occupies 0.06 nm^2 and each CH3 group occupies 0.08 nm^2, first proposed by Dorris and Grey, and applied by Sun and Berg (2002). A liquid density model assuming a spherical molecular shape and hexagonal packing was used to approximate the cross-sectional areas of the polar probes:

$$a_{mol} = 1.33 N^{\frac{1}{3}} v_{mol}^{\frac{2}{3}} \tag{79}$$

where a_{mol} is the molar area, υ_{mol} the liquid molar volume, and N is Avogadro's number.

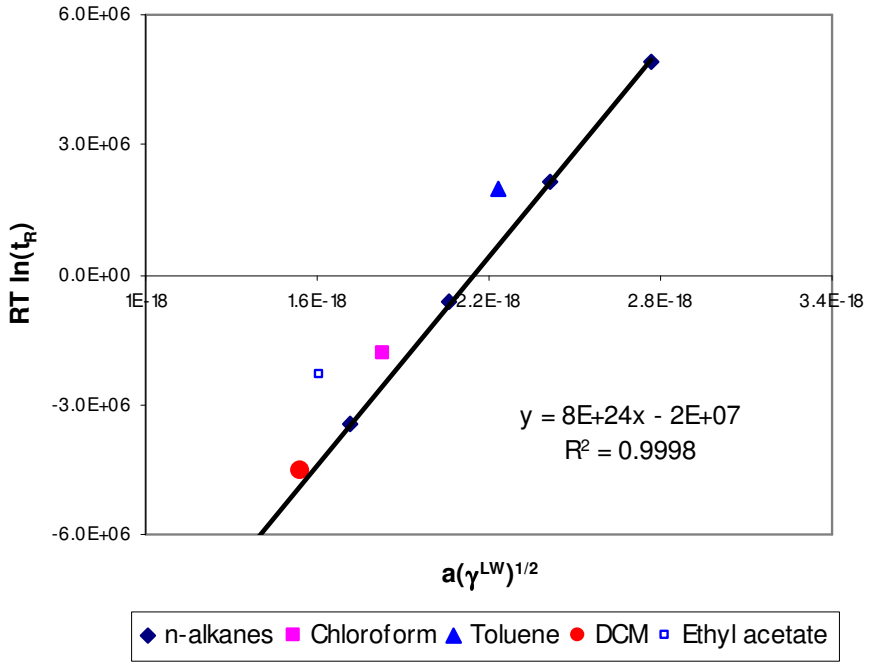

Figure 40. Typical IGC analysis plot for bitumen: ABD

Table 14. Characteristics of probe molecules used in IGC experiments

Probe	Surface Energy Characteristics, mJ/m^2 (20˚C)				Cross-sectional area (m^2)
	γ^{Total}	γ^{LW}	γ^{+}	γ^{-}	
n-Pentane (C_5H_{12})	16.1	16.1	0	0	3.399×10^{-19}
n-Hexane (C_6H_{14})	18.4	18.4	0	0	3.999×10^{-19}
n-Heptane (C_7H_{16})	20.1	20.1	0	0	4.598×10^{-19}
n-Octane (C_8H_{18})	21.6	21.6	0	0	5.198×10^{-19}
n-Nonane (C_9H_{20})	22.8	22.8	0	0	5.799×10^{-19}
Toluene (C_7H_8)	28.5	28.5	0	2.3	4.200×10^{-19}
EA ($CH_3CO_2C_2H_5$)	23.9	23.9	0	19.2	3.293×10^{-19}
DCM (CH_2Cl_2)	26.5	26.5	5.2	0	2.986×10^{-19}
Chloroform ($CHCl_3$)	27.2	27.2	3.8	0	3.505×10^{-19}

Legend:
γ : Surface energy; LW: Lifshitz van der Waals; +: acid (electron acceptor); -: base (electron donor)
s denotes standard deviation; EA: ethyl acetate; DCM: dichloromethane
Note:
[1] Negative surface energy values set equal to zero. Standard deviation associated with these values are only reported for completeness.

Results and Discussion

The parameters presented in Table 15 were derived only from the measured retention times and are essentially free from any theoretical manipulations. These parameters may therefore be used to establish a precision statement for the inverse gas chromatography technique to determine bitumen surface energies. Reproducibility of the technique for the conditions of one operator and one laboratory are presented in Table 16.

With the Lifshitz-van der Waals component presented in Table 15, surface energy components derived from different polar probes are presented in Table 17. Similar to the values obtained from the contact angle approach, the Lifshitz components are dominant. Although the acid and base components obtained from IGC are also small, they are never zero, i.e. this approach does not lend itself to calculation of negative square roots.

Table 15. Parameters calculated from IGC retention times (25˚C)

Bitumen	γ^{LW} n-Alkanes		ΔG^+ Toluene		ΔG^+ Ethyl Acetate		ΔG^- Chloroform		ΔG^- DCM	
	Avg.	S	Avg.	s	Avg.	s	Avg.	s	Avg.	s
	mJ/m^2		kJ/mol		kJ/mol		kJ/mol		kJ/mol	
AAB-1	48.3	0.9	1.3	0.04	1.6	0.02	0.6	0.04	0.5	0.1
AAD-1	45.4	0.6	1.5	0.03	1.9	0.12	0.9	0.03	0.5	0.1
AAF-1	47.5	0.5	1.4	0.02	1.8	0.05	0.5	0.03	0.7	0.1
AAM-1	44.9	0.4	1.1	0.01	1.3	0.01	0.2	0.03	0.1	0.1
ABD	44.8	0.2	1.3	0.01	2.0	0.03	0.7	0.02	0.4	0.04
AAB-1+L	44.5	0.3	1.2	0.1	1.3	0.0	0.5	0.03	0.3	0.03
AAM-1+L	45.0	0.2	1.0	0.01	1.4	0.08	0.3	0.1	0.3	0.1
ABD+L	43.5	0.4	1.2	0.01	1.9	0.01	0.7	0.04	0.5	0.001

Legend:
Avg.: average; s: standard deviation; γ^{LW} : Lifshitz van der Waals surface energy components;
ΔG^+: specific free energy (acid); ΔG^-: specific free energy (basic); L: liquid anti-strip agent (Akzo-Nobel C-450)

Table 16. Pooled standard deviations (Sp) for specific free energy parameters from IGC

γ^{LW} (mJ/m^2)	ΔG^+ (kJ/mol)		ΔG^- (kJ/mol)	
n-Alkanes	**Toluene**	**Ethyl Acetate**	**Chloroform**	**DCM**
0.481	0.029	0.074	0.046	0.068

The magnitude of γ^- derived from ethyl acetate compares to those obtained from contact angles. It is interesting that the acidic components derived from toluene are higher than the base components derived from both chloroform and dichloromethane. While this may seem to coincide with the generally acidic character of bitumen, these values simply imply that the ratio between water and bitumen (AAB-1, for example) is 25.5/2.6 for the acidic component and 25.5/0.8 for the base component (if ethyl acetate

is selected). No matter which combination of acidic or basic probes is selected, the total surface energy remains between 45.1 and 50.4 mJ/m^2 as summarized in Table 18. Generally, the magnitudes of γ^{LW} and γ^{Total} compare to those obtained from receding contact angles. In addition, γ^{LW} values for untreated bitumens rank the same as those obtained from receding contact angles while no correlation exist between γ^{Total} values, or between the components.

Table 17. Surface energy components determined by IGC at 25˚C, mJ/m^2

Bitumen	γ^+ **(Toluene)**		γ^+ **(Ethyl Acetate)**		γ^- **(Chloroform)**		γ^- **(DCM)**	
	Avg.	S	Avg.	s	Avg.	s	Avg.	s
AAB-1	2.6	0.1	0.8	0.02	0.5	0.1	0.4	0.2
AAD-1	3.1	0.1	1.1	0.15	1.2	0.1	0.4	0.1
AAF-1	2.9	0.1	1.1	0.06	0.4	0.05	0.6	0.2
AAM-1	1.7	0.01	0.6	0.01	0.1	0.02	0.01	0.01
ABD	2.3	0.03	1.3	0.04	0.8	0.03	0.3	0.1
AAB-1+L	2.1	0.2	0.6	0.0	0.4	0.05	0.1	0.02
AAM-1+L	1.5	0.04	0.6	0.07	0.1	0.1	0.2	0.1
ABD+L	2.1	0.03	1.3	0.01	0.7	0.1	0.3	0.001

Legend:
Avg.: average; s: standard deviation; γ : Surface energy; LW: Lifshitz van der Waals; +: acid (electron acceptor); -: base (electron donor); L: liquid anti-strip agent (Akzo-Nobel C-450)

No statistically significant difference exists between the base components of each of the untreated and corresponding binders treated with 0.5% liquid anti-strip agent. Not one of the surface energy parameters show any difference between each of the AAB-1 and AAM-1 untreated and treated binders, while γ^{LW} , γ^+ and γ^{Total} indicate a statistically significant difference in the case of AAB-1. These differences are still small

and can, however, not be elucidated by the addition of an amine anti-strip agent because the γ^- parameters were not significantly affected. As discussed previously, boil tests confirmed that 0.25% of liquid anti-strip agent is sufficient to increase adhesion of these binders with approximately 90%.

Table 18. Total surface energies (γ^{Total}) determined by IGC at 25˚C, mJ/m^2

Bitumen	Toluene/ Chloroform		Toluene/ DCM		Ethyl Acetate/ Chloroform		Ethyl Acetate/ DCM	
	Avg.	S	Avg.	s	Avg.	s	Avg.	s
AAB-1	50.4	0.9	50.2	1.2	49.5	0.9	50.4	0.9
AAD-1	49.2	0.5	47.7	0.7	47.7	0.7	48.0	0.8
AAF-1	49.6	0.5	50.2	0.8	48.8	0.5	50.0	0.4
AAM-1	45.7	0.4	45.1	0.6	45.4	0.4	46.5	0.4
ABD	47.4	0.3	46.4	0.3	46.8	0.3	47.4	0.2
AAB-1+L	46.2	0.4	45.5	0.4	45.4	0.3	46.2	0.3
AAM-1+L	45.8	0.5	45.9	0.4	45.5	0.4	46.6	0.3
ABD+L	46.0	0.2	45.2	0.4	45.4	0.3	46.0	0.4

Legend:
Avg.: average; s: standard deviation; L: liquid anti-strip agent (Akzo-Nobel C-450)

GENERAL DISCUSSION ON BITUMEN SURFACE ENERGY CHARACTERIZATION

Precision of the two methods based on reproducibility of the 'measured' parameters were discussed and presented in previous paragraphs. Table 19 summarizes the pooled standard deviations for the surface energy parameters obtained with the two techniques.

Table 19. Pooled standard deviations (Sp) of bitumen surface energies

Parameter	**Wilhelmy Plate**		**Inverse Gas Chromatography**			
LW	**Advancing**	**Receding**	**n-Alkanes**			
γ^{LW}	0.22	0.21	0.48			
Polar	**Advancing**	**Receding**	**T**	**E**	**C**	**D**
γ^+	0.40	0.31	0.09	0.07		
γ^-	0.93	0.38			0.06	0.12
Total	**Advancing**	**Receding**	**TC**	**TD**	**EC**	**ED**
γ^{Total}	1.29	2.15	0.50	0.65	0.51	0.49

Legend:
T: toluene; E: ethyl acetate; C: chloroform; D: dichloromethane
TD: total surface energy obtained from γ^+ (T) and γ^- (D) etc.

The precision based on surface energy parameters is statistically different in each case. The pooled standard deviation for the Lifshitz-van der Waals component, obtained from the Wilhelmy plate technique, is lower than that obtained from IGC. These differences are not practically significant with resulting coefficient of variations in the order of 1 to 2%. In general, the polar components itself are small and in many cases negligible. In the latter cases, standard deviations of these components are close to or larger than the components itself and cannot be considered as a realistic measure of precision. Although the standard deviation of the total surface energy derived from contact angles is an approximation, IGC produces higher precision based on this parameter.

In order to address the accuracy of a technique, it is necessary to know the bias or deviation from the true value. These intrinsic values are not known, especially for surface energy components, but total surface energies could be compared with surface tension values measured by classic mechanical means. These techniques are of course not perfect and have their own inherent problems when used to measure the surface tension of bitumen. Elphingstone (1997) used the pendant drop method to measure surface tensions of bitumen at 80˚C, while WRI (2001) employed the du Nöy ring to

obtain surface tension values at 60˚C. Due to the convenience offered by IGC to perform tests at different temperatures, surface energies were also determined at 60˚C. A consistent factor of 0.8 was obtained between measurements performed at 25˚C and 60˚C. Assuming that this factor is generic, it was used to convert Wilhelmy plate results from 25˚C to 60˚C. The total surface energies of four different bitumen types are presented in Figure 41.

The fact that surface energy decreases with temperature can be conceptually explained by recalling the definition of surface energy: the work required to increase the surface by a unit area. Heating results in mobility of the molecules and less resistance, and hence less work to increase the surface area. Theoretically, Equation (1) in Chapter II implies that increased temperature (thus entropy) will result in a decrease of the free energy of the system. Figure 41 suggests that surface tension values at 60˚C and 80 ˚C do not differ substantially.

It is interesting that both du Nöy ring and pendant drop results show that the differences between bitumen types are not significant. As previously pointed out, surface energies derived from the advancing contact angles appears to indicate differences among the binders to some extent. Figure 41 further reveals that Wilhelmy plate results obtained from receding angles and IGC results at 60˚C compare to du Nöy ring and pendant drop values.

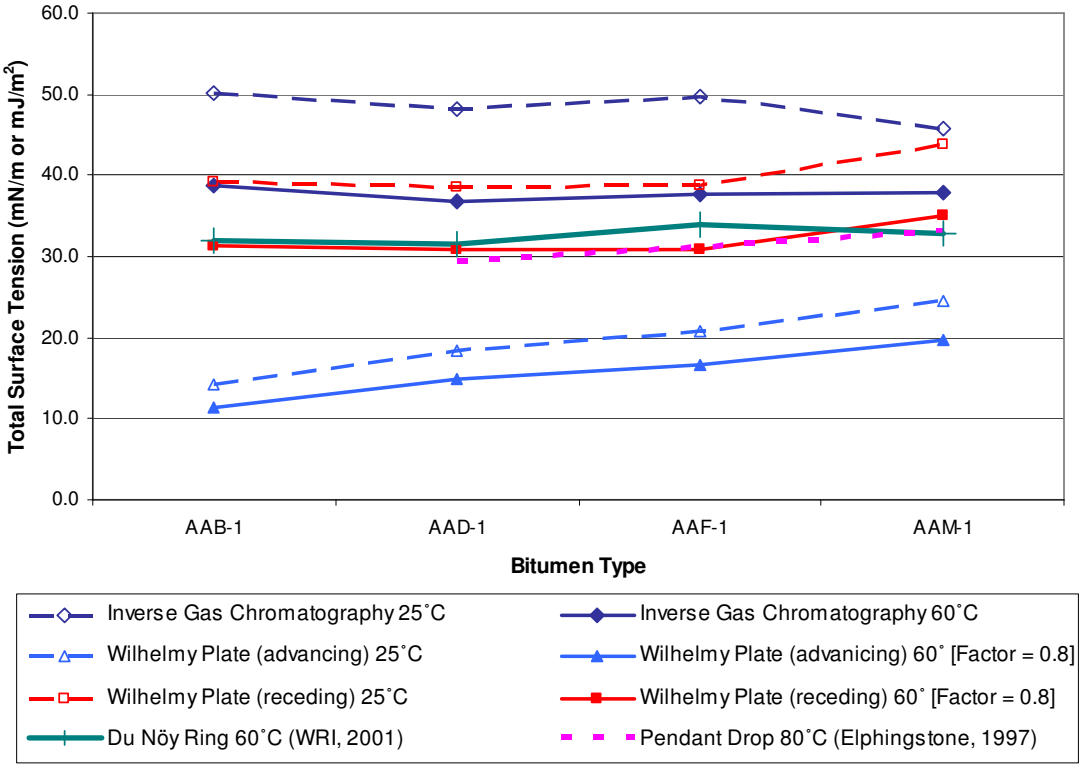

Figure 41. Comparison of total surface energy values

Rationale for Inability of Current Approaches to Detect the Effect of Additives

Results presented in previous subsections indicated that surface energy characterization using both the Wilhelmy plate technique and IGC do not clearly distinguish untreated bitumen, and bitumen treated with amine liquid anti-strip additive. Boil tests conducted during this research showed that 0.25% of the amine anti-strip agent would be sufficient to increase the adhesive properties of these binders substantially.

Schultz et al. (1984) were faced with a similar problem when they studied the effect of 1 percent acrylic acid grafted onto polyethylene in order to improve its adhesion. Peel tests of these polymers from aluminum plates indicated that the grafted polymer improves the work of adhesion significantly, while initial surface energies obtained from contact angle measurements for polyethylene (PE) and grafted polyethylene (PEg)

appeared to be identical. In this work the two-component theory, or Owens-Wendt theory, was used as a first approximation. In this theory, the geometric mean rule is used to combine polar surface energy components. Criticism against this type of approach was presented in Chapter II (p. 62). A dispersive component (γ^d, similar to Lifshitz-van der Waals component) of 40 mJ/m^2, and a polar component (γ^p, similar to the acid-base component) of 0.02 mJ/m^2 were obtained for these polymers. Interestingly, the values are similar to that obtained for bitumen in the current research.

The researchers proposed that grafting improves adhesion properties of polyethylene by orientation of the acrylic groups in the polymer surface towards the polar metal oxide surface. The orientation ability of PE and PEg in contact with model orientation environments (water and formamide) was investigated using a two-liquid phase contact angle technique illustrated in Figure 42. A plate of polymer (S) is placed in contact with an 'orienting' polar liquid (L). In this approach, 2 µl drops of n-alkanes (H) are placed on the S/L interface at different contact times.

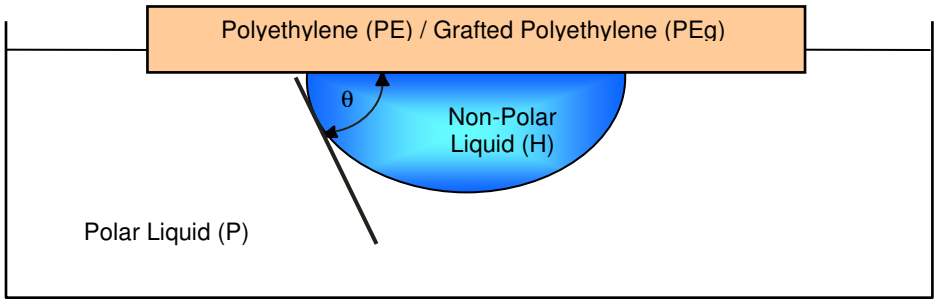

Figure 42. The two-liquid phase contact angle technique (Schultz et al., 1984)

The contact angle (θ) of the alkane on the polymer in the polar liquid medium satisfies the following relationship:

$$\gamma_H - \gamma_L + \gamma_{HL}\cos\theta = 2\left(\gamma_S^d\right)^{\frac{1}{2}}\left[\left(\gamma_H\right)^{\frac{1}{2}} - \left(\gamma_L^d\right)^{\frac{1}{2}}\right] - \Delta G_{SL}^p \qquad (80)$$

where ΔG_{SL}^p is the polar free energy component of adhesion between the polymer plate (S) and the orienting liquid (L). For two immiscible polar liquids, the generalized form of Equation (80) is:

$$\gamma_H - \gamma_L + \gamma_{HL}\cos\theta = 2\left(\gamma_S^d\right)^{\frac{1}{2}}\left[\left(\gamma_H\right)^{\frac{1}{2}} - \left(\gamma_L^d\right)^{\frac{1}{2}}\right] - \Delta G_{SL}^p + \Delta G_{SH}^p \qquad (81)$$

where ΔG_{SH}^p is the polar free energy of adhesion between the solid and a drop of polar liquid, replacing the non-polar hydrocarbon, H, in Equation (80).

By using a series of n-alkanes (hexane, heptane, octane, decane, dodecane, and hexadecane) the left side of Equation (80) plotted against the first term on the right allows determining γ^d from the slope and ΔG_{SL}^p from the intercept. Alternatively, two equations can be solved simultaneously by using two different n-alkanes.

The evolution of γ^d and γ^p of PE and PEg as a function of contact time with water at 20˚C is shown in Figure 43. The dispersive components of PE and PEg did not change significantly and were of the same order, between 37 and 41mJ/m^2. The polar component, γ^d, of PE remained small, whereas γ^d of PEg increased to reach a maximum value of 22 mJ/m^2 after 13 days of contact with water. Measurements with formamide produced a γ^d for PEg of 8.8 mJ/ m^2.

Schultz et al. (1984) report that the increase of polarity due to molecular orientation has been verified using other analytical techniques. They also state that the kinetics of orientation is influenced by temperature. Due to higher mobility at higher temperatures, 1 hour of contact with water at 90˚C, for example, could have the same effect on surface energy as 2 weeks contact at 23˚C.

The researchers concluded that, in contact with a model orientation medium, the polymer chains move thereby modifying the conformation of the chains within the surface layer. The polar acryclic acid groups orient towards the water interface, which increases the surface polarity of the polymer. They introduce the concept of 'potential surface energy'. Based on these observations, surface energy of a polymer (or polymer-like material such as bitumen) can no longer be considered as an intrinsic property of the polymer. The surface energy of these materials depends on, and can vary drastically with the history and the contact medium.

The techniques used in this research should be adequate for characterization of the Lifshitz-van der Waals component of surface energy. It is envisioned that this approach can be adopted to study bitumen surface energies, especially the polar components. It should, however, be pointed out that the use of n-alkanes in contact angle experiments will dissolve the bitumen and that other sets of immiscible liquids need to be selected. Equation (80) or (81) can easily be extended to the theory proposed by van Oss et al. (1988) adopted in the current research.

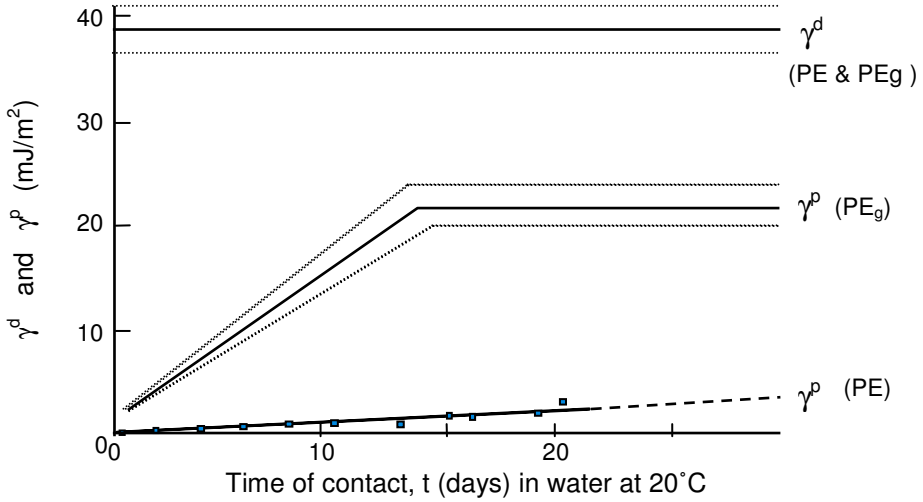

Figure 43. Surface energy components of polyethylene (PE) and grafted polyethylene (PEg) plates in contact with water at 20˚ C with time (Adapted from Schultz et al., 1984)

STATIC VAPOR SORPTION EXPERIMENTS

General concepts and theory underlying the static vapor sorption approach using the universal sorption device (USD) were presented in Chapter III. The detail sample preparation and test methodologies used in this research are furnished in the following paragraphs.

USD Method

The aggregate fraction passing the No.4 (4.75mm) sieve and retained on the No.8 (2.35mm) sieve was used for surface energy characterization of aggregate. Approximately 150g of aggregate is collected by a laboratory scoop and washed with distilled water over the retaining sieve. The sample is allowed to dry in an oven at 120˚C for four to six hours and then moved to a desiccator to cool down to ambient temperature for another four to six hours. A fine-screen aluminum sample holder, 27mm in diameter and 55 mm in height, is used in this research. The sample holder is prepared by washing it with distilled water and then acetone after which it is oven dried and allowed to cool to ambient temperature. One replicate of 20 to 25g of aggregate is transferred with a clean funnel to the sample holder.

The magnetic suspension balance is in a calibrated condition during these experiments in accordance with the manufacturer's specifications. The sample holder with aggregate is suspended onto the measuring hook of the magnetic suspension balance. After sliding the sample chamber cover with gasket into position, the retaining bolts were fastened evenly. The suspension control, vacuum pump, and temperature bath are switched on. Sorption Operation, Measurement and Analysis Software developed at Texas Transportation Institute (TTI) was used in these experiments. This software suite comprises of three modules, namely, a centering balance module, degassing module and, a testing and analysis module. The balance centering procedure, performed next, takes alternate mass readings at "zero point" (the electromagnet and permanent magnet are uncoupled) and "measuring point" (coupled) until stable readings

are achieved. No magnetic material is allowed within a radius of one meter from the magnetic suspension balance when measurement is in progress.

Degassing of the sample chamber follows. During this operation, a valve is opened to allow the system to reach a vacuum of approximately 100 mTorr. The system temperature increases to 60˚C while the degassing continues to approximately 5 mTorr (0.0005 psi) over a period of approximately 3 hours. In the final stage of the degassing sequence, the temperature is decreased to the testing temperature of 25˚C and the sample is allowed to equilibrate for 3 hours. At this point, the stability of the balance is checked again using the centering balance module.

Testing with the first vapor proceeds. The testing and analysis module controlled the testing sequence, acquired data and performed data analysis to produce the equilibrium spreading pressure based on the theory presented in Chapter III. The software divides the saturation vapor pressure of the selected probe vapor into 10 pressure levels and proceeds with opening the valve to allow vapor into the system until the first pressure level is reached. The adsorbed mass is monitored until equilibrium is reached and the sequence continues until the equilibrium mass at the final pressure level is recorded. After testing with the first probe vapor, the sample chamber is opened and the sample removed. The sample is washed with distilled water and the sample preparation procedure is repeated for the same sample before testing with the next probe vapor. Testing with all probe vapors on the same sample constitute one replicate. The probe vapors used in this research were n-hexane, methyl propyl ketone, and distilled water (HPLC grade, Sigma-Aldrich). Three replicates were performed with each aggregate type.

Analysis

Surface energy characteristics of the probe molecules used in USD experiments are summarized in Table 20. The detail analysis of isotherms to obtain equilibrium-spreading pressure (π_e) was presented in Chapter III. The only significant deviation of this procedure was that the specific surface areas of the aggregate samples were based on

the cross-sectional area of the non-polar probe n-hexane. In addition, a molecular cross-sectional area of 56.2 Å was used in accordance with the value recommended by McClellan and Harnsberger (1967) which is based on adsorption data on several surfaces, in lieu of Equation (32) which is based on liquid density and the assumption of hexagonal close packing.

Table 20. Surface energy characteristics of USD probe liquids at 20˚C, mJ/m^2

Probe / Adsorbate	γ^{LW}	γ^+	γ^-	γ^{Total}
Water	21.8	25.5	25.5	72.8
MPK	24.7	0	19.6	24.7
n-Hexane	18.4	0	0	18.4
Legend: MPK = methyl propyl ketone				

Equation (34), Chapter III, gives the relationship between spreading pressure and work of adhesion, which in turn can be expressed in terms of surface energy components following the theory proposed by van Oss et al. (1988).

The Lifshitz-van der Waals component of the surface energy is then calculated from the "measured" π_e and surface energy characteristics for n-hexane using the following expression.

$$\gamma_S^{LW} = \frac{\left(\pi_e + 2\gamma_L^{tot}\right)^2}{4\gamma_L^{LW}} \tag{82}$$

Knowing γ^{LW}, the acidic or electron acceptor component of solid surface energy is calculated using π_e obtained for the monopolar basic liquid MPK and its associated surface energy characteristics.

$$\gamma_s^+ = \frac{\left(\pi_e + 2\gamma_L^{tot} - 2\sqrt{\gamma_S^{LW}\gamma_L^{LW}}\right)^2}{4\gamma_L^-} \tag{83}$$

The two surface energy components obtained allows calculation of the basic or electron donor component using π_e obtained for distilled water, a bipolar liquid, and its surface energy characteristics.

$$\gamma_s^- = \frac{\left(\pi_e + 2\gamma_L^{tot} - 2\sqrt{\gamma_S^{LW}\gamma_L^{LW}} - 2\sqrt{\gamma_S^+\gamma_L^-}\right)^2}{4\gamma_L^+} \tag{84}$$

Finally, the total surface energy of the aggregate is calculated based on Equation (11), Chapter II.

$$\gamma_S^{tot} = \gamma_S^{LW} + 2\sqrt{\gamma_S^+\gamma_S^-} \tag{85}$$

Results and Discussion

Parameters derived from adsorption isotherms are summarized in Table 21. Little et al. (2004) determined specific surface areas (SSAs) of the same fractions of RA granite and RK basalt used in USD experiments, employing a commercial surface area analyzer. SSAs for RA and RK were found to be approximately 0.13 m^2/g and 10.1 m^2/g, respectively. These results, from nitrogen adsorption, correspond well with those obtained with the USD from n-hexane adsorption presented in Table 21. Although limited, this data supports the suitability, and establishes some confidence in applying this approach to these materials. This is especially corroborated by the fact that RK basalt is one of the most difficult materials to use in sorption experiments due to its high surface area and high adsorptive characteristics, facilitated by high-energy sites and clay inclusions. Table 22 summarizes the pooled standard deviations calculated for the different sorption parameters.

Table 21. Sorption parameters determined by USD measurements at 25˚C

Aggregate	SSA		π_e (water)		π_e (MPK)		π_e (n-hexane)	
	Avg.	s	Avg.	s	Avg.	s	Avg.	s
RD Limestone	0.30	0.05	94.5	8.09	32.1	5.1	20.2	1.4
RK Basalt	10.54	1.27	59.3	3.3	31.1	3.9	25.3	3.9
RG Sandstone	0.83	0.12	255.7	(1)	61.5	6.5	28.7	4.4
RA Granite	0.12	0.03	124.7	28.8	19.3	3.4	23.2	0.4
RL Gravel	1.06	0.12	288.7	9.2	69.7	4.9	28.7	4.9

Legend:
SSA: specific surface area in g/m^2; π_e: equilibrium spreading pressure in mJ/m^2
Avg.: Average; s: standard deviation
Note: (1) Only one test result

Despite good correspondence between specific surface areas compared to the conventional nitrogen technique, it is evident that results are not very reproducible with a coefficient of variation that typically varies between 3 and 23 percent. This variability can primarily be attributed to the heterogeneity of the materials; even if the same sample is used. In addition, aggregates with low surface areas tend to produce high variability in the sorption parameters due to closeness of mass measurements to the resolution of the balance. It is expected that water will produce higher variability due to its high polarity. Time to measure a full adsorption isotherm also tends to be the longest with water. It should be possible to reduce variability and testing time by selection of a more suitable organic vapor.

Table 22. Pooled standard deviations (Sp) of sorption parameters

SSA	π_e (water)	π_e (MPK)	π_e (n-hexane)
0.58	15.76	4.89	3.26

Legend:
SSA: specific surface area in g/m^2; π_e: equilibrium spreading pressure in mJ/m^2

Surface energies calculated for the different aggregates are presented in Table 23. It is apparent that the difference between these aggregates should be sought in the polar surface energy components. The Lifshitz-van der Waals component only varies over a relatively small range, i.e. between about 44 and 58 mJ/m^2. From these results, the controlling component in adhesive bonding would be the base component (γ^-). As previously mentioned, the high base components (relative to acid components) is a manifestation of the selected scale proposed by van Oss and co-workers. The true effect of these numbers can only be assessed through work of adhesion calculations, which is presented in the following chapter.

Table 23. Surface energy results determined from USD measurements at 25˚C

Aggregate	γ^{Total}		γ^{LW}		γ^+		γ^-	
	Avg.	s	Avg.	s	Avg.	s	Avg.	s
RD Limestone	99.39	5.7	44.1	2.1	2.5	1.1	263.3	15.4
RK Basalt	73.6	3.4	52.4	4.8	0.8	0.1	150.2	1.1
RG Sandstone	293.0	5.6	58.4	7.9	13.3	7.4	869.3	(1)
RA Granite	61.2	3.6	49.0	0.6	0.1	0.05	420.1	61.2
RL Gravel	357.6	17.8	57.7	7.0	19.9	8.8	1023.3	11.1

Notes: (1) Only one test result
Legend:
γ : Surface energy; LW: Lifshitz van der Waals; +: acid (electron acceptor); -: base (electron donor)
Avg.: average; s: standard deviation;

Although the magnitude of the basic numbers may seem to be excessive, similar values were reported by Li (1997) and Elphingstone (1997). Another interesting aspect is the fact that limestone has a lower base number and a higher acid number compared to limestone. This is intrinsically correct, knowing that elements such as calcium on limestone act as strong electropositive Lewis acid bonding sites and that oxygen in silica can act as Lewis base sites in granite. Limestone and granite tested by Cheng (2002)

showed dominant basic and acidic character for the aggregate types, respectively. Although this is more intuitive, these characteristics are typically encountered in aqueous environments, which can be attributed to the extent of preconditioning of the specimens tested. In this research, specimens were subjected to a less intense heat treatment, with no vacuum desiccation before being transferred to the USD sample cell. Vacuum degassing of the sample cell was performed to approximately 5 mTorr in this research, while Cheng (2002) vacuum degassed to below 1 Torr. It therefore appears that these levels of vacuum degassing can make a difference and that careful attention should be paid to this experimental parameter in future. Although vacuum degassing is inherently part of the static gravimetric sorption approach, it is difficult to relate this form of preconditioning to real conditions.

Finally, more user-friendly techniques should be explored for surface energy characterization of aggregates. While thin-layer wicking is simple, samples can only be tested in a powdered from and effective preconditioning of the material retained onto a slide by suction may be problematic. Dynamic vapor sorption techniques can be used to produce sorption isotherms without the need for vacuum degassing. It is envisioned that the latter technique holds the key to implementation of aggregate surface energy characterization on a routine basis.

CONCLUSIONS

In this chapter, detailed methodologies of two techniques for surface energy characterization of bitumen, and one technique for surface energy characterization of aggregate were presented. Five bitumen types and five aggregate types, used during the Strategic Highway Research Program (SHRP), were obtained from the Materials Reference Library (MRL) for surface energy characterization in this research.

The Wilhelmy plate technique is based on contact angle measurements of selected probe liquids on bitumen coated glass slides. Emphasis is placed on the selection of a balanced set of liquids based on the condition number (CN) of the coefficient matrix which consists of the known surface energy components of the probe liquids. A CN

below 10 represents a well-balanced liquid set. The key ingredient to achieve this condition is the inclusion of a non-polar or dispersive liquid into the set. Methylene iodide is proposed, and appears to be the only liquid of this kind, with known surface energy components, that does not dissolve bitumen readily. Due to the errors typically associated with contact angle measurements, large liquid sets do not necessarily offer any advantage in eliminating negative square roots. In addition, contact angles obtained with each liquid can be further assessed by plotting $\gamma_L \cos\theta$ versus γ_L. Any liquid that shows substantial deviation from the curve, may violate the assumptions of Young's equation and should be considered carefully for inclusion. The receding angle is more prone to large deviations.

Most bitumen types exhibit a slip-stick phenomenon induced by both chemical and physical surface features. Despite this phenomenon, confirming deviations from the assumptions of Young's equation, reproducibility of the method is acceptable as reflected by contact angle statistics. Manifestation of this phenomenon is pronounced in the advancing contact angles.

Inverse gas chromatography is introduced as an alternative technique to determine surface energies of bitumen. A fused silica capillary column of less than a millimeter in diameter is coated with bitumen from a toluene solution. Retention time is the measured parameter used to calculate the thermodynamic properties of the surface. Reproducibility of the technique is generally acceptable. In addition, this technique is not prone to producing zero-value components induced by negative square roots.

Both techniques suggest that the Lifshitz-van der Waals component of bitumen is dominant which is in line with the known non-polar character of bitumen. Acid and base components are small, in many cases negligible, and therefore not suitable parameters to assess the reproducibility of the techniques. Total surface energies determined by both techniques were compared with mechanical surface tension values obtained from du Nöy ring and pendant drop measurements at 60˚C and 80˚C, respectively. Firstly, these values indicate that different bitumen types are not

significantly different (at least practically), and secondly, total surface energies from IGC and receding contact angles compare well with mechanical surface tension data.

Testing of bitumen types AAB-1, AAM-1 and ABD treated with 0.5% amine liquid anti-strip agent generally show inconsistent or no effect. Boil tests indicated that only 0.25% of the anti-strip agent required to improve adhesion by about 90%. A rationale is presented based on research from the literature. It is proposed that molecular orientation due to chain mobility plays an important part in the adhesion process of polymeric materials. The concept of 'potential' surface energy is introduced and states that polymeric materials do not possess an intrinsic surface energy but that surface energy varies depending on the chemistry of the surface that it is in contact with. It is proposed that the polar components of bitumen surface energy be characterized by a similar approach where the surface is placed into contact with a reference polar medium. It should be noted that the current approaches are adequate for characterization of the Lifshitz-van der Waals component of bitumen surface energy.

The universal sorption technique was employed to characterize surface energies of five aggregates. The polar components of surface energy were identified as the important parameters that differentiate between aggregates. The magnitude of these components confirms that aggregate plays a dominant role in bitumen-aggregate adhesion. The fact that base components are generally higher than acid components is attributed to the original scale proposed by van Oss and co-workers. The true effect of these numbers can only be assessed through work of adhesion calculations. Preconditioning by vacuum degassing is an important variable, which needs further investigation in order to relate the extent of degassing to practical conditions.

It is proposed that other, more user-friendly techniques for aggregate surface energy characterization should be explored. A dynamic vapor sorption approach is simpler and eliminates the need for vacuum degassing. This approach should be investigated as a candidate for surface energy characterization of aggregates on a routine basis.

CHAPTER V

QUANTIFICATION OF BITUMEN-AGGREGATE ADHESION IN THE PRESENCE OF WATER

INTRODUCTION

Moisture damage, sometimes called stripping, in hot-mix asphalt is a major cause of pavement failure. This chapter concentrates on the effect of water at the bitumen-aggregate interface after diffusion through the bitumen (Fromm, 1974, Nguyen et al., 1992, Cheng, 2002) has taken place. Chapter II illustrated how moisture damage may occur when water is thermodynamically favored at the bitumen-aggregate interface and bitumen consequently displaced from the aggregate surface. While the theory adopted thus far (van Oss, 1988) corroborates this phenomenon, it does not account for the effect of overlapping double layers in the presence of water. The electric double layer effect may be important in quantifying adhesion in the presence of water.

Moisture damage is a complex phenomenon involving several mechanisms. Some of these mechanisms were discussed in Chapter II. For example, water may lead to dissolution of the aggregate surface, causing a cohesively weak boundary layer. WRI (2003) showed that water could cause oxidative aging of bitumen. The increased polar nature of the aged bitumen may in some cases increase adhesion with the polar aggregate, while it is also known that oxidative products are typically more hydrophilic and tend to attract more moisture than the original compound. More than 50 years ago, Gzemski (1948) showed that more emphasis should be placed on the influence of pH of water on stripping.

The pH of natural surface waters depends on a number of factors including geology, human activities, topography, climate and season, and vegetation. The distribution of pH values, for example, in the Delaware, Susquehanna, and Ohio basins of Pennsylvania were found to vary between 2 and 10 and shows the potential extremity of these values

in natural waters (Gzemski, 1948). Gzemski states that since surface waters are the products of subterranean drainage, it is reasonable to believe that a similar range of pH is likely to exist in the proximity of the roadbed.

Researchers such as Scott (1978), and Yoon and Tarrer (1988) illustrated how aggregate surface chemistry can influence the pH of the contacting water (See Chapter II, Figure 7). Although it can be argued that the time dependency of this process may render it a secondary effect, many petroleum recovery studies indicate that the process of water displacement can be quite slow (WRI, 2003a).

The objective of this chapter is to assess the feasibility of including electric double layer effects and the ability of this approach to quantify the effect of pH of the interface water on the adhesive bond. The effect of pH on the surface energy components of water is addressed, followed by assessment of the free energy of electrostatic interaction as a third term following the generalize theory proposed by van Oss (1994). The significance of this term and its ability to reflect the role of pH are assessed based on data from the literature. An alternative mechanism that relates pH to electron donor-acceptor properties of surfaces are introduced following the work by Labib (1992).

EFFECT OF pH ON THE SURFACE ENERGY COMPONENTS OF WATER

With the application of the current theory, the surface energy components of water at the interface may be different from the values of "neutral" water if the pH is different. Chapter II showed that the pH of water in contact with most aggregate surfaces is in the upper pH range, i.e. between nine and ten. Situations, however, may arise where other environmental factors introduce more acidic pH levels.

As far as it is known, a study of this nature has not been done before. Two potential approaches were identified to investigate whether pH will alter the surface energy components of water, namely, inverse gas chromatography and a contact angle approach.

The literature shows that surface characterization of liquids can be performed using inverse gas chromatography (Hartkopf and Karger, 1973; Dorris and Gray, 1981;

Castells et al., 1982). If a hydrophilic particle (support) is saturated with water, then a surface is provided that approaches that of free water. Coated particles are packed into a chromatographic column and vapors of different polarities are then eluted through the column to measure different retention times that can be used to obtain thermodynamic properties of water. This technique would require a supporting material stable at various pH levels and careful selection and control of testing parameters to prevent evaporation.

Due to the influence of pH on surface charge as discussed in Chapter II, an additional degree of freedom is introduced should the contact angle approach be followed. The change in contact angle of water due to a pH change can, however, be investigated by selecting an electrostatically neutral surface (van Oss, 2004). After corresponding with Prof. Carel van Oss at the New York State University at Buffalo, his interest in the subject led to a study conducted in his laboratory. The fact that this study was inspired by the current research at Texas Transportation Institute was acknowledged and the work submitted for publication in the Journal of Adhesion, as part of the Chaudhury Collection (van Oss and Giese, 2004). The contact angle approach and results are presented in the following paragraphs.

Experimental

Dextran, a polymer of maltose (also called dextrose) is a material that exhibits negligible change in zeta-potential for different electrolyte pH levels. Microscope glass slides were covered with a 10 % (w/v) solution of dextran (ICN Pharmaceuticals) and reverse osmosis (RO) water. The covered glass slides were air-dried for 24 hours and placed in a vacuum desiccator until used. The RO water was used in the contact angles experiments and had a pH of 6.1. Acidified water was prepared by adding drops of approximately 0.1 M HCl to pH 1.94, while basic water was prepared by adding drops of approximately 0.1 M NaOH to a pH of 12.8.

Contact angle measurements were performed with a Gaertner instrument with a 10X telescope provided with crosshairs and ocular rim divided into 360˚. The telescope was mounted in an optical bench with a movable track. A Teflon micrometer syringe,

clamped on a support stand was used to facilitate placement of liquid drops onto the horizontal mounted slides. All measurements were performed at 20˚.

For each pH level, i.e. 1.94, 6.1, and 12.8, a total of 22 to 24 observations were made and the contact angles averaged. Apart from contact angles measured on dried dextran surfaces, control measurements were also done on untreated glass microscope slides as a control.

Results and Discussion

Contact angle results obtained on the untreated glass and dextran surfaces are furnished in Table 24. In this experiment, any changes in the contact angles on the dextran films would be as a result of different pH levels because the effect of surface charge is eliminated by the fact that dextran is electrostatically neutral.

Table 24. Contact angles with drops of water at different pH levels

pH	Glass	Dextran
1.94	9.7˚ ± 3.04˚	34.8± 3.00˚
6.1	10.5˚ ± 2.06˚	35.8± 3.35˚
12.8	6.8˚ ± 1.91˚	36.7± 2.52˚

While no significant difference exists between contact angles of water at pH 6.1 and pH 1.94 (P-value 0.35) measured on clean glass, a decrease in contact angle is evident with water at the alkaline pH of 12.8 compared with other levels. The later is substantiated by P-values close to zero. This increase at high alkaline pH is attributed to a large increase in the ζ-potential with a concomitant increase in the γ^- of the glass under these conditions.

The results show that there was essentially no change between the contact angles on dextran as a function of pH if values at pH 1.94 and pH 12.8 are compared with that obtained at pH 6.1. Respective P-values of 0.26 and 0.19 substantiate this observation. The small but modestly significant difference (P-value of 0.016) between the contact angles at the two extremes, pH 1.94 and pH 12.8, can be disregarded on account of the fact that HCl slightly decreases surface energy and NaOH increases surface energy of water. This is because HCl in itself has a lower surface energy than water while NaOH has a higher surface energy than water. The fact that these solutes have an influence on surface energy is important. It is known that organic and inorganic solutes influence surface tension of water, which can result in osmotic suction in fine-grained soils (Lytton, 2004: personal communication). In conclusion, the change in the pH of water therefore has no substantial effect on its acid and base surface energy components especially at pH values within three or four pH points from pH 7.

ELECTRIC DOUBLE LAYER THEORY

The background to electrostatic interactions and relevance to bitumen-aggregate interaction was presented in Chapter II. In the presence of water, surfaces are usually charged due to adsorption of ions and/ or the ionization of dissociable groups on the surface. Counter ions are ions with charge of sign opposite that of the surface charge and tend to neutralize the surface charge. Thermal motion prevents these ions to accumulate on the surface so that an ionic cloud, or diffuse layer, consisting of counter ions and co-ions exists. Together with the ions tightly bound to the surface (Stern layer), an electric double layer is formed. When two charged surfaces approach each other, their electric double layers overlap so that attractive or repulsive electric forces are acting between them.

When the electrokinetic potential, or ζ-potential, was introduced in Chapter II it was defined as the potential at the shear plane. In calculating interactions between electric double layers, ζ-potential can be used as an approximation of the surface potential ψ_o even though the location of the shear plane is about a hydrated ion away from the

surface (Ohshima, 1998; van Oss, 1994; Goodwin, 2004). Even though the surface potential (not directly measurable) can be extrapolated from ζ-potential (measurable), the dielectric constant on the inside of the shear plane can be much smaller than the dielectric constant of the bulk due to strong orientation of the water molecules close to the surface. From the shear plane outward, this orientation decays rapidly which makes it more reasonable to use the measured ζ-potential rather than ψ_o extrapolated from it (van Oss, 1994).

The Debye-Hückel parameter,κ, is commonly used in the theory of electrolytes and controls the rate of decay of potential with distance, *x*, from the surface (see Figure 5, Chapter II, p. 27). The parameter, 1/κ, is called the Debye length or thickness of the electric diffuse double layer. For a general electrolyte and units of m^{-1} (Ohshima, 1998):

$$\kappa = \left(\frac{e^2 \sum_i^N z_i^2 n_i}{\varepsilon_r \varepsilon_o kT} \right)^{\frac{1}{2}} \tag{86}$$

Where the elementary electronic charge $e = 1.6\times10^{-19}$ C, the relative permittivity in water at 25˚C $\varepsilon_r = 78.54$, the permittivity in vacuum $\varepsilon_o = 8.854\times10^{-12}$ $C^2m^{-1}J^{-1}$, Boltzmann's constant $k = 1.3805\times10^{-23}$ J/K, and *T* is the absolute temperature in degree Kelvin. The concentration of each ionic species, n_i, is expressed in ions/m^3, and the valence of each ionic species, z_i, is dimensionless. The term $\Sigma z_i^2 n_i$ is related to the ionic strength, and therefore molarity. In this calculation, the stoichiometry of the dissociation should be taken into account. For an electrolyte concentration (*M*) in moles/liter, relative number of moles for each ionic species m_i, and Avogadro's number $N_A = 6.022\times10^{23}$ mol^{-1}, this term (in units of m^{-3}) can be calculated as follows:

$$\sum_{i=1}^{N} z_i^2 n_i = 1000 \cdot M \cdot N_A \sum_{i=1}^{N} z_i^2 m_i \tag{87}$$

The expressions for the free energy of interaction between two flat plates for 1-1, 2-1, and a mixture of 1-1 and 2-1 electrolytes are presented in detail in the following paragraphs according to Ohshima (1998). The plate-plate configuration was selected based on the assumption that at a microscopic scale, the thickness of the electric double layers is much smaller than the size of the interacting particles under consideration.

For practical purposes, the most widely applied approximation is the linear superposition approximation (LSA) in which the potential between two approaching surfaces is approximated by the sum of the asymptotic values of the two individual and unperturbed potentials in the absence of interaction. This approach, which applies to large separations, is a good approximation even at intermediate separation. In addition, these expressions are valid for relatively low potentials (Ohshima, 1998).

The asymptotic form of the interaction energy per unit area (J/m^2) between two parallel plates 1 and 2 with surface potentials ψ_{o1} and ψ_{o2}, at separation x in a symmetrical (1-1) electrolyte with bulk concentration n is given by Equations (88) to (90). In all equations, ψ_{oj} can be set equal to ζ-potential with units in volts (V).

$$\Delta G_{1-1}^{EL} = \frac{64\gamma_1\gamma_2 nkT}{\kappa}\exp(-\kappa x) \tag{88}$$

where,

$$\gamma_j = \frac{\exp(e\psi_{oj}/2kT)-1}{\exp(e\psi_{oj}/2kT)+1}\ ,\quad j = 1,2 \tag{89}$$

and,

$$\kappa = \left(\frac{2ne^2}{\varepsilon_r\varepsilon_o kT}\right)^{\frac{1}{2}} \tag{90}$$

with all constants as previously described. Closer examination of Equation (88) reveals that the treatment of two different surfaces is equivalent to the application of Berthelot's geometric mean rule (introduced in Chapter II) to γ_1 and γ_2, associated with the two surface potentials. For two identical surfaces, $\gamma_1\gamma_2$ takes the form γ^2. Hence, when the geometric mean rule is applied, then:

$$\left(\sqrt{\gamma_1\gamma_2}\right)^2 = \gamma_1\gamma_2 \tag{91}$$

For a 2-1 electrolyte, the free energy of electrostatic interaction can be calculated according to Equations (92) to (94).

$$\Delta G_{2-1}^{EL} = \frac{192 n \gamma_1' \gamma_2' kT}{\kappa} \exp(-\kappa x) \tag{92}$$

where,
$$\gamma_j' = \frac{3}{2}\left(\frac{\left[(2/3)\exp\left(e\psi_{oj}/2kT\right)+1/3\right]^{\frac{1}{2}}-1}{\left[(2/3)\exp\left(e\psi_{oj}/2kT\right)+1/3\right]^{\frac{1}{2}}+1}\right), \quad j = 1,2 \tag{93}$$

and,
$$\kappa = \left(\frac{6ne^2}{\varepsilon_r \varepsilon_o kT}\right)^{\frac{1}{2}} \tag{94}$$

For a mixed solution of a 1-1 electrolyte of bulk concentration n_1 and a 2-1 electrolyte of concentration n_2, the free energy of electrostatic interaction can be calculated according to Equations (95) to (98).

$$\Delta G_{(1-1)+(2-1)}^{EL} = \frac{64(n_1+n_2)\gamma_1''\gamma_2'' kT}{\kappa} \exp(-\kappa x) \tag{95}$$

where,
$$\gamma_j'' = \frac{1}{1-\eta/3}\left(\frac{\left[(1-\eta/3)\exp\left(e\psi_{oj}/2kT\right)+\eta/3\right]^{\frac{1}{2}}-1}{\left[(1-\eta/3)\exp\left(e\psi_{oj}/2kT\right)+\eta/3\right]^{\frac{1}{2}}+1}\right), \quad j = 1,2 \tag{96}$$

with,
$$\eta = \frac{3n_2}{n_1+3n_2} \tag{97}$$

and,
$$\kappa = \left(\frac{2(n_1+3n_2)e^2}{\varepsilon_r \varepsilon_o kT}\right)^{\frac{1}{2}} \tag{98}$$

CALCULATION OF FREE ENERGY OF ELECTROSTATIC INTERACTION

The bitumen-aggregate interaction diagrams developed by Labib (1992) and presented in Figures 8 and 9 (Chapter II, p. 31) inspired this investigation into the potential integration of the electrostatic interaction to better describe the adhesion between bitumen and aggregate in the presence of water. Two data sets from previous research were utilized to calculate the free energy of electrostatic interaction. Detail descriptions of the aggregates are provided in the following subsection, and in the table on p. 165. The key parameters in these calculations are the ζ-potentials of the two interacting surfaces that can lead to attraction or repulsion depending on the signs of the charged surfaces in the presence of water.

Labib (1992) and Labib and McClelland (1993) investigated and developed reliable methods to determine the electrokinetic properties of the two main types of aggregates, namely, siliceous and calcareous. MRL core aggregates RJ granite and RD limestone represented the two respective groups and measurements were presented at different pH levels. In addition, Labib (1992) and Labib and Schujko (1993) developed a method to measure the ζ-potential of bitumen. In earlier work during the SHRP Program, ζ-potentials of all the MRL core aggregates were measured following ASTM procedure D 4187-82: Blue-White Light, Method B. These results were reported at the equilibration pH (similar to Figure 7, Chapter II) of each aggregate type (SHRP, 1991). Since that time, the ASTM standard used for these measurements was discontinued. The methods developed by Labib and his colleagues, specifically for measurement of electrokinetic properties of these materials, are reported in the following paragraphs.

Method for ζ-Potential Measurement of Aggregate

Aggregates are complex mixtures of mineral and soluble ions that leach out in the presence of water and determine the pH and ionic strength of the aqueous environment at the surface of the aggregate. These factors were investigated by Labib and

McClelland (1993) to develop reliable methods for measuring the ζ-potential of siliceous and calcareous aggregates which are presented in this section.

Aggregate particles were first reduced to a size smaller than the No.70 mesh by passing it through a Micro Hammer-Cutter Mill (Gibson Company, Glen Mills Inc.). Further reduction to a median particle size of 10 mm by means of a Pulverisette 6 Laboratory Centrifugal Mill (Gibson Company, Fristsch GmbH), which is essentially a ball mill.

Two techniques were employed to determine ζ-potentials of the aggregates under investigation. The electrophoretic mobility of the aggregate particles was measured by the acoustophoretic technique and a Dopler-Shift electrophoreses technique was used as a calibration experiment.

Based on the acoustophoretic technique, electrophoretic mobility of particles were measured using a PenKem System 7000 instrument. In this technique, a hydrophone is used to impose sonic oscillations (1kHz) to polarize the double layers around the particles in suspension. A 10% by weight suspension was used in these experiments. The potential drop produced by the polarization is measured. The Smoluchowski equation, Equation (99), was used to calculate the ζ-potential. This equation is commonly used for the situation where the particles are relatively large with thin but quite dense electric double layers (van Oss, 1994). Derivation of ζ-potential from relative acoustic mobility (RAM) was facilitated by using the correction proposed by O'Brien (1988) due to the size of particles.

A Zetasizer IIc (Malvern Instruments Company) was used to measure electrophoretic mobility by the laser Dopler-Shift electrophoreses technique. In this technique, the availability of particles for reliable measurement is detected by a particle counter. Computation of ζ-potential is facilitated by the Smoluchowski equation:

$$U_E = \frac{\zeta \varepsilon}{\eta} \tag{99}$$

where, U_E is the electrophoretic mobility, ε is the permittivity of the medium, η is the viscosity of the medium, and ζ is the zeta-potential. The ζ-potential results generated from the two techniques produced a standard deviation of ± 5mV .

The electrokinetic properties of both aggregate types were significantly affected by soluble leachable ions, type and concentration of electrolyte, as well as electrolyte equilibration time. For siliceous aggregates (RJ granite) it was found that chloride and sulfate ions act as potential determining ions which changed the ζ-potential-pH characteristics of the aggregate. Labib and his co-workers recommend KNO_3 as a supporting electrolyte since the nitrate ions does not interfere with the chemistry of the granite surface. In addition, an 18-hour equilibration time of the aggregate in the electrolyte is necessary for reliable electrokinetic characterization. It is recommended that the measurements be conducted over a pH range of 2.0 to 10.0.

Results obtained for the calcareous aggregate RD limestone, suggest that potassium sulfate (K_2SO_4) interacts with the limestone surface and should therefore not be used as a supporting electrolyte. Chloride and nitride ions in the supporting electrolytes did not interfere with the electrokinetic properties of the limestone. Consistent results were obtained with KCl at different molar concentrations where the ζ-potential decreased with increase in ionic strength as predicted by the theory of electric double layers. KNO_3 were not as consistent as those obtained with KCl after the 18-hour equilibration time. The authors emphasize that limestone is soluble in acids at pH < 6.5 and that electrokinetic measurements should be conducted above this pH level.

Method for ζ-Potential Measurement of Bitumen

The methodology presented in this section was developed and reported by Labib and Schujko (1993). Five core SHRP bitumen types including AAA, AAD, AAG, ABD, and AAM were used in this investigation. The key consideration in the successful measurement of electrophoretic mobility was to produce a dilute bitumen emulsion without introducing extraneous organic groups that may mask the surface chemistry of the bitumen. Some form of stabilization of the emulsion was required in order to

produce reliable electrophoretic results. This was accomplished by using a 0.1% solution of peroxide-free nonionic surfactant. The 0.1% concentration was sufficiently low to avoid the formation of large micelles or stabilized air bubbles that could interfere with the measurements.

Electrophoretic mobility of the bitumen droplets was measured by the laser Dopler-shift technique and using the Smoluchowski equation to calculate ζ-potential as described above. The instrument was calibrated by using a standard latex solution (Interfacial Dynamics Corporation). One gram of bitumen was emulsified in 100 ml of 0.1% surfactant solution using a Polytron homogenizer (Brinkmann Instruments). Short intervals (approximately 30 seconds) of homogenization were necessary before a sufficient particle count was detected by the Zetasizer IIc instrument. A reasonable particle count was achieved within three to five minutes due to collapse of the bitumen droplets. The pH of the emulsions was controlled by NaOH or HCl solutions. No supporting electrolyte could be used due to the low stability of the bitumen emulsions.

Measurements were made in duplicate and the average value used. The standard deviation in the measurements was ± 3mV.

Calculation of the Gibbs Free Energy of Electrostatic Interaction

The objective in this investigation was to determine the order of magnitude of interaction induced by electrostatic forces between bitumen and aggregate in an aqueous environment. As mentioned above, aggregates produce natural electrolytes by dissolution of ionic species from their surfaces. Using the molar concentrations of the supporting electrolytes would therefore not be a true reflection of the actual ionic strength. Labib (1992) and Labib and Wielicki (1993a) determined the specific conductance and pH values for four MRL aggregate slurries after several soaking and decanting cycles. These results are presented in Table 25.

Specific conductance at equilibrium pH for the electrolytes produced was used to approximate the bulk molar concentrations for use in free energy calculations. A

common relationship between specific conductance and concentration is given by (Bard and Faulkner, 1980; Atkins, 1986):

$$\Lambda = \frac{k}{1000 \cdot C} \tag{100}$$

where specific conductivity (k) is in μS/cm, equivalent or molar conductivity (Λ) in $S.cm^2$/equivalent, and concentration (C) in moles/liter.

Table 25. pH and specific conductance of aggregate slurries (Labib, 1992)

Cycles[1]	RJ Granite		RL Gravel		RC Limestone		RD Limestone	
	pH	K[(2)]	pH	k	pH	k	pH	k
I	9.6	75	9.5	113	9.0	143	9.1	125
II	9.4	41	9.4	70	8.1	56	9.2	60
III	9.3	37	9.4	61	9.1	46	9.3	49
IV	9.5	33	9.6	54	9.1	45	9.5	44
V	9.3	36	9.4	56	9.5	42	9.5	42

Notes: [1] Hourly soaking - decanting, except Cycle V where soaking was 12 hours.
[2] Specific conductance in micro siemens per cm (μS/cm)

Equivalent conductivity for known electrolytes at infinite dilution (Λ_o) is available from the literature and can be used to calculate Λ at 25˚C following Equation (101).

$$\Lambda = \Lambda_o - (60.32 + 0.2289\Lambda_o)\sqrt{C} \tag{101}$$

The molar concentration can then be obtained by solving equations (100) and (101) simultaneously through an iterative process. In this research, it was assumed that ions in the natural electrolyte are represented by the ions used in the supporting electrolytes. A fair correspondence exists between the pH values after five soaking cycles presented in Table 25, and the pH values for the same aggregates characterized and documented as a reference during the SHRP Research (SHRP, 1991). Molar concentrations based on the

corresponding specific conductivities were calculated for the four aggregates and are furnished in Table 26.

Table 26. Molar concentration derived from specific conductivity

Aggregate	Electrolyte	Λ_o S.cm^2/equivalent	k μS/cm	C Moles/liter
RJ	KNO_3	144.96	36	2.51×10^{-4}
RD	KCl	149.86	42	2.83×10^{-4}
RL	KCl	149.86	56	3.78×10^{-4}
RC	KCl	149.86	42	2.83×10^{-4}

Based on the plate-plate configuration and 1-1 electrolytes (KCl and KNO_3), the free energy of electrostatic interaction was calculated utilizing Equations (88) through (90). Free energies were calculated at points that represent different pH regions according to Figures 7 and 8 (Ch II, pp. 30 and 31) for aggregates RJ and RD, respectively. As indicated above, ζ-potential measurements for limestone at pH levels lower than 6.5 is not meaningful. In addition, the free energy at the isoelectric point is zero, and therefore not applicable in those regions of the diagrams. ζ-potential measurements were not performed over the full pH range for aggregates RL and RC and are therefore only calculated at the equilibrium pH levels.

The interaction diagrams show that the ζ-potential-pH curves for the bitumen types are grouped close together and AAM-1 was therefore selected for bitumen-aggregate free energy calculations. The separation distance between the two surfaces is unknown but can be assumed similar to the equilibrium distance for van der Waals and acid-base interactions, i.e. approximately 1.6Å or 16nm (van Oss, 1994). The results, including selected parameters are presented in Table 27.

The results indicate that the assumption of large separations is satisfied since the thickness of the double layer is almost the same as the interaction distance. This also confirms that the assumption of low potential is correct. At this distance, the interaction takes place at the outer edge of the electric double layers where the potential is low. As expected based on surface charge or ζ-potential values, most of the combinations indicate repulsion and corresponds to a positive free energy value.

Zeta-potential values for the rest of the MRL aggregates at equilibrium pH conditions were also obtained from the literature (SHRP, 1991). Sodium chloride was used as a supporting electrolyte in all the measurements. Although specific conductance tests were not performed, Table 18 showed that the molar concentrations do not vary much for the siliceous and carbonate aggregates and the two electrolytes considered. A value of 2.83×10^{-4} M were used to calculate the free energies of electrostatic interactions for the rest of the aggregates. Results are reported in Table 28.

Table 27. Free energy of electrostatic interaction based on data from Labib (1992)

Aggregate		Bitumen		pH	κ^{-1} nm	γ_a	γ_b	ΔG^{EL} mJ/m^2
Code	ζ_a mV	Code	ζ_b mV					
RJ	-16.0	AAM-1	-57.0	6.0	19	-0.154	-0.504	0.026
RJ	-44.0	AAM-1	-61.8	9.0	19	-0.404	-0.538	0.072
RD	60.0	AAM-1	-57.0	6.0	18	0.525	-0.504	-0.089
RD	-16.0	AAM-1	-66.7	10.0	18	-0.154	-0.571	0.030
RL	-22.0	AAM-1	-65.5	9.8	16	-0.211	-0.563	0.040
RC	-16.0	AAM-1	-63.7	9.5	18	-0.154	-0.551	0.029

Table 28. Free energy of electrostatic interaction based on aggregate data from SHRP (1991)

Aggregate		Bitumen		pH	κ^{-1} nm	γ_a	γ_b	ΔG^{EL} mJ/m^2
Code	ζ_a mV	Code	ζ_b mV					
RA	-28.1	AAM-1	-54.5	7.7	18	-0.267	-0.486	0.043
RB	-17.1	AAM-1	-61.8	9.1	18	-0.165	-0.538	0.030
RC	-6.12	AAM-1	-65.5	9.8	18	-0.059	-0.563	0.011
RD	-13.6	AAM-1	-66.7	9.9	18	-0.132	-0.571	0.025
RE	-24.2	AAM-1	-57.0	8.1	18	-0.231	-0.504	0.039
RF	-5.8	AAM-1	-64.2	9.5	18	-0.056	-0.554	0.010
RG	-9.4	AAM-1	-65.5	9.8	18	-0.091	-0.563	0.017
RH	-20.5	AAM-1	-54.5	7.6	18	-0.197	-0.486	0.032
RJ	-27.5	AAM-1	-63.6	9.5	18	-0.261	-0.550	0.048
RK	-23.4	AAM-1	-54.5	7.6	18	-0.224	-0.486	0.036
RL	-22.3	AAM-1	-64.8	9.7	18	-0.241	-0.558	0.040

FREE ENERGY OF ADHESION IN THE PRESENCE OF WATER

In this subsection, the free energy of electrostatic interaction (ΔG^{EL}) is brought into perspective. First, this term is assessed on its own, then its contribution to the total Gibbs free energy of adhesion (ΔG^{Tot}) in the presence of water is evaluated.

In order to assess the ability of the free ΔG^{EL} to distinguish between moisture sensitive mixtures, WRI moisture susceptibility test data on MRL asphalt mixtures were obtained (WRI, 2001). Table 29 ranks the aggregate mixtures based on calculated ΔG^{EL} ($\times 10^3$) values. A description of the aggregates, major elemental composition and, observed performance of mixtures are included.

Table 29. Aggregate description and moisture damage performance of mixtures

RANK $\Delta G^{EL} \times 10^3$	MRL Code	Aggregate Type and Origin	Major Elements (Oxide %)	Visual[3]	F-T[4] Cycles
10.48 [(1)]	RF	Glacial Gravel, IL	Ca 25.9 Mg 16.7 Si 15.8 Al 1.89	Intermediate Stripping	40, 30[(5)] (8 – 50)[(6)] 32
11.23 28.54 [(1)]	RC	Limestone, KS	Ca 48.9 C 40.3 Si 6.5 Mg 2.5	Non-Stripping	> 50, >50 (29 – 50) 46
17.22	RG	Sandstone, PA	Si 52.8 Ca 23.8 Al 2.3 K 0.9	Intermediate Striping	41, 44 (4 – 44) 16
25.19 29.57	RD	Limestone, MD	Ca 39.1 C 35.0 Si 16.4 Mg 3.5	Non-Stripping	>50, >50 (26 – 50) 47
32.06	RH	Graywacke, CA	Si 66.0 Fe 12.9 Al 10.4 Na 2.57	Non-Stripping[7]	5, 5 (1 – 5) 3
36.45	RK	Basalt, OR	Si 50.1 Fe 15.7 Al 13.7 Ca 10.3 Mg 6.88	Non-Stripping	>50, >50 (2 – 50) 15
39.08	RE	Piedmont Gravel, MD	Si 93.7 Al 1.86 Fe 1.46 Ca 0.42	Intermediate Stripping	2, 2 (1 – 3) 2

Notes:
1. Based on data from SHRP (1991)
2. Second row based on data from Labib (1992)
3. Water stripping classification from visual observation
4. WRI Pedestal Test freeze-thaw cycles to failure
5. Two specimens tested with bitumen AAM-1
6. Range over nine MRL bitumen mixtures
7. Appears to be considered anomalies by researchers

Table 29 (Continued). Aggregate description and moisture damage performance of mixtures

RANK $\Delta G^{EL} \times 10^3$	MRL Code	Aggregate Type and Origin	Major Elements (Oxide %)	Visual[3]	F-T[4] Cycles
40.01 40.09	RL	Gulf Coast Gravel, TX	Si 63.1 Ca 14.5 Al 4.7 K 1.72	Stripping	2, 2 (1 – 2) 1
43.45	RA	Lithonia Granite, GA	Si 73.4 Al 13.4 K 4.9 Na 3.4	Stripping	>50, >50[(7)] (3 – 12) 16
48.23 72.22	RJ	Granite, WY	Si 76.5 Al 12.2 K 4.3 Na 2.9	Stripping	2, 2 (1 – 2) 1

Notes:
[1] Based on data from SHRP (1991)
[2] Second row based on data from Labib (1992)
[3] Water stripping classification from visual observation
[4] WRI Pedestal Test freeze-thaw cycles to failure
[5] Two specimens tested with bitumen AAM-1
[6] Range over nine MRL bitumen mixtures
[7] Appears to be considered anomalies by researchers

All the free energy values in the table are positive and imply repulsion between bitumen and aggregate in the presence of water. The ranking is in ascending order and therefore increased electrostatic repulsion, which should correspond to increased moisture susceptibility of the mixtures. Mixtures with aggregate AAM-1 manufactured with limestone (RC, RD) should not be prone to stripping while siliceous gravel and granite mixes (RL, RA, RJ) are expected to be moisture sensitive. Indeed, the comparison shows that the free energy of electrostatic interaction is able to distinguish between these materials. Aggregates that are classified as intermediate strippers exhibit large variation in performance with different bitumen types which is evident from the range of freeze-thaw cycles recorded. Visual assessment of stripping is quite subjective

and can be misleading, especially for dark aggregates such as basalt. The relationship between the scaled ΔG^{EL} and the average freeze-thaw cycles to failure are graphically presented in Figures 44 and 45.

Figure 44 is based on the two replicate pedestal test results for AAM-1 mixtures manufactured with different aggregate types. The range suggested by the researchers for aggregate RA implies that the data may not be completely reliable. In addition, testing was terminated at 50 cycles. Surface energy testing as well as electrokinetic measurements on bitumen confirm that aggregate plays a dominant role in bitumen-aggregate adhesion. Figure 45 presents the same-scaled free energy values plotted against the number of freeze-thaw cycles averaged for each aggregate type over all mixtures produced from different bitumen types. Figures 41 and 42 reveal that a shift exists between ΔG^{EL} calculated from SHRP data (1), and ΔG^{EL} calculated from Labib's data (2). This could be attributed to different techniques used and emphasizes the fact that ΔG^{EL} appears to be sensitive under the same conditions of testing.

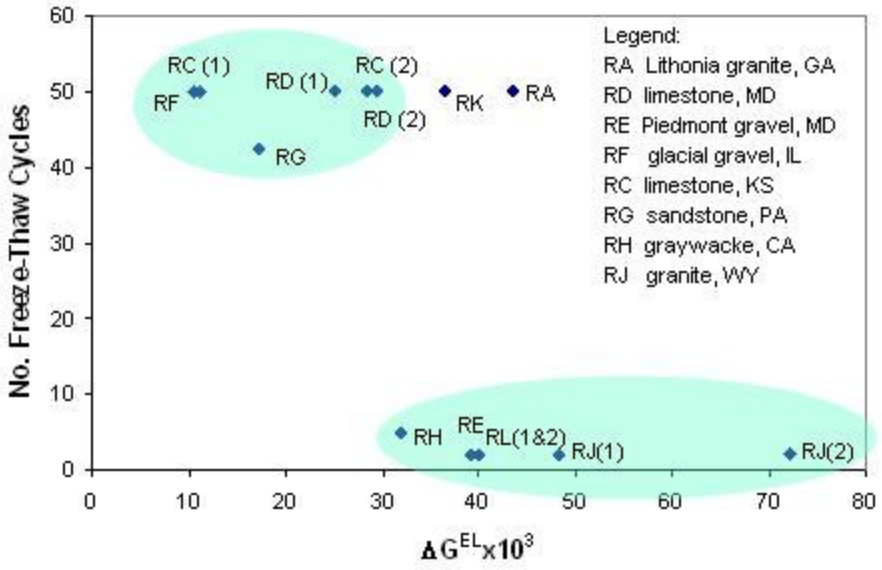

Figure 44. Relationship between freeze-thaw cycles to failure (AAM-1 mixtures) and free energy of electrostatic interaction (AAM-1 with different aggregates)

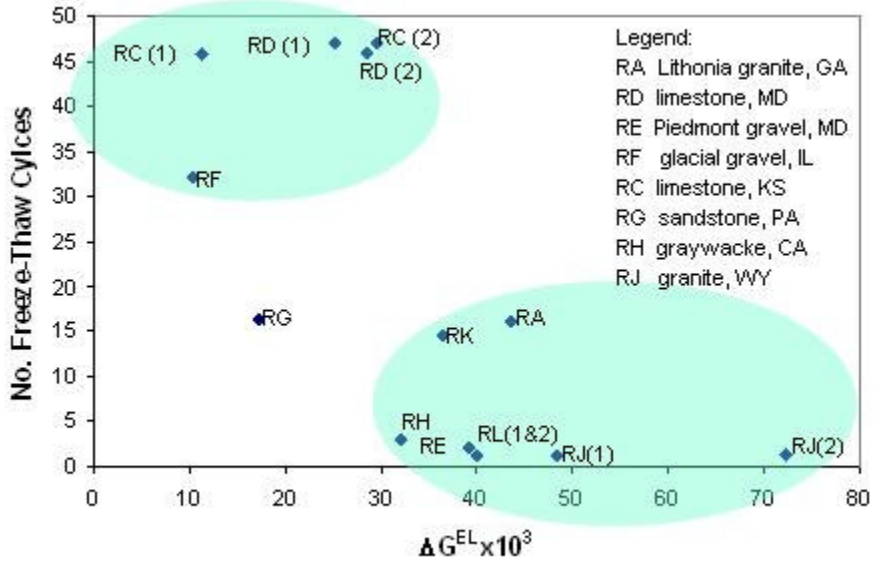

Figure 45. Relationship between average freeze-thaw cycles to failure and free energy of electrostatic interaction (AAM-1 with different aggregates)

An important consideration in this research is to evaluate the contribution of the free energy of electrostatic interaction following the generalized theory of van Oss (1994).

$$\Delta G_{1w2}^{Tot} = \Delta G_{1w2}^{LW} + \Delta G_{1w3}^{AB} + \Delta G_{1w2}^{EL} \qquad (102)$$

The acid and base terms of the Gibbs free energy of adhesion was calculated employing Equation (19) (Chapter II, p. 63) utilizing the surface energy results obtained from experimental work in this research, as presented in the previous chapter. The results based on surface energies for AAM-1 are furnished in Table 30. Surface energy values for bitumen AAM-1 calculated from IGC data were used to compile this table.

Table 30. Comparison of typical magnitudes of free energy terms, specifically ΔG^{EL}

Aggregate + AAM-1	ΔG_{1w2}^{LW} mJ/m^2	ΔG_{1w2}^{AB} mJ/m^2	ΔG_{1w2}^{EL} mJ/m^2	ΔG_{1w2}^{Tot} mJ/m^2	$\%\Delta G^{EL}$
RK	-10.4	18.0	0.036	7.6	0.48
RD	-8.0	49.5	0.025	41.6	0.06
RA	-9.8	66.0	0.043	56.3	0.08
RG	-12.0	166.1	0.017	154.1	0.01
RL	-11.8	196.1	0.040	184.2	0.02

From Table 30, the Lifshitz-van der Waals term is negative as expected, since these interactions are always attractive. The acid-base and electrostatic terms are repulsive. It is evident that ΔG^{EL} is rather insignificant with a contribution of less than 0.5%, and in most cases less than 0.1%, to the total free energy of adhesion in the presence of water. This finding appears to be anomalous considering the correlation of the electrostatic term with performance data.

Having established that the effect of overlapping electric double layers can be neglected, the ability of ΔG_{1w2}^{Tot} to predict adhesion in the presence of water should be investigated with the data at hand. Figure 46 depicts the relationship between the free energy of adhesion and freeze-thaw cycles to failure. This data looks promising considering that tests were terminated at 50 cycles with the RK, RD and RA mixtures exhibiting lower positive free energy values, i.e. less repulsion between the two surfaces in the presence of water. Mixtures produced with AAM-1 were, however, the only ones that produced number of cycles in excess of 50 with aggregate RK and RA. It is rather uncommon for granites to perform this well under wet conditions.

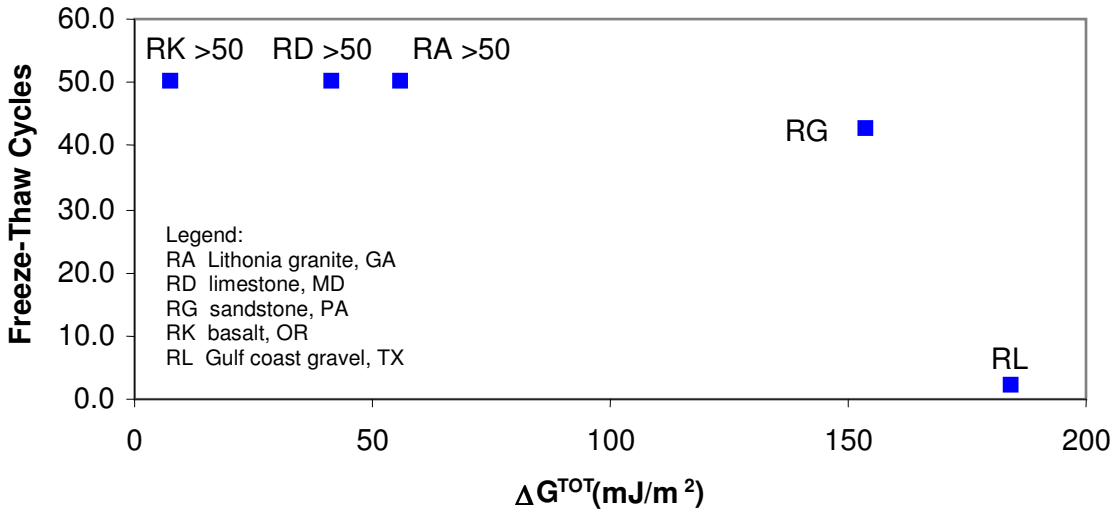

Figure 46. Relationship between freeze-thaw cycles to failure and free energy of adhesion in the presence of water (AAM-1 with different aggregates)

Figure 47 is more representative of the freeze-thaw data in relation to the calculated free energy values. This figure shows both freeze-thaw data for mixtures manufactured with bitumen AAD-1 and averaged over all eight binders (2 replicates each) for each aggregate. The fact that all other asphalt mixtures follow this trend, shows that aggregate characteristics control the strength of the adhesive bond. Performance data for asphalt mixtures with aggregates RD, RG, and RL is consistently explained by the calculated free energy values.

RK and RA performance data do not relate well with free energy values. It is interesting that the same two aggregates showed inconsistencies in the comparison of performance data with electrostatic free energy results. The free energy results for the two aggregates under consideration are somewhat counter intuitive since it is known that granite exhibits quite hydrophilic surfaces. In this research, thin sections of RK basalt

revealed that this aggregate has started to decompose and contain clay which would of course increase its affinity for water dramatically.

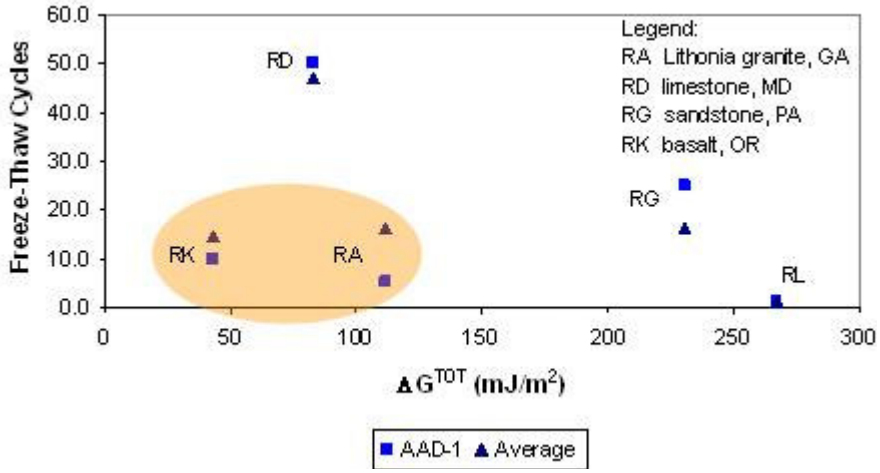

Figure 47. Relationship between freeze-thaw cycles to failure for different mixtures with bitumen AAD-1 and free energy of adhesion in the presence of Water. "Average" represents the average number of cycles over all bitumen types

Although Gibbs free energy of adhesion between bitumen and aggregate relates to moisture damage test results for some aggregates, the calculated thermodynamic parameters do not explain performance observed for others. It should be kept in mind that the freeze-thaw test is yet another laboratory test intended to produce relative numbers, which could be related to performance in a phenomenological way. However, some of these complexities are sometimes captured without knowing what they are.

Table 26 showed that the pH of water in contact with aggregate surfaces remains high after several soaking-decanting cycles. In the first section of this chapter, it was shown that the surface energy components of water are not significantly influenced by

pH. This is not necessarily true for the contacting surface. The surface energies determined experimentally in Chapter III do not account for effects such as pH of the interface water. The fact that a relationship exists between the moisture sensitivity of mixtures and the free energy of electrostatic interaction suggests that ζ-potential (or surface charge) plays a fundamental role in bitumen-aggregate adhesion. Table 30, however, suggests that overlapping of electric double layers is not the controlling mechanism. It is hypothesized that the real manifestation of the effect of these electric properties, is induced by another mechanism.

SIGNIFICANCE OF pH AND ITS RELATION TO DONOR-ACCEPTOR INTERACTIONS

Despite the fact that free energy of electrostatic interaction is insignificant if compared to interfacial free energy, the importance of the effect of pH on the adhesive bond in water cannot be neglected. The latter is reiterated in the following paragraphs before this research concludes with suggestions on how these effects can be incorporated into the current theory.

The proposed dissociation of hydrogen bonds between bitumen and aggregate functional groups with decrease or increase of pH was presented in Chapter II (p. 51).

Yoon and Tarrer (1988) illustrated how an increase in the pH of water aggravates stripping by conducting boil tests on asphalt mixtures manufactured with different aggregates. Figure 48 clearly shows the detrimental effect of pH on the adhesive bond.

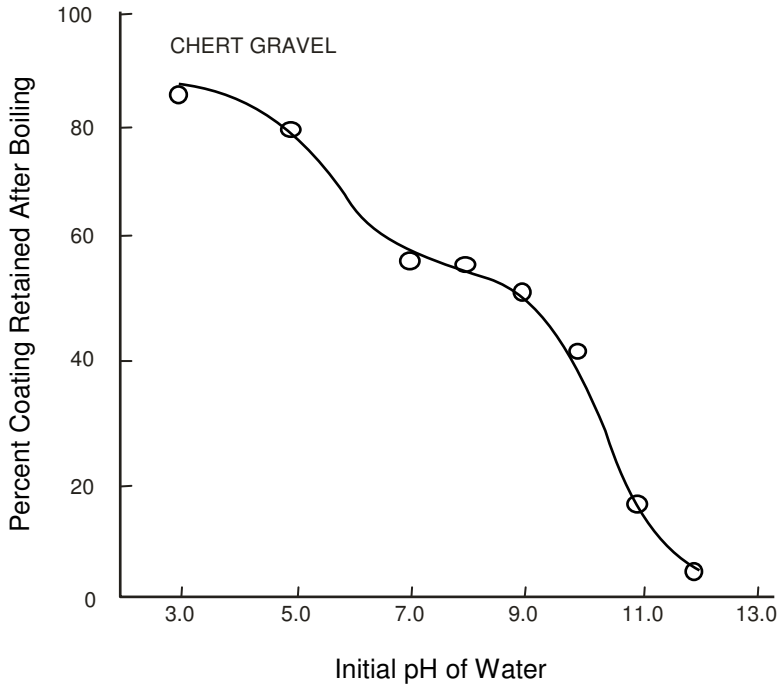

Figure 48. Effect of pH of water used in boiling water tests on a chert gravel asphalt mixture (Yoon and Tarrer, 1988)

Yoon and Tarrer (1988) also conducted a series of boil tests at the natural pH levels imparted by different aggregates in an aqueous environment. This result is depicted in Figure 46. In harmony with previous data (Table 25), pH of the contacting water in all cases is basic. Granite, which produced a high pH also had a higher propensity for stripping than quartz gravel or chert gravel, both of which imparted a lower pH to the contacting water.

Figure 49 reveals another important aspect of bitumen-aggregate adhesion, and that is the fact that limestone was not significantly affected by the high pH surroundings. As illustrated and discussed in Chapter II (p. 45) and also proposed by Yoon and Tarrer, free calcium in limestone associates strongly with acidic functional groups in bitumen, such as carboxylic acids, to form carboxylate salts that are not easily dissolved in the

presence of water. Figure 49 suggests that these bonds are preserved even at high pH levels.

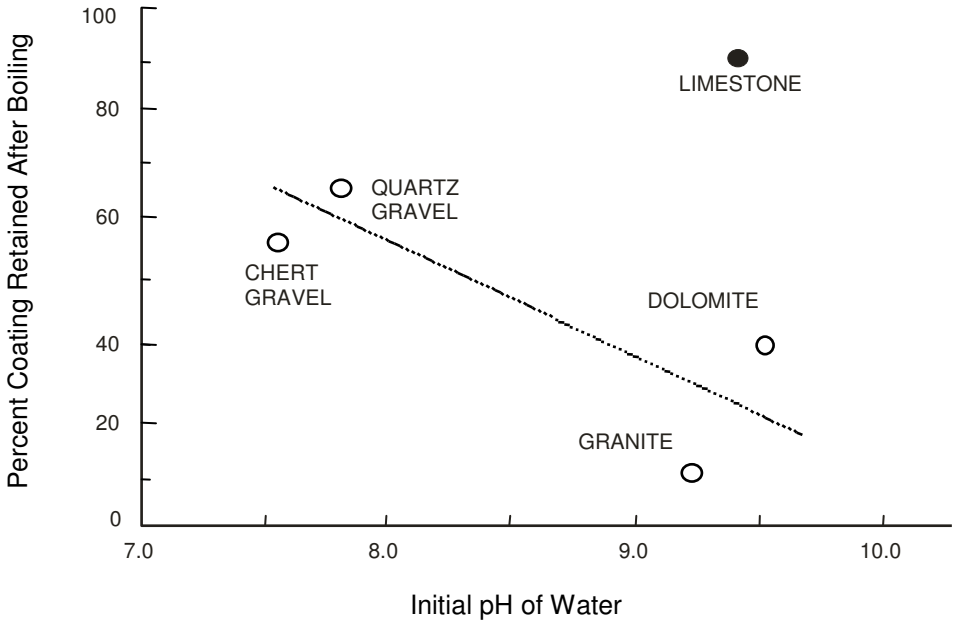

Figure 49. Stripping propensity as a function of the natural pH of water in contact with different aggregates (Yoon and Tarrer, 1988)

Data presented in Table 27 showed the influence of pH on the free energy of electrostatic interaction. By decreasing the pH from 9 to 6, repulsion reduced with approximately 63% for granite RJ. More significantly, in the case of limestone RD, a reduction in pH from 10 to 6 changed the electrostatic free energy from an already low repulsion to attraction. Based on the data presented in the previous subsection, a link between the changes in these minute forces and performance on a more significant level exists.

Surface charge of a solid particle and counter ions in an organic liquid are induced by donor-acceptor interactions between the solid surface and the liquid. The energy levels of the solid and liquid determine the direction of electron transfer and the sign of the surface charge (Labib, 1988). The donor-acceptor properties of surfaces can be characterized in terms of both proton and electron transfer. The pH scale defines the acidity of aqueous media and is a measure of hydrogen activity and therefore acid-base reactions that involve proton transfer phenomena. Electron transfer properties involve donor-acceptor reactions according to the generalize Lewis acid-base theory. Gutmann's donor and acceptor numbers have defined the donor and electron strengths of a series of organic liquids (non-aqueous). The series of donor numbers is known as the donicity scale (Labib and Williams, 1986; Labib, 1988). Labib and Willams (1986) illustrated that a correlation exist between the aqueous pH scale and the non-aqueous electron donicity scale through electrokinetic measurements. In the following subsections, the donicity and pH scales are explained and illustrated with reference to aggregate characterization. In addition, this data is used to relate the two scales to demonstrate how the donor-acceptor properties of these surfaces depend on the aqueous pH environment.

The Donicity Scale

Van Oss (1994) refers to work done by Fowkes and his colleagues where electrophoreses of electron-accepting (+) and electron donating (-) particles suspended in electron donating (-) and electron accepting (+) organic liquids, respectively. The following rules pointed out by van Oss, are of importance in this context:

- "(+) particles suspended in (-) liquids are negatively charged"
- "(-) particles suspended in (+) liquids are positively charged"

Labib (1990) derived the donor-acceptor properties of inorganic solid particles from ζ-potential measured in organic liquids. In this approach, ζ-potential of a solid surface is plotted as a function of liquid donicity, defined according to the Gutmann scale in kcal/mol. The donicity of a solvent is the enthalphy of reaction between the solvent and

a solution of Lewis acid, $SbCl_5$, in reference dichloroethane (DCE). DCE thus have a donicity of zero kcal/mol and liquids with higher values are stronger electron donors. The isoelectric point (IEP, where ζ-potential is zero) on the *donicity scale* is considered to be the donicity of the solid surface. At this point no net electron transfer between the liquid and solid surface occurs. Labib and Willliams (1987) also investigated the effect of moisture testing dry and "wet" (50% humidity) particles in dried organic liquids. A schematic illustration of a zeta-donicity plot is presented in Figure 50 showing three characteristic regions of donor-acceptor interactions.

In Region I, the solid surface acquires a positive charge in more acidic (acceptor) liquids. A lower ζ-potential represents weaker interactions in the presence of moisture. Region II is the water-sensitive region. The surface properties change from an acceptor to a donor and the surface charge changes from negative to positive. The adsorbed moisture induces a shift in the donicity of the solid, i.e. IEP. In addition, the surface charge can be positive or negative depending on the presence or absence of moisture. The surface acts as an acceptor and acquires a negative charge in Region III. Moisture weakens the interaction evident from the decrease in ζ-potential.

Labib and Wielicki (1993b) investigated the donor-acceptor properties of MRL aggregates using a number of donor-acceptor organic liquids that represents functional groups in bitumen. The effect of moisture was also investigated. The ζ-potential - donicity curve for RL gravel from Dopler-shift electrophoreses measurements is furnished in Figure 51.

RL Gravel exhibits electron acceptor behavior with organic liquids having donicities higher than 2.7 kcal/mol. Adsorption of water changes the surface from and acceptor to a donor in dichloroethane. A decrease in ζ-potential in the presence of moisture indicates a weaker bond and RL aggregate was found to be the most water susceptible aggregate tested with intermediate accepticity. It is reported that RJ Granite was the most acidic (acceptor) material, while the two calcite-based materials, RC and RL showed basic character as expected.

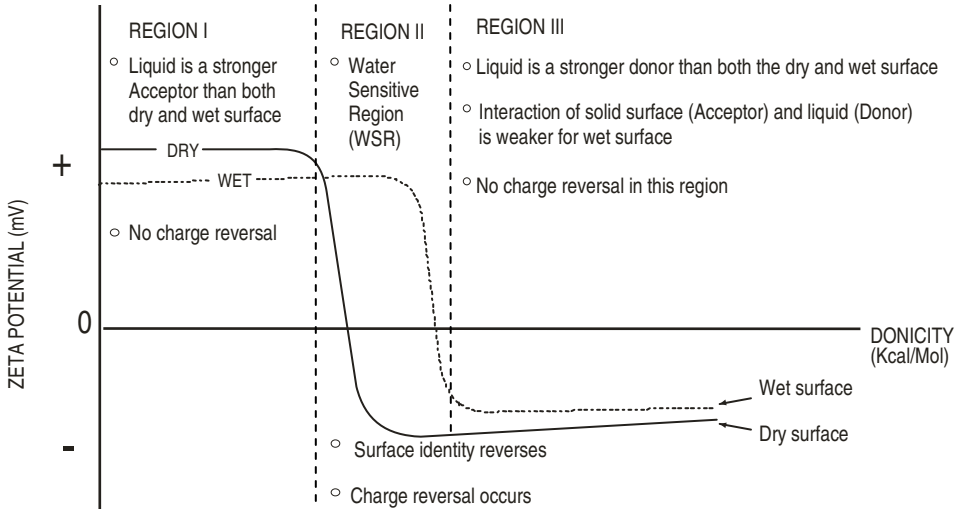

Figure 50. Schematic description of three regions describing donor-acceptor interaction based on the donicity scale (Labib and Williams, 1987)

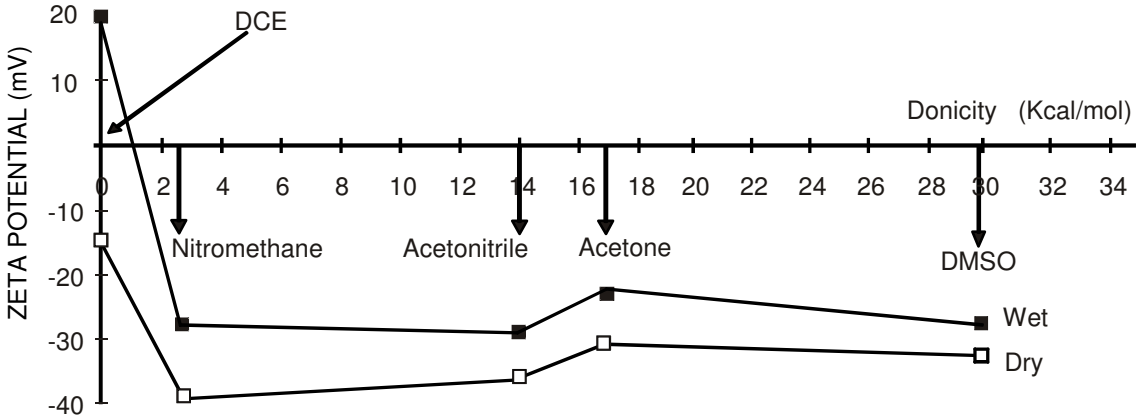

Figure 51. ζ-potential vs. donicity curve for RL aggregate (Labib and Wielicki, 1993b)

In Chapter II it was stated that bitumen generally exhibits an excess of acidic functional groups if compared to basic functional groups. It can therefore be reasoned that aggregate with stronger electron donor character should form stronger and more durable bonds. Since isoelectric point on the donicity scale is an indicator of the donicity of the solid surface, these parameters were obtained for the four aggregates tested by Labib and Wielicki and plotted against the average number of freeze-thaw cycles. Although the data is limited to four aggregates, Figure 52 shows that aggregates that produced more moisture sensitive mixtures relate to lower donicity values. Although the freeze-thaw test results do not show a difference between performance aggregate RJ and aggregate RL, the higher donicity value for RL can be explained by the fact that this is a mixed gavel, containing about 15% limestone.

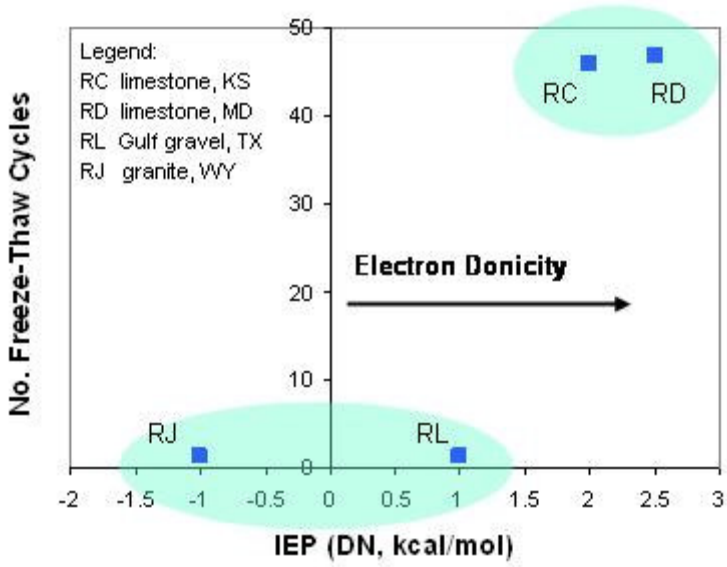

Figure 52. Performance related to isoelectric point on donicity scale

The pH Scale

Measuring ζ-potential as a function of pH was introduced in Chapter II and formed an integral part of the discussions presented thus far. Interesting and important aspects related to the interpretation of these results within the context of this subsection are briefly introduced. Figure 53 is a schematic typical for sileceous aggregates showing three distinct pH regions that characterize the surface under these conditions. The isoelectric point (IEP, zero ζ-potential) of a solid on the *pH scale* describes the acid-base proton transfer properties of the solid surface. Labib and Wielicki (1993a) explains the surface chemistry based on the three regions depicted in Figure 53 as follows.

In Region I, adsorption of protons lead to a positive charge on the surface. Region II includes the IEP, defined by the equillibrium adsorption of protons and hydroxyl ions. In general, siliceous aggregate shown in Figure 53 behaves as a strong acid with IEP 3.4. Region III is characterized by hydroxil group dissociation with associated increase in ζ-potential. Surface dissolution takes place in this region (refer to Weak Bounday Layer Theory, Chapter II). The authors point out that dissolution rate depends on the pH, ion composition, organic compounds and temperature. As discussed in Chapter II, dissolution of calcite based aggregates will take place in low pH environment.

In a similar way as described above for the donicity scale, aqueous isoelectric points for the four aggregates were related to the average number of freeze-thaw cycles to failure as depicted in Figure 54. This parameter shows a similar relationship with moisture sensitivity data and distinguishes the more basic aggregates from the more acidic ones. Since bitumen generally has a net acidic character, functional groups such as carboxylic acids will act as proton donors which will tend to form more durable bonds with strong proton accepting aggregate surfaces.

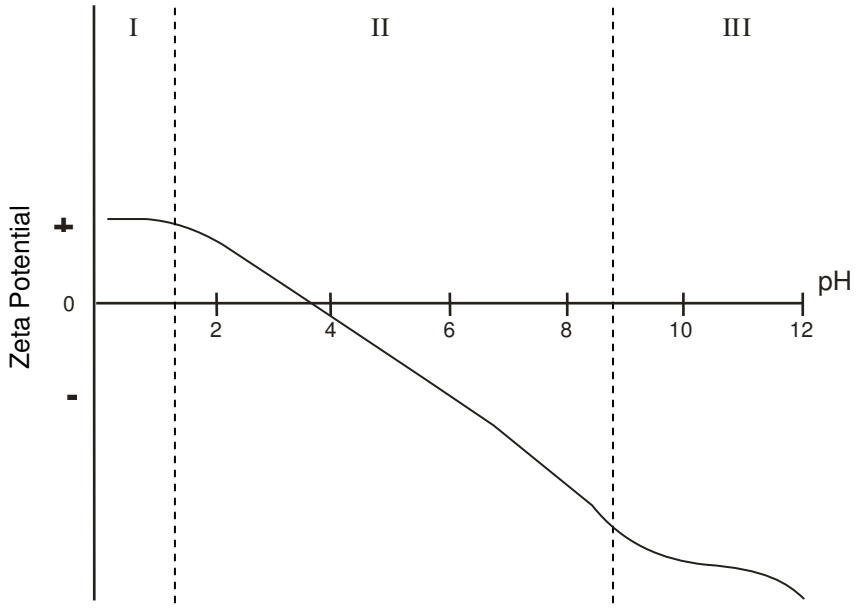

Figure 53. Typical ζ-potential vs. pH curve for siliceous aggregates (Labib and Wielicki, 1993a)

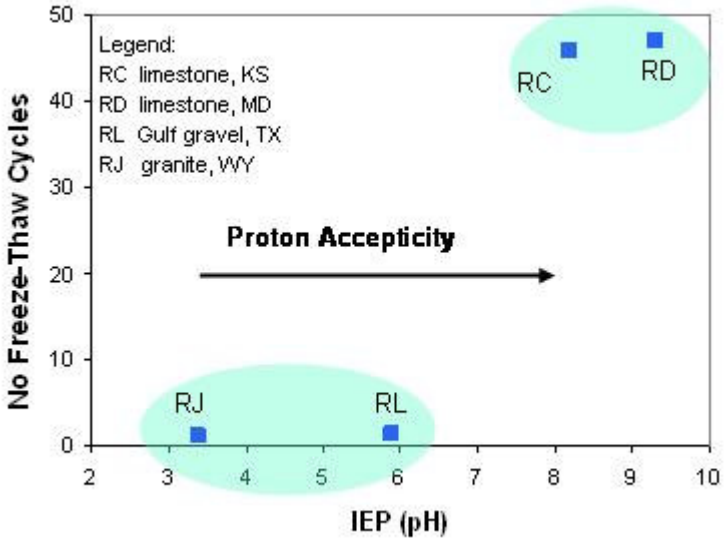

Figure 54. Performance related to isoelectric point on the pH scale

Comparison of Scales

Both the pH and donicity scales are energy related scales since both could be expressed in terms of free energy of reactions, and thus constitutes a measure of electron transfer. The free energies can be expressed in the following form (Labib and Williams, 1986):

$$\Delta G_{pH} = -RT \ln\left(a_{H^+} / a_{oH^+}\right) = 2.303RT\left(pH\right) \tag{103}$$

$$\Delta G_{DA} = -RT \ln K \tag{104}$$

Where ΔG_{pH} is the free energy for transfer of an electron between two hydrogen electrodes with H^+ activities, a_{H^+} and a_{oH^+} respectively, gas cas constant R, and absolute temperature T. ΔG_{DA} is the free energy of donor-acceptor chemical reactions, where K is the equilibrium constant (Labib and Williams, 1986).

Experimental alignment of the scales based on the isoelectric points of the four aggregates determined by electrophoretic mobility at various pH values discussed in the preceding sections. In addition, isoelecric points of the aggregates obtained from electrophoretic mobility measurements in organic liquids are required. Restated, donicity of a solid is defined by the isoelectric point and equates to the donicity of a liquid that neither donates nor accepts electrons in contact with the solids. Only the "wet" IEPs were used for scale comparison. The IEPs of the two scales provides a good correlation as shown in Figure 55. Having established this common relationship between pH and donicity, an "absolute" scale can be established for each aggregate by assigning zero donicity to the aqueous IEPs. The final relationship is shown in Figure 56.

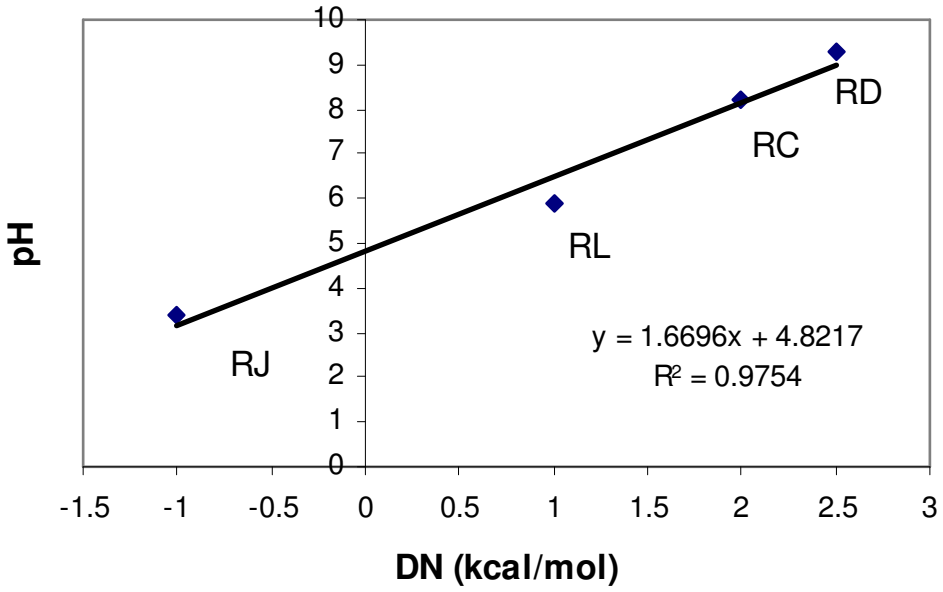

Figure 55. Relationship between pH scale and donicity scale

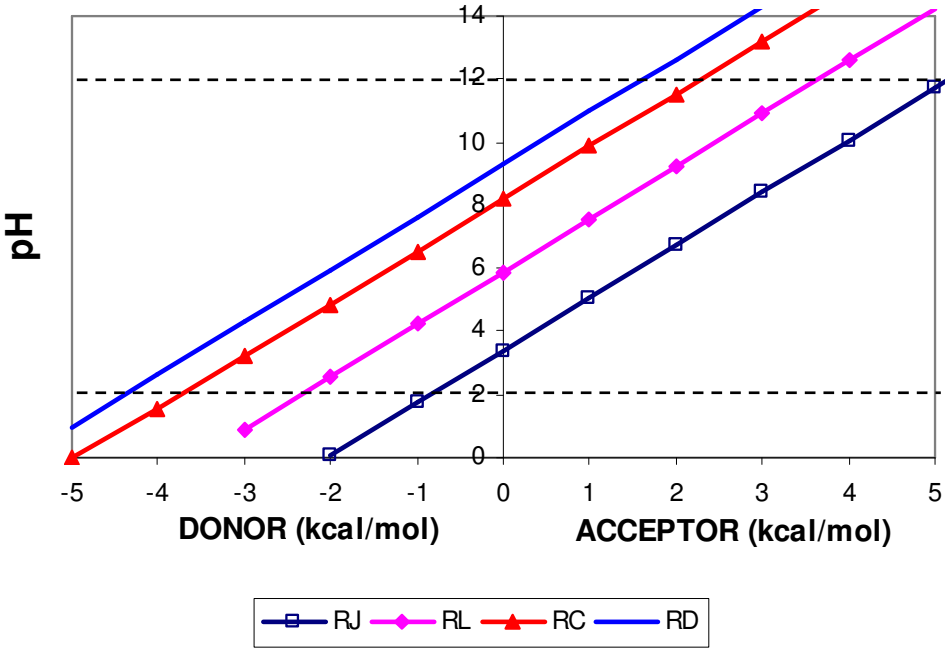

Figure 56. Donor-acceptor properties of aggregates at different pH levels

Figure 56 indicates that the surface of RJ aggregate dominantly shows electron acceptor behavior over a wide range of pH conditions, but changes to donor characteristics in aqueous environments with a pH of less than about 3,4. RD aggregate on the other hand mostly exhibits electron donor properties which can change to electron acceptor properties at high pH levels. In addition, RJ has the strongest acceptor properties and RD the strongest donor properties under any given pH condition.

While the Labib approach presents only the dominant character of the surface, i.e. either electron acceptor or electron donor properties, these results relates to the expected acid-base characteristics of these surfaces. In addition, this initial attempt to relate these numbers to performance data revealed promising results.

These acceptor and donor numbers, in kcal/mol, are in fact free energies and if they could be converted to mJ/m^2, then the values could be used in the van Oss- Chaudhury-Good theory to calculate the work of adhesion. Such a conversion should, if possible, be unique to the proposed approach, separated from the scales originally used with the aforementioned theory.

CONCLUSIONS

Based on work done by Professor van Oss at the State University of New, York, at Buffalo, the effect of pH on surface energy of water was found to be insignificant for practical considerations. Therefore, although it is known that the pH of water in contact with aggregates is altered, there is no need to adjust the surface energy components to account for this effect when the free energy of adhesion is calculated in the presence of water. It is a well-known fact, however, that dissolved salts do influence the surface tension of water. This effect, for example, is responsible for osmotic suction in fined-grained soils. This effect on surface energy components of water needs further work.

Electric double layer effects as a contributory part of adhesion in the presence of water was investigated. A plate-plate configuration was assumed to calculate the free energy of electrostatic interaction. Data from electrophoreses measurements performed

by Labib and co-workers on selected MRL bitumen and aggregate types, played an important role in this study. The aggregate data was supplemented by electrophoreses results reported as part of the official MRL aggregate characteristics during the SHRP Program. These data sets were utilized to calculate the free energy of electrostatic interaction (ΔG^{EL}) between bitumen and aggregate. Comparison of these results with moisture sensitivity performance data from the literature reveals that ranking of aggregates in terms of strippers, intermediate strippers and non-strippers, is consistent with performance data. Despite this initial finding, comparison of the electrostatic term (ΔG^{EL}) with free energy of adhesion ($\Delta G^{LW}+\Delta G^{AB}$) indicates that the contribution of the electrostatic term is negligible. It was hypothesized that the correlation of the electrostatic term with performance suggests the existence of another mechanism associated with electrical phenomena at the interface, which is manifested at a more significant level.

Work by Labib and co-workers showed that a relationship exists between donor-acceptor properties of surfaces and ζ-potential. In addition, they illustrated that a relationship between the pH scale and donicity scale exist because both are intrinsically energy scales. Limited data on four aggregates suggests a logical relationship between isoelectric points derived from both scales and performance data. More testing is needed in this regard. Based on Labib's data on four MRL aggregates, the relationship between the pH and donicity scales for these materials is presented. This relationship is significant and paves the way to quantifying adhesion in the presence of water at pH levels expected in the field. The parameters suggested by the Labib approach can be used to identify moisture sensitive aggregates. Alternatively, the free energy of electrostatic interaction can be used as such. Ideally, the Labib approach should be explored in order to express the donor-acceptor numbers in terms of mJ/m^2. It is envisioned that these numbers could then be used to calculate the free energy of adhesion in the presence of water utilizing the theory developed by van Oss-Chaudhury and Good. Apart from the fact that the effect of pH would be quantifiable, this approach offers the potential to replace the current scale with a more 'absolute' scale.

CHAPTER VI

CONCLUSIONS AND RECOMMENDATIONS

SUMMARY

This research aimed at advancement of a materials design process which would enable assessment of adhesion in bitumen-aggregate systems based on a more fundamental, macroscopic approach. The theory developed by van Oss, Chaudhury and Good forms the core of this approach, and allows quantification of adhesion through known surface energy parameters of the materials under consideration.

This research focused on surface energy characterization of bitumen and aggregate, and quantification of the effect of water with special reference to the pH of the interface water. To place this effort in perspective and to gain an understanding of the theories and mechanisms of bitumen-aggregate adhesion, a synthesis was carried out. Findings from this synthesis served as the basis for selecting key research needs pursued during this research. An important part of the scope of this research included a comprehensive review and assessment of existing and potential techniques for surface energy characterization of bitumen and aggregate.

Materials from the Strategic Highway Research Program (SHRP) Materials Reference Library (MRL) were selected for surface energy characterization; five bitumen types and five aggregate types that represent a wide range of chemical composition. Existing methodologies and analysis procedures for bitumen surface energy characterization with the Wilhelmy plate technique were evaluated, and refined procedures documented. Inverse gas chromatography (IGC) was identified as a feasible alternative to the Wilhelmy plate technique and detailed test methodologies and analysis procedures were documented. Precision statements for both techniques were made based on reproducibility of the results obtained. Total surface energies were compared with mechanical surface tension values from the literature, obtained by the du Nöy ring and pendant drop techniques.

A rationale for the inability of the techniques used in this research to effectively distinguish between untreated bitumen and bitumen treated with liquid anti-strip agent is presented, and the concept of 'potential' surface energy introduced.

A refined methodology for aggregate characterization is presented and surface energy results for the five aggregates reported. Precision of the technique was evaluated and discussion presented. Surface energy data for bitumen and aggregate served as an important input to calculation of the free energy of adhesion in the presence of water and evaluation of proposed refinements in this regard.

This research inspired a study conducted by Professor van Oss, co-founder of the adopted theory, on the effect of pH on the surface energy components of water. The free energy of electrostatic interaction (ΔG^{EL}) was introduced as a third term following the generalized theory proposed by van Oss. This term, which describes the forces generated when electric double layers overlap, was calculated based on data obtained from the literature. It was hypothesized that this term held the potential to quantify the effect of pH of the interface water on the adhesive bond. Relations of ΔG^{EL} with moisture sensitivity performance data were evaluated. The contribution of this term, and therefore its practical significance, was investigated by comparison with the total free energy of adhesion calculated from surface energy values of the materials tested during this research.

The relationship between ζ-potential and donor-acceptor surface properties was studied and presented as an alternative mechanism through which the effect of pH could manifest. Based on the work done by Labib and co-workers, the relationship between the pH scale and donicity scale was investigated and recommended future research identified.

FINDINGS

A vast amount of literature exists on adhesion between bitumen and aggregate. Synthesis of this information is presented within the framework of theories and mechanisms, well established within the general field of adhesion science. The theories presented include the (weak) boundary layer theory, mechanical theory, electrostatic theory, chemical bonding theory, and thermodynamic theory. The thermodynamic theory is the most widely applied due to its convenience in calculating free energies of adhesion and use of the universal energy concept. Table A1, Appendix A, is a simplified summary of this synthesis.

A comprehensive review of techniques for surface energy characterization of solid surfaces is presented. The techniques were assessed in terms of the ability to produce quantities that are compatible with the surface energy theory adopted in this research, practicality, and potential effectiveness. Contact angle techniques, vapor sorption techniques, force microscopy, and microcalorimetry were considered. The Wilhelmy plate and sessile drop methods, both contact angle techniques, are proposed as well-established and relatively simple techniques. Inverse gas chromatography is identified as a strong candidate. Aggregate surfaces, however, present a more complex situation, which limits the applicability of most techniques, investigated. Vapor sorption appears to be the best approach and has been used by previous researchers. The family of sorption techniques that relies on the development of sorption isotherms are intrinsically time consuming due to the times required to reach equilibrium stages. In addition, static vapor sorption techniques require a sample vacuum preconditioning process. Dynamic vapor sorption techniques differ in that vacuum degassing is not required and preconditioning processes could be followed that relate in a more intuitive way to field conditions. Inverse gas chromatography has been used extensively for mineral characterization, but its applicability to heterogeneous surfaces on a macroscopic level, is not a simple matter. The thin layer wicking method is a simple indirect contact angle technique for solid particles less than approximately a 100 μm in size.

Apart from refining the Wilhelmy plate tests methodology, analysis procedures were also scrutinized. It was found that the condition number (CN) can be used to select a balanced set of probe liquids and that inclusion of methylene iodide, a non-polar or dispersive liquid, is imperative. Despite this selection process, as well as the use of a single value decomposition (SVD) analysis approach, negative square roots were inevitable in some solutions. The selection of larger liquid sets did not take care of this problem either. While advancing contact angles predominantly showed slip-stick phenomena, receding contact angles obtained with most liquids deviated substantially from a plot of $\gamma_L \cos\theta$ versus γ_L. Although both these observations imply deviation from the assumptions of Young's equation, acceptable errors were generally obtained. The addition of additives did seem to aggravate these conditions.

Inverse gas chromatography (IGC) was used successfully to characterize bitumen surface energies. The technique is relatively simple and lends itself to perform these measurements at different temperatures with ease. Different from the contact angle approach, problems with negative square roots (components that are set to zero) are eliminated with this technique.

In both techniques, the Lifshitz-van der Waals component of bitumen is dominant. Values obtained from receding angles are in the order of 38 mJ/m^2 and compare with IGC values, which are in the order of 45 mJ/m^2. These dispersive components are much lower when derived from advancing contact angles, typically in the order of 20 mJ/m^2, and show slightly larger differences between bitumen types. Total surface energies follow similar trends and comparison with mechanical surface tension data revealed that values from receding contact angles and IGC are of the same order. The differences between different bitumen types are not significant, and were confirmed by mechanical surface tension data. The Lifshitz-van der Waals component was identified as the most appropriate parameter to compare precision between the two techniques. Both techniques exhibited comparable, and acceptable precision based on the Lifshitz-van der Waals component.

Slightly higher polar components were obtained with IGC. Values up to approximately 3 mJ/m^2 were determined for the acid component with toluene, while base components were generally below 1 mJ/m^2. These components derived from contact angles were generally below 1 mJ/m^2, except for the base components obtained from receding angles. It should be noted, that acid and base components can be manipulated depending on the selection of the liquids set, but that these numbers generally remain small. It seems that the receding angle might be a more sensitive parameter to use for calculation of surface energies. This is indeed the only parameter that logically showed an increase in the base component with addition of 0.5% amine anti-strip agent for one bitumen, namely, AAB-1. Although boil tests showed a dramatic increase in adhesion with the addition of only 0.25% of this additive for both bitumen types AAB-1 and ABD, these observations could not be consistently confirmed with the two techniques evaluated in this research.

A literature study of polyethylene grafted with 1% acrylic acid (polar compound) showed that polymeric materials cannot be considered to have intrinsic surface energies and that the polar component(s) of surface energy changes with time due to molecular orientation towards the surface in contact. The concept of 'potential' surface energy states that different surface energies are possible for a particular polymeric material depending on the chemistry of the surface in contact. This research from the literature suggests that the acid and base components of surface energy cannot be quantified realistically based on a surface prepared and tested in air or in the presence of an inert carrier gas. It should be noted that the Lifshitz-van der Waals component, obtained with the techniques adopted in this research, is acceptable. Alteration of the methods or another technique, such as the two-liquid phase contact angle technique (a static, therefore sessile drop type approach) should be investigated to obtain realistic numbers for acid and base components. This is especially important when additives are used.

Surface energy results were obtained from experiments with the universal sorption device (USD) using a more efficient test methodology. While bitumen surface energies are dominated by the Lifshitz-van der Waals component, aggregate surface energies are

dominated by the polar components. This explains the controlling role of aggregate on bitumen-aggregate adhesion. Manifestation of the scale problem, i.e. all surface energy components referenced to water with an assumed acid-base ratio of 1:1, is pronounced in the case of aggregates with exhibition of exceptionally high base components in all cases. The precision of this technique based on such heterogeneous materials is unrealistic and needs further investigation. Specific surface areas determined with a commercial nitrogen adsorption device for two aggregates compared favorably with the numbers generated from experiments with the USD. The effects of vacuum degas preconditioning process as an integral part of the static sorption technique was identified as an important variable that needs further consideration. In addition, it is difficult to relate this process to asphalt mixing plant conditions. It is envisioned that a dynamic vapor sorption approach would be more user-friendly and would eliminate the need for vacuum degas preconditioning.

Inspired by this research, the effect of pH on the electron donor-electron acceptor properties of water were investigated by Professor C.J. van Oss and colleagues. Contact angle measurements of water at an acidic, close to neutral and basic pH, on a electrostatically neutral surface revealed that the pH effect is practically insignificant. No adjustment of the surface energy components of water is therefore required to compensate for the effect of pH when adhesive bonding in the presence of water is calculated. It should, however, be noted that the effect of organic or inorganic solutes will still influence surface tension and that this effect has not been considered thus far.

Following the generalized theory proposed by van Oss (1994), it was hoped that the introduction of a third term, called the free energy of electrostatic interaction, would be able to elucidate the effect of pH on the adhesive bond. Calculation of this term utilizing ζ-potential data from the literature showed that these values correlate with moisture sensitivity performance data for the same aggregate mixtures. Surprising, however, is the fact that the term itself is very small and negligible if compared to the total free energy of adhesion, which is essentially based on surface energy of the two materials

under consideration. This apparent anomaly indicates that another, more significant mechanism related to electrical phenomena at the interface is at work.

Research by Labib and co-workers suggest that a relationship exist between ζ-potential and donor-acceptor surface properties. In addition, they proposed a relationship between the aqueous pH scale and the non-aqueous donicity scale. This relationship was illustrated utilizing data available on four aggregates from electrophoreses experiments conducted by these researchers in the early 1990s. While it is anticipated that the Labib approach holds the key to quantifying the effect of pH of the interface water on the adhesive bond, it also presents another attractive potential. It should be possible to replace the original scale (proposed by van Oss and his colleagues) with the more 'absolute' scale following the Labib approach.

RECOMMENDATIONS

While the two techniques evaluated for surface energy characterization of bitumen can be used to obtain realistic values for the Lifshtiz-van der Waals components, this research showed that effective characterization of polar (acid and base) components needs further investigation. The two-liquid phase contact angle approach was briefly described as a possible solution. The key issue identified is the exposure of the bitumen surface to a reference polar medium over time. This is especially important when bituminous materials with additives need to be characterized.

More user-friendly devices should be explored for aggregate surface energy characterization. Van Oss (1993) showed that the specific surface areas of powders obtained from thin layer wicking, compared well to that obtained from the BET approach (sorption). These findings warrant research into the use of thin layer wicking for surface energy characterization of aggregate particles. It is anticipated, however, that effective preconditioning may be a problem. In addition, this technique can only be applied to powder sized particles. Dynamic vapor sorption devices are commercially available nowadays. This approach is considered a strong candidate for aggregate surface energy characterization. Similar to static techniques, isotherms are also

produced, but no vacuum degassing is required. Specimens can be heat treated in the presence of inert gas or air flow. While inverse gas chromatography is similar to dynamic vapor sorption, an adsorption-desorption process needs to take place before elution and signal detection can occur. The success of this process depends on specimen surface area and porosity, and abundance of high-energy sites which necessitate selection of the right sample mass. In addition, the test is carried out at infinite dilution, which complicates testing of heterogeneous materials. Static and dynamic vapor sorption approaches which rely on 'monolayer coverage' and isotherm development can be used to obtain either adsoption data, desorption data, or both. Desorption experiments are more difficult to perform, especially on high-energy, high absorptive type of materials. It remains therefore a balance between the significance of these measurements and practicality of the test with implementation in mind. Furthermore, a device is needed where at least relative values can be obtained with options to explore the significance of others.

The possible use of electrophoreses for surface energy characterization of aggregate was not addressed in this research although the literature suggests that this can, and has been done in the past. Chibowski and Holysz (1986) and Holysz et al.(1991) determined dispersive and polar surface energies of quartz and glass in the past using this approach. According to Chibowski (2004: personal communication), however, this is not a very effective way to characterize surface energies of solid particles and can be time consuming. The author has not seen any work in recent literature where this approach has been applied to determine surface energies specifically. Based on research presented in this document, the significance of the work done by Dr. M. Labib is an incentive to investigate the use of electrophoreses for surface energy characterization more closely. This technique appears to be the key in studying adhesive bonding in aqueous environments, especially with regard to the effect of pH of the interface water.

The relationship between the electron donor-electron acceptor numbers derived from the Labib approach and the compatibility of these numbers (kcal/mol versus mJ/m^2) with the combining rule or theory proposed by van Oss, Chaudhury and Good needs to be

explored. The emphasis of these discussions focused on aggregates. The effect of pH on bitumen surface energies can easily be studied by performing contact angle measurements with water at different pH levels as one of the liquids in the set. Such an experiment is simplified by the fact that pH does not effect the surface energy components of water significantly.

Although the effect of pH on surface energy components of water was found to be negligible, it is well known that surface tension of water is altered when organic or inorganic solutes are present. Further research is needed to gain a full understanding of this effect on the surface energy components of water.

Finally, the current thermodynamic theory only addresses physical interactions. Chapter II suggests that insoluble salts may form at interfaces when certain bitumen and aggregate types interact or when additives are present. This is therefore chemical bonding in the true sense. It is interesting that bonding energy calculations for RD limestone correlated well with moisture sensitivity data. This aggregate is expected to form strong insoluble coordination complexes at the interface. It may indicate that a relatively stronger physical interaction is predicted by this theory and that this approximation is sufficient for practical purposes. This hypothesis needs to be verified.

REFERENCES

Adamson, A.W., and Gast, A.P. (1997). Physical chemistry of surfaces (6th edition). New York: John Wiley & Sons.

Adão, M.H., Saramago, B. and Fernandes, A.C. (1998). Estimation of the surface tension components of thiodiglycol. Langmuir, 14, 4198-4203.

Allan, K.W. (1992). Mechanical theory of adhesion. In D.E. Packham (Ed.), Handbook of adhesion (pp. 273-275). Essex, England: Longman Group UK Ltd.

Ardebrant, H., and Pugh, R.J. (1991a). Surface acidity/ basicity of road stone aggregates by adsorption from non-aqueous solutions. Colloids and Surfaces, 53, 101-116.

Ardebrant, H., and Pugh, R.J. (1991b). Wetting studies on silicate minerals and rocks used in bitumen highways. Colloids and Surfaces, 58, 111-130.

Atkins, P.W. (1986). Physical chemistry (third edition). New York: W.H. Freeman and Co.

Barbour, A.F., Barbour, R.V., and Petersen, C.J. (1974). A study of asphalt-aggregate interactions using inverse-liquid chromatography. Journal of Applied Chemistry and Biotechnology, 24, 11, 645-654.

Bard, A.J. and Faulkner, L.R. (1980). Electrochemical methods: Fundamentals and applications. New York: Wiley.

Beach, E.R., Tormoen, G.W., and Drelich, J. (2002). Pull-off forces measured between hexadecanethiol self-assembled monolayers in air using an atomic force microscope: Analysis of surface free energy. Journal of Adhesion Science and Technology, 6(7), 845-868.

Bhasin, A. (2004). CASE software manual. Unpublished manuscript. NCHRP Project 9-37. College Station, Texas: Texas Transportation Institute.

Bose, A. (2002). Measurement of work of adhesion between asphalt and rock. Unpublished Report. Rhode Island: Department of Chemical Engineering, University of Rhode Island.

Brannan, C.J., Jeon, Y.W., Perry, L.M., and Curtis, C.W. (1991). Adsorption behavior of asphalt models and asphalts on siliceous and calcareous aggregates, Transportation Research Record, 1323, 10-21.

Brendlé, E., and Papirer, E. (1997a). A new topological index for molecular probes used in inverse gas chromatography. Journal of Colloid and Interface Science, 194, 217-224.

Brendlé, E., and Papirer, E. (1997b). A new topological index for molecular probes used in inverse gas chromatography for the surface nanorugosity evaluation. Journal of Colloid and Interface Science, 194, 207-216.

Brewis, D.M. (1992). Weak boundary layers. In D.E. Packham (Ed.), Handbook of adhesion (pp. 501-502). Essex, England: Longman Group UK Ltd.

Butt, H-J., Graf, K., and Kappl, M. (2003). Physics and chemistry of interfaces. Weinheim: WILEY-VCH Verlag GmbH & Co. KgaA.

Castells, R.C., Arancibia, E.L., and Nardillo, A.M. (1982). Solution and adsorption of hydrocarbons in glycerol as studied by gas-liquid chromatography. Journal of Physical Chemistry, 86, 4456-4460.

Chadan, C., Sivakumar, K., Masad, E., and Fletcher, T. (2004). Application of imaging techniques to geometry analysis of aggregate particles. Journal of Computing in Civil Engineering, ASCE, 75-82.

Charmas, B., and Leboda, R. (2000). Effect of heterogeneity on adsorption of solid surfaces: Application of inverse gas chromatography in the studies of energetic heterogeneity of adsobents. Journal of Chromatography A, 886, 133-152.

Chaudhury, M.K., and Good, R.J. (1991). Chapter 3. in L.H. Lee.(Ed.), Fundamentals of adhesion, New York: Plenum Press.

Cheng, D. (2002). Surface free energy of asphalt-aggregate systems and performance analysis of asphalt concrete based on surface free energy. PhD Dissertation, Texas A&M University, College Station, Texas.

Cheng, D., Little, D.N., and Holste, J.C. (2002). Use of surface free energy of asphalt-aggregate systems to predict moisture damage potential. Journal of Association of Asphalt Paving Technologists, 71, 59-84.

Chibowski, E. (2003). Surface free energy of a solid from contact angle hysteresis. Advances in Colloid and Interface Science. 103, 149-172.

Chibowski, E., and Holysz, L. (1986). Correlation of surface free energy changes and flotability of quartz. Journal of Colloid and Interface Science, 112(1), 15 – 23.

Companion, A.L. (1979). Chemical bonding (second edition). New York: McGraw-Hill Book Co.

Curtis, C.W. (1992). Investigation of asphalt-aggregate interactions in asphalt pavements. American Chemical Society, Fuel, 37, 1292-1297.

Curtis, C.W., Clapp, D.J., Jeon, Y.W., and Kiggundu, B.M. (1989). Adsorption of model asphalt functionalities, AC-20, and oxidized asphalts on aggregate surfaces. Transportation Research Record, 1228, 112-127.

Curtis, C.W., Ensley, K., and Epps, J. (1993). Fundamental properties of asphalt-aggregate interactions including adhesion and absorption, Report SHRP-A-341, Washington, D.C.: National Research Council.

Curtis, C.W., Lytton, R.L., and Brannan, C.J. (1992). Influence of aggregate chemistry on the adsorption and desorption of asphalt. Transportation Research Record, 1362, 1-9.

Curtis, C.W., Terrel, R.L., Perry, L.M., Al-Swailmi, S., Brannan, C.J. (1991). Importance of asphalt-aggregate interactions in adhesion. Journal of Association of Asphalt Paving Technologists, 60.

Davis, T.C., and Petersen, J.C. (1966). An adaptation of inverse-liquid chromatography to asphalt oxidation studies. Analytical Chemistry, 38, 138-1940.

Davis, T.C., and Petersen, J.C. (1967). An inverse GLC study of asphalts from the Zaca-Wigmore Experimental Test Road. Journal of the Association of Asphalt Paving Technologists, 36, 1-5.

Della Volpe, C. and Siboni, S. (1997). Some reflections on acid-base solid surface free energy theories. Journal of Colloid and Interface Science, 195, 121-136.

Della Volpe, C. and Siboni, S. (2000). Acid-base surface free energies of solids and the definition of scales in the Good-van Oss- Chaudhury theory, Journal of Adhesion Science and Technology, 14(2), 235 -272.

Digital Instruments. (1998). MultiMode™ SPM instruction manual. Tucson, Arizona: Veeco Metrology Group.

Divito, J.A. and Morris, G.R. (1982). Silane pretreatment of mineral aggregate to prevent stripping in flexible pavements. Transportation Research Record, 843, 104.

Dorris, G.M., and Gray, D.G. (1981). Adsorption of hydrocarbons on silica-supported water surfaces. Journal of Physical Chemistry, 85, 3628-3635.

Elphingstone, G.M. (1997). Adhesion and cohesion in asphalt-aggregate systems. P.h.D. Dissertation, Texas A&M University, College Station, Texas.

Endersby, V.A., Griffin, R.L., and Sommer, H.J. (1947). Adhesion between asphalts and aggregates in the presence of water. Proceedings of the Association of Asphalt Paving Technologists, 16, 411-451.

Ensley, E.K. (1973). A study of asphalt-aggregate interactions and asphalt molecular interactions by microcalorimetric methods: Postulated interaction mechanisms. Journal of the Institute of Petroleum, 59(570), 279-289.

Ensley, E.K., and Sholz, H.A., (1972), A study of asphalt-aggregate interactions by heat of immersion. Journal of the Institute of Petroleum, 58(560), 95-101.

Ensley, E.K., Petersen, J.C., and Robertson, R.E.. (1984). Asphalt-aggregate bonding energy measurments by microcalorimetric methods. Thermochimica Acta, 77, 95-107.

Ernstsson, M. and Larsson, A. (1999). A multianalytical approach to characterize acidic adsorption sites on a quartz powder. Colloids and Surfaces, 168, 215-230.

Finston, H.L. and Rychtman, A.L. (1982). A new view of current acid-base theories. New York: John Wiley & Sons, Inc.

Fowkes, F.M. (1964). Attractive forces at interfaces. Industrial Engineering & Chemistry, 56(12), 40-52.

Fromm, H.J. (1974). The mechanisms of asphalt stripping from aggregate surfaces. Proceedings of the Association of Asphalt Paving Technologists, 43, 191-223.

Gast, R. (1977). Surface and colloid chemistry. In J.B. Dixon and S.B. Weed (Eds.), Minerals in soils environments (pp. 27-73), Madison, Wisconsin: Soil Science Society of America.

Good, R.J. (1966). Intermolecular and interatomic forces. In Patrick, R.L (Ed.), Treatsie on adhesion and adhesives, Volume 1: Theory (pp. 10-65). New York: Marcel Dekker, Inc.

Good, R.J. and van Oss, C.J. (1991). The modern theory of contact angles and the hydrogen bond component of surface energies. In M.E. Schrader and G. Loeb (Eds.), Modern approach to wettability: Theory and applications (pp. 1-27). New York: Plenum Press.

Goodwin, J.W. (2004). Colloids and interfaces with surfactants and polymers – An introduction. England: John Wiley & Sons Ltd.

Goss, K-U. (1997). Considerations about the adsorption of organic molecules from the gas phase to surfaces: Implications for inverse gas chromatography and the prediction of adsorption coefficients. Journal of Colloids and Interface Science,190, 241-249.

Graf, P.E. (1986). Factors affecting moisture susceptibility of asphalt concrete mixes. Proceedings of the Association of Asphalt Paving Technologists, 55, 191-175.

Gutierrez, M.C., Rubio, F., and Oteo, J.L. (1999). Inverse gas chromatography: A new approach to the estimation of specific interactions. Journal of Chromatography A, 845, 53-56.

Gzemski, F.C. (1948). Factors affecting adhesion of asphalt to stone. Proceedings of the Association of Asphalt Paving Technologists, 17, 74-92.

Harnsberger, M. (2003). Catalytic effects of aggregate on oxidation. Presented at Aging of Paving Asphalts Conference. Laramie, Wyoming: Western Research Institute.

Harter, R.D. (1977). Reactions of minerals with organic compounds in soil. In J.B. Dixon and S.B. Weed (Eds.), Minerals in soil environments. Madison, Wisconsin: Soil Science Society of America.

Hartkopf, A., and Karger, B.L. (1973). Study of the interfacial properties of water by gas chromatography. Accounts of Chemical Research, 6, 209-216.

Hicks, G.R. (1991). Moisture damage in asphalt concrete. National Cooperative Highway Research Program Synthesis of Highway Practice 175. Washington, D.C.: Transportation Research Board.

Hicks, R.G., Santucci, L., and Aschenbrener, T. (2003). Introduction to moisture sensitivity of hot mix asphalt pavements. National Seminar in Moisture Sensitivity, San Diego, California.

Holysz, L., Dawidowicz, A.L., Chibowski, E., and Stefaniak, W. (1991). Influence of surface modification of porous glasses on their surface free energy. Journal of Material Science, 26, 4344 – 4350.

Houston, J.E. and Kim, H.I. (2002). Adhesion, friction, and mechanical properties of functionalized alkanethiol self-assembled monolyaers. Accounts of Chemical Research, 35, 547-553.

Huang, S-C., Branthaver, J.F., and Robertson, R.E. (2000). Effects of aggregates on asphalt-aggregate interaction. 8th Annual Symposium of the International Centre for Aggregate Research, Denver, Colorado, 1– 20.

Hubbard, P. (1938). Adhesion of asphalt to aggregate in the presence of water. HRB Bulletin 8 (Part 1). Washington D.C.: Highway Research Board.

Israelachvili, J.N., Chen, Y.L., and Yoshizawa, H. (1994). Relationship between adhesion and friction forces. Journal of Adhesion Science & Technology, 8, 1231 – 1249.

Jacobasch, H-J., Grundke, K., Schneider, S., and Simon, F. (1995). Surface characterization of polymers by physico-chemical measurements. Journal of Adhesion, 48, 57-73.

Jamieson, I.L., Moulthrop, J.S., and Jones, D.R. (1995). SHRP results on binder-aggregate adhesion and resistance to stripping. Asphalt Yearbook 1995, 17-21.

Jeon, Y.W., and Curtis, W.C., (1990). A literature review of the adsorption of asphalt functionalities on aggregate surfaces. Strategic Highway Research Program (Report SHRP-A/IR-90-014). Washington, D.C.: National Research Council.

Johnston, C.T. (1996). Sorption of organic compounds on clay minerals: A surface functional group approach. In B.Sawhney (Ed.), Organic pollutants in the environment (Chapter 1). Boulder, Colorado.: Clay Minerals Society.

Kiggundu, B.M. and Roberts, F.L. (1988). Stripping in HMA mixtures: State-of-the-art and critical review of test methods. NCAT (Report No.88-2). Alabama: National Centre for Asphalt Technology.

Kim, S-S., Gardner, G.W., McKay, J.F., Robertson, R.E., and Branthaver, J.F. (1997). Detection of strongly acidic compounds in extensively aged asphalts. In A.M. Usmani (Ed.), Asphalt science and technology (pp. 103-117). New York: Marcel Dekker, Inc.

Kittrick, J.A. (1977). Mineral equilibria and the soil system. In J.B. Dixon and S.B. Weed (Eds.), Minerals in soils environments (pp. 1-25). Madison, Wisconsin: Soil Science Society of America.

Kolasinski, K.W. (2002). Surface science: Foundations of catalysis and nanoscience. Chichester: John Wiley & Sons Ltd.

Krchma, L.C., and Loomis, R.J., (1943). Bituminous-aggregate water resistance studies. Journal of the Association of Asphalt Paving Technologists, 15, 153-187.

Kwok, D.Y. (1999). The usefulness of the Lifshitz-van der Waals/ acid-base approach to surface tension components and interfacial tension. Colloids and Surfaces A: Physiochemical and Engineering Aspects, 156, 191-200.

Kwok., D.Y., and Neumann, A.W. (2003). Contact angle measurements and criteria for surface energetic interpretation. Contact Angle Wettability and Adhesion, 3, 117-159.

Labib, M.E. (1988). The origin of the surface charge on particles suspended in organic liquids. Colloids and Surfaces, 29, 293-304.

Labib, M.E. (1992). Asphalt-aggregate interactions and mechanisms for water stripping. American Chemical Society, Fuel, 37, 1472-1481.

Labib, M.E., and McClelland, K. (1993). Electrokinetic properties of siliceous and calcareous road aggregates. Unpublished manuscript. Princeton: David Sarnoff Research Center.

Labib, M.E., and Schujko, A. (1993). Donor-acceptor properties of asphalts. Part I: Proton transfer properties. Unpublished manuscript. Princeton: David Sarnoff Research Center.

Labib, M.E., and Wielicki, H. (1993a). Donor-acceptor properties of inorganic aggregates used in asphalt pavements. Part I: Proton transfer surface properties. Unpublished manuscript. Princeton: David Sarnoff Research Center.

Labib, M.E., and Wielicki, H. (1993b). Donor-acceptor properties of inorganic aggregates used in asphalt pavements. Part II: Electron transfer surface properties. Unpublished manuscript. Princeton: David Sarnoff Research Center.

Labib, M.E. and Williams, R. (1986). An experimental comparison between the aqueous pH scale and the electron donicity scale. Colloid and Polymer Science, 264, 533-541

Labib, M.E. and Williams, R. (1987). The effect of moisture on the charge at the interface between solids and organic liquids. Journal of Colloid and Interface Science, 115(2), 330-338.

Lee, L.H. (1991). Fundamentals of adhesion. New York: Plenum Press.

Li, W. (1997). Evaluation of the surface energy of aggregate using the Chan balance. Unpublished manuscript. College Station, Texas: Texas A&M University, Chemical Engineering Department.

Little, D.N. and Jones, D.R. (2003). Chemical and mechanical mechanisms of moisture damage in hot mix asphalt pavements. National Seminar in Moisture Sensitivity, San Diego, California.

Little, D.N., Lytton, R.L., and Williams, D., (1997), Propagation and healing of microcracks in asphalt concrete and their contributions to fatigue. In A.M. Usmani (Ed.), Asphalt science and technology (pp. 149-195). New York: Marcel Dekker, Inc.

Little, D.N., Bhasin, A., Lytton R.L., and Hefer, A.W. (2003). Using surface energy measurements to select materials for asphalt pavements. NCHRP Project 9-37, Interim Report. College Station, Texas: Texas Transportation Institute.

Little, D.N., Bhasin, A., and Hefer, A.W. (2004). Using surface energy measurements to select materials for asphalt pavements. NCHRP Project 9-37, July Quarterly Report. College Station, Texas: Texas Transportation Institute.

Logaraj, S. (2002). Chemistry of asphalt-aggregate interaction – Influence of additives. Presented at the Moisture Damage Symposium, Laramie, Wyoming.

Lytton, R.L. (2000). Characterizing asphalt pavements for performance. Transportation Research Record, 1723, 5-16.

Lytton, R.L. (2003). Adhesive fracture in asphalt concrete mixtures. Chapter in Youtcheff, J. (Ed.), In Press.

Lytton, R.L., Chen, C.W., and Little, D.N. (2001). Microdamage healing in asphalt and asphalt concrete, Volume 3: A micromechanics fracture and healing model for asphalt concrete. Report FHWA-RD-98-143. College Station, Texas: Texas Transportation Institute.

Malandrini, H., Clauss, F., Partyka, S., and Douilard, J.M. (1997). Interactions between talc particles and water and organic solvents. Journal of Colloid and Interface Science, 194, 183-193.

Masad, E., Tashman, L., Little, D.N., and Zbib, H. (2004). Viscoplastic modeling of asphalt mixes with the effects of anisotropy, damage and aggregate characteristics. Submitted to the Journal of Mechanics of Materials.

McBain, J.W. and Hopkins, D.G. (1925). On adhesives and adhesive action. Journal of Physical Chemistry, 29, 294.

McBain, J.W. and Hopkins, D.G. (1929). Adhesives and adhesive action (Appendix IV). Second report of the Adhesive Research Committee. London: Dept. of Scientific and Industrial Research.

McClellen, A.L. and Harnsberger, H.F. (1967). Cross-sectional areas of molecules adsorbed on solid surfaces. Journal of Colloid and Interface Science, 23, 577-599.

McMurry, J. (2000). Organic chemistry (5th edition). Pacific Grove, California: Brooks/Cole.

Médout-Marére, V., Belarbi, H., Thomas, P., Morato, F., Guintini, J.C., and Douillard, J. (1998). Thermodynamic Analysis of immersion of swelling clay. Journal of Colloid and Interface Science., 202, 139-148.

Merril, W.W. and Pocius, A.V. (1991). Direct measurement of molecular level adhesion forces between biaxially oriented solid polymer films. Langmuir, 7, 1975-1980.

Mertens, E.W. and Wright, J.R. (1959). Cationic emulsions: How they differ from conventional emulsions in theory and practice. Highway Research Board Proceedings, 38, 386-397.

Morgan, P. and Mulder, A. (1995). The shell bitumen industrial handbook. London: Thomas Telford Publishing.

Myers, D., (1991). Surfaces, interfaces, and colloids: Principles and applications. New York: VCH Publishers, Inc.

Myers, D., (2002). Some general concepts about interfaces. Interfaces and colloids (Part 1), retrieved from http://www.cheresources.com/interfaces2.shtml. Cheresources, Inc

Nguyen, T., Byrd, E., and Bentz, D. (1992). Insitu measurement of water at the asphalt/ siliceous aggregatei. Americal Chemical Society, Fuel, 37, 1466 – 1471.

Nicholson, V. (1932). Adhesion tension in asphalt pavements, its significance and methods applicable in its determination. Proceedings of the Association of Paving Technologists, 3, 28 -48.

Niemantsverdriet, J.W., (200), Spectroscopy in catalysis, an introduction (2nd edition). Weinheim, Germany: Wiley-VCH Verlag GmbH.

O'Brien, R.W. (1988). Electro-acoustic effects in a dilute suspension of spherical particles. Journal of Fluid Mechanics, 190, 71-86.

Ohshima, H. (1998). Interaction of electrical double layers. In H. Ohshima and K. Furusawa (Eds.), Electrical phenomena at interfaces; fundamentals, measurements and applications, 2nd edition, surfactant science series volume 76 (Chapter 3). New York: Marcel Dekker, Inc.

Packham, D.E. (1992). Handbook of adhesion. Essex, England: Longman Group UK Ltd.

Packham, D.E. (1998). The mechanical theory of adhesion – A seventy year perspective and its current status. In W.J. van Ooij and H.R. Anderson Jr.. (Eds.), First International Congress on Adhesion Science and Technology (pp. 81-108). The Netherlands: VSP.

Park, S., Jo, M.C., and Park, J.B. (2000). Adsorption and thermal desorption behaviour of asphalt-like functionalities on silica. Adsorption Science & Technology, 18, 675-684.

Pearson, R.G. (1968). Hard and soft acids and bases, HSAB, Part 1, fundamental principles. Journal of Chemical Education, 45 (9), 581.

Perry, L.M. and Curtis, C.W. (1992). Effect of aggregate modification by organosilane coupling agents on the adsorption behavior of asphalt models and asphalt. American Chemical Society, Fuel, 37, 1482-1489.

Petersen, C.J. (1986). Quantitative functional group analysis of asphalts using differential infrared spectrometry and selective chemical reactions – Theory and application. Transportation Research Record, 1096, 1.

Petersen, C.J. and Plancher, H., (1998). Model studies and interpretive review and the competitive adsorption and water displacement of petroleum asphalt chemical functionalities on mineral aggregate surfaces. Petroleum Science & Technology, 16, 89-131.

Petersen, J.C., Ensley, E.K., and Barbour, F.A. (1974). Molecular interactions of asphalt in the asphalt-aggregate interface region. Transportation Research Record, 515, 67.

Petersen, J.C., Plancher, H., Ensley, E.K., Miyake, G., and Venable, R.L. (1982). Chemistry of asphalt-aggregate interaction: Relationship with moisture damage prediction test. Transportation Research Record, 843, 95.

Pimentel, G.C. and McClellan, A.L (1960). The hydrogen bond. New York: Reinhold Publishing Co.

Plancher, H., Dorrence, S.M., and Petersen, C.J. (1977). Identification of chemical types in asphalts strongly adsorbed at the asphalt-aggregate interface and their relative displacement by water. The Association of Asphalt Paving Technologists, 46, 151.

Pocius, A.V. (1997). Adhesion and adhesives technology. Cincinnati, Ohio: Hanser/ Gardner Publications, Inc.

Podoll, R.T. and Becker, C. (1991). Surface analysis by laser ionization of the asphalt-aggregate bond. March Progress Report SHRP-87-AIIR-07. Menlo Park, California: SRI International.

Podoll, R.T. and Irwin, K.C. (1990). Flow microcalorimetry studies of the asphalt/aggregate interface, American Chemical Society. Division Petroleum Chemistry, 35(3), 346-352

Press, W.H., Flannery, B.P., Teukolsky, S.A., and Vetterling, W.T. (1989). Numerical Recipies. Cambridge, UK: Cambridge Univ. Press.

Rice, J.M. (1958). Relationship of aggregate characteristics to the effect of water on bituminous paving mixtures. Symposium on effect of water on bituminous paving mixtures, ASTM STP No. 240, 17 – 34.

Roberts, A.D. (1977). Surface charge contribution in rubber adhesion and friction. Journal of Physics, D10, 1801.

Robertson, R.E. (2000). Chemical properties of asphalts and their effects on pavement performance. Transportation Research Circular No. 499. Washington, D.C.: Transportation Board.

Ross, D., Mirsalis, J., Loo, B., and Rhee, S. (1991a,b,c). Fundamentals of the asphalt-aggregate bond. Progress Reports (SHRP-87-AIIR-11): (a) January, (b) May, (c) June,. California: SRI International.

Saville, V.B., and Axon, E.O. (1937). Adhesion of asphaltic binders to mineral aggregates. Journal of the Association of Asphalt Paving Technologists, 9, 86-101.

Schapery, R.A. (1984). Correspondence principles and a generalized J-integral for large deformation and fracture analysis of viscoelastic media. International Journal of Fracture, 25, 194-223.

Schapery, R.A. (1989). On the mechanics of crack closing and bonding in linear viscoelastic media. International Journal of Fracture, 39, 163-189.

Schmidt, R.J. and Graf, P.E. (1972). The effect of water on the resilient modulus of asphalt treated mixes, Proceedings. Journal of the Association of Asphalt Paving Technologists, 41, 118-162.

Schultz, J. and Nardin, M. (1994). Theories and mechanisms of adhesion. In A. Pizzi and K.L. Mittal (Eds.), Handbook of Adhesive Technology (pp. 19-33). New York: Marcell Dekker, Inc.

Schultz, J., Carré, A., and Mazeau, C. (1984). Formation and rupture of grafted polyethylene/ aluminum interfaces. International Journal of Adhesives, 4(4), 163-168.

Scott, J.A. N. (1978). Adhesion and disbonding mechanisms of asphalt used in highway construction and maintenance. Journal of the Association of Asphalt Paving Technologists, 47, 19 - 48.

Shanahan, M.E.R. (1992). Wetting and spreading. In D.E. Packham (Ed.), Handbook of adhesion (pp. 506-509). Essex, England: Longman Group UK Ltd.

SHRP (1991). SHRP Materials Reference Library aggregates: Chemical, mineralogical, and sorption analyses. Report SHRP-A/ UIR-91-509. Washington D.C.: Strategic Highway Research Program, National Research Council.

SHRP (1993). SHRP Materials Reference Library: Asphalt cements: A concise data compilation. Report SHRP-A-645. Washington D.C.: Strategic Highway Research Program, National Research Council.

Simmons, G.W. and Beard, B. (1987). Characterization of acid-base properties of the hydrated oxides on iron and titanium metal surfaces. Journal of Physical Chemistry, 91, 1143.

Skoog, D.A., and Leary, J.J. (1992). Principles of instrumental analysis (4^{th} edition). Philadelphia, Pennsylvania: Saunders College Publishing.

SMS (2004). Dynamic vapor sorption. Allentown, Pennsylvania: Surface Measurement Systems Ltd.

Sun, C., and Berg, J.C. (2002). Effect of moisture on the surface free energy and acid-base properties of mineral oxides. Journal of Chromatography A, 969, 59-72.

Tarrer, A.R. and Wagh, V.P. (1990). Innovative tests to predict the strength and type of asphalt-aggregate bonds. American Chemical Society, Division of Petroleum Chemistry, 35 (3), 361-369.

Tarrar, A.R. and Wagh, V.P. (1992). The effect of the physical and chemical characteristics of the aggregate on bonding. Report SHRP-A/ UIR-91-507. Washington, D.C.: Strategic Highway Research Program, National Research Council.

Thelen, E. (1958). Surface energy and adhesion properties in asphalt-aggregate Systems. HRB Bulletin 192 (pp. 63-74). Washington D.C.: Highway Research Board.

Thomas, RC., Houston, J.E., Crooks, R.M., Kim, T. and Michalske, T.A. (1995). Probing adhesion forces at the molecular scale. Journal of the American Chemical Society,117, 3830-3834.

Titova, T.I., Kosheleva, L.S., and Zhdanov, S.P. (1987). IR study of hydroxylated silica, Langmuir, 3, 960.

Tsukruk, V.V. and Bliznyuk, V.N. (1998). Adhesive and friction forces between chemically modified silicon and silicon nitride surfaces. Langmuir, 14, 446-455.

Uhlmann, P., and Schneider, S. (2002). Acid-base surface energy characterization of grafted polyethylene using inverse gas chromatography. Journal of chromatography A, 969, 73-80.

Van Oss, C.J. (1994). Interfacial forces in aqueous media. New York: Marcel Dekker, Inc.

Van Oss, C.J., and Giese, R.F. (2003). Surface Modification of clays and related materials. Journal of Dispersion Science and Technology, 24 (3&4), 363-376.

Van Oss, C.J., and Giese R.F. (2004). Influence of the pH of water on its electron-accepticity and donicity. Submitted to the Journal of Adhesion for the Chaudhury Collection.

Van Oss, C.J., Chaudhury, M.K., and Good, R.J. (1988). Interfacial Lifshitz-van der Waals and polar interactions in macroscopic systems. Chemical Review, 88, 927.

Van Oss, C.J., Wu, W., and Giese, R.F. (1993). Measurement of the specific surface area of powders by thin layer wicking. Particulate Science and Technology, 11, 193-198

Walker, P. (1994). Silane and other adhesion promoters in adhesive technology. In A. Pizzi and K.L. Mittal (Eds.), Handbook of adhesive technology (pp. 50-52). New York: Marcel Dekker, Inc.

Woodward, R.P. (2000). Prediction of adhesion and wetting from Lewis acid-base measurements. Automotive 2000: http://www.firsttenangstorms.com

WRI (2001). Fundamental properties of asphalts and modified asphalts, Volume 1: Interpretive report. FHWA-RD-99-212. Laramie, Wyoming: Western Research Institute.

WRI (2003a). Fundamental properties of asphalts and modified asphalts, Volume 1: Interpretive report. Draft final report (Contract DTFH61-99C-0022). Laramie, Wyoming: Western Research Institute.

WRI (2003b). Fundamental properties of asphalts and modified asphalts, Volume 2: New test methods. Draft final report (Contract DTFH61-99C-0022). Laramie, Wyoming: Western Research Institute.

Yildirim, I. (2001). Surface free energy characterization of powders. PhD Dissertation, Mining and Minerals Engineering, Faculty of the Polytechnic Institute and State University, Blacksburg, Virginia.

Yoon, H.H. and Tarrar, A. (1988). Effect of aggregate properties on stripping. Transportation Research Record, 1171, 37-43.

APPENDIX A

SUMMARY OF THEORIES AND MECHANISMS OF BITUMEN-AGGREGATE ADHESION

Table A1. Summary of theories and mechanisms of adhesion

Theory	Mechanisms
(Weak) Boundary Layer Theory	• Low molecular weight organic contaminants on aggregate surface with low cohesive strength • Dust preventing effective wetting • Surface roughness and insufficient mixing temperature prevent effective wetting • Porosity acts as molecular sieve, absorbing low molecular fractions leaving polar species, forming a brittle interphase. • Dissolution of aggregate surface induced by pH of contacting water causes aggregate cohesive failure • Catalytic effect of aggregate on oxidative aging may cause brittle interphase • Long range polarization effect of aggregate on organic bitumen groups may cause more stable interphase

Mechanical Theory	• Macroscopic Scale
	  • Contribution of size/ angularity/ gradation differs depending on magnitude of applied stress/ induced strain
	  • Porosity: lock and key effect
	  • Surface texture: redistribution of stresses and increased contact area
	• Microscopic scale
	  • Fractal aggregate surface at microscopic scale
	  • Phases of different hardness and morphology on bitumen surfaces

Electrostatic Theory	• Opposite charges attract • Surface charges develop in aqueous environments. At least a monolayer of water left on aggregate surfaces at temperatures below 500 to 1000˚C • Electric double layers (EDLs) that interact or overlap cause EDL forces that can attract or repel two surfaces. • Aggregate surfaces induce high pH environments in the presence of water. • pH of interface water affects surface charge of contacting surfaces. • Changes in surface charge affect the magnitude of electrostatic interactions.

Chemical Bonding Theory	• Lewis acids and bases interact through variety of bonds, which may include: covalent, donor-acceptor, coordination, and hydrogen bonding.
	• The nature of aggregate: More variable than bitumen and heterogeneous on macroscopic scale, comprising of different minerals with different functional groups. Aggregate dominates adhesion in bitumen-aggregate systems.
	• The nature of bitumen: Essentially a non-polar organic material with excess weak acidic compounds compared to basic compounds.
	• Interaction: The most prominent polar fraction in bitumen, acidic fraction, readily adsorbs onto aggregate surface forming bonds of variable durability, depending on the dominant mineral type in the aggregate under consideration.
	  • Siliceous aggregates: Hydrogen bonds form with hydroxilated surfaces (silanol groups), which is easily displaced in the presence of water.
	  • Calcareous aggregates: Free calcium prerequisite to form insoluble salt links, not easily displaced by water.
	  • Intermediate aggregates: Siliceous and calcareous minerals or fractions, and/ or presence of other minerals. Transition metals form stronger hydrogen bonding, or if alkali earth metals present, ‘soaps’ or water-soluble salts form.

Table A1 (Continued)

Theory	Mechanisms

Chemical Bonding Theory (continued)	• Additives
	  • Lime added to bitumen: Tie up carboxylic acids (or acids) allowing nitrogen containing and other groups to form more durable bonds with siliceous surface groups.
	  • Lime added to aggregate: Higher valence cations (Ca^{+2}) displaces lower valence cations on aggregate surface and bond with bitumen in a similar fashion as calcareous aggregate.
	  • Amines added to bitumen: Nitrogen groups exhibit lone pairs of electrons that can take part in bonding. The strength of basic molecule depends on the hydrocarbon chain length; C_{18} for example, forms a strong basic molecule, easily protonized, forming a stable ionic/ coordination bond. Naturally, the number of nitrogen head groups increases bond strength.
	  • Coupling agents added to aggregate (organosilanes): Covalent bonds formed through hydrolyses, coupling, and condensation processes.
	• pH effect: influences donor-acceptor interactions which leads to unstable bonds within certain pH ranges.

Thermodynamic Theory	• Although it is listed as a theory, thermodynamics encompasses some of the theories/ mechanisms listed above and simplifies offers quantification following a macroscopic approach. • Free energy is minimized in order for system to approach an equilibrium state. • The nature of bitumen: Comprises of mobile hydrocarbons (polar and non-polar), which in contact with different polar surfaces may exhibit varying 'potential' surface free energies due to molecular orientation, depending on the chemistry of the contacting surface. • The nature of aggregate: Rigid atomic lattice structure, comprises of different minerals each with its own intrinsic surface free energy. The energy of the total system is, however, additive. • Different extensions of classical thermodynamic theory exist. In the approach adopted in this research, microscopic contributions to adhesion are approximated on a macroscopic level by assigning surface energy components to each material. According to the van Oss-Chaudhury-Good theory, these are: a non-polar Lifshitz-van der Waals component, acid or electron acceptor component, and a base or electron donor component. • Physical surface chemistry combining rules or theories can be used estimate the free energy of adhesion between different materials. The theory by van Oss and co-workers are widely used and has been applied to bitumen-aggregate systems. The work of adhesion, or free energy of adhesion, can also be estimated in the presence of a third medium, such as water. • The energy approach is universal and allows incorporating these thermodynamic parameters into holistic, damage prediction models that include other important physical measurable properties such as compliance.

VITA

Arno Wilhelm Hefer, son of Gideon Daniël (Danie) and Henriëtta (Hettie) Petronella Hefer was born in Port Elizabeth, South Africa on June 19, 1972. He grew up on the East Rand, near Johannesburg, and married Masha Botha on March 7, 2000.

The author graduated from the University of Pretoria with a bachelor's degree in civil engineering in 1995, and received a fellowship with the Centre for Transportation Development to pursue a master's degree in civil engineering. With the emphasis on employment creation after the political reform in South Africa, research during his master's degree contributed to reconcile modern pavement engineering technology with the art of constructing macadam pavements in a labor-based fashion. After obtaining his master's degree in 1997 he joined the pavement and materials team of AFRICON Engineering International (Pty) Ltd, a consulting engineering firm with head office in Pretoria, South Africa. During the period 1997 to 2001, the author gained valuable experience from challenging projects in a number of countries including South Africa, Mozambique, Botswana, Namibia, Zambia, and Malaysia. He registered as a professional engineer at the Engineering Council of South Africa in February 2002.

In 2002, the author commenced with a PhD degree at Texas A&M University and was employed as a graduate research assistant by Texas Transportation Institute. After receiving his doctorate in 2004, the author returned to South Africa to continue with a career in industry.

Mailing address: P.O. Box 36765
Menlo Park
0102
Pretoria
South Africa.